

Dissertation
submitted to the
Combined Faculty of Natural Sciences and Mathematics
of the Ruperto Carola University Heidelberg, Germany
for the degree of
Doctor of Natural Sciences

Presented by
M.Sc. Lukas Freund

Born in: Langen, Germany
Oral examination: September 14th 2021

Therapeutic targeting of CD8 T cells and molecular
mechanisms of keratinocyte cell death in acute graft-versus-
host disease

Referees:

Prof. Dr. Hans-Reimer Rodewald

Prof. Dr. Knut Schäkel

Table of Contents

Abstract	6
Zusammenfassung	7
List of Abbreviations	9
Table of Figures	11
1 Introduction	12
1.1 Immune system	12
1.1.1 Innate immunity	12
1.1.2 Adaptive immunity	12
1.1.3 Type I immune response	13
1.2 Skin	13
1.2.1 Keratinocytes.....	14
1.2.2 Immune system of the skin	14
1.2.3 Biology of IFN γ	15
1.3 Hematopoietic stem cell transplantation (HCT)	16
1.3.1 Allogeneic activation	16
1.4 Graft-versus-Host Disease (GVHD)	17
1.4.1 Pathomechanisms of aGVHD.....	17
1.4.2 Cutaneous aGVHD	18
1.4.3 Management of GVHD	20
1.4.4 Experimental models to study cutaneous aGVHD.....	20
1.5. Immunotherapy	21
1.5.1 Near-infrared photoimmunotherapy (NIR-PIT)	21
1.5.2 NIR-PIT in clinical context	22
1.6 Regulated cell death	23
1.6.1 Necroptosis.....	23
1.7 Aim of this study	26
2 Material and Methods	27
2.1 Material	27
2.1.1 Antibodies for flow cytometry.....	27
2.1.2 Reagents for flow cytometry	27
2.1.3 Antibodies for depletion and neutralization	27
2.1.4 Antibodies for histology	27
2.1.5 Histology kits and reagents	28
2.1.6 Antibodies for western blot.....	28
2.1.7 Western Blot kits and reagents	28
2.1.8 Enzyme-linked Immunosorbent Assay (ELISA) kits	29
2.1.9 Cell lines.....	29

2.1.10 Media.....	29
2.1.11 Cell culture reagents.....	29
2.1.12 Magnetic activated cell sorting (MACS).....	29
2.1.13 Oligonucleotides.....	30
2.1.14 qRT-PCR Kits and reagents	30
2.1.15 Biological compounds.....	30
2.1.16 Buffers and solutions.....	30
2.1.17 Laboratory instruments.....	31
2.2. Methods	32
2.2.1 Study approval.....	32
2.2.2 Antibody conjugation	32
2.2.3 Blood samples	32
2.2.4 <i>In vitro</i> depletion	32
2.2.5 Flow cytometry.....	32
2.2.6 Skin samples	33
2.2.7 Mouse model.....	33
2.2.8 CD8 T cell transfer experiments	34
2.2.9 Histology.....	34
2.2.10 Cell culture.....	34
2.2.11 Subcellular fractionation	35
2.2.12 Western Blot.....	35
2.2.13 Expression analysis	35
2.2.14 Enzyme-linked immunosorbent assay.....	36
2.2.15 <i>Ex-vivo</i> organ culture	36
2.2.16 Statistics.....	36
3 Results	37
3.1 Characterization of cutaneous aGVHD.....	37
3.2 NIR-PIT in cutaneous aGVHD	37
3.2.1 Targeting CD8 T cells by NIR-PIT.....	37
3.2.2 Mouse model of humanized cutaneous aGVHD.....	40
3.2.3 CD8 NIR-PIT prevents histopathology of cutaneous aGVHD	43
3.2.4 NIR-PIT ablates targeted skin CD8 T cells thereby inhibiting cutaneous aGVHD.....	45
3.2.5 NIR-PIT targeting CD8 antigen selectively depletes skin localized CD8 T cells	48
3.2.6 CD8 NIR-PIT inhibits delayed aGVHD.....	49
3.2.7 Purified CD8 T cells alone are incapable of inducing cutaneous aGVHD.....	52
3.3 Necroptosis in cutaneous aGVHD	54
3.3.1 Necroptotic signaling is activated in the epidermis of cutaneous aGVHD	54
3.3.2 Allogeneic leukocyte activation induces necroptotic keratinocyte cell death	56

3.3.3 IFN γ induces RIP3 dependent necroptotic keratinocyte cell death.....	58
3.3.4 IFN γ -driven keratinocyte cytotoxicity is regulated by STAT1 signaling	61
3.3.5 <i>De novo</i> expressed ZBP1 facilitates keratinocyte necroptosis	63
3.3.6 IFN γ induces epidermal necroptosis in an <i>ex vivo</i> organ culture model	64
3.3.7 Necroptosis is activated in a mouse model of human aGVHD.	65
3.3.8 Serum levels of RIP3 are associated with clinical aGVHD.....	69
4 Discussion	70
4.1 NIR-PIT for dermatological use	70
4.1.1 NIR-PIT for local therapy of skin diseases.....	71
4.1.2 Role of CD8 T cells in cutaneous aGVHD	72
4.2 Epidermal homeostasis	74
4.3 Pathology of type I driven interface dermatitis.....	75
4.4 Necroptosis in interface dermatitis.....	76
4.5 Concept of IFNγ in the context GVHD	76
4.6 Necroptosis in cutaneous aGVHD	77
4.6.1 Pro-necroptotic properties of IFN γ on epidermal keratinocytes.....	78
4.6.2 Clinical implication of necroptosis during acute GVHD	80
4.6.3 Keratinocyte cell death in aGVHD	81
4.7 JAK/STAT inhibitors for aGVHD	82
4.8 Conclusion.....	83
5 References.....	86
Acknowledgements	99

Abstract

Graft-versus-host disease (GVHD) remains a major complication following hematopoietic stem cell transplantation (HCT), affecting the skin as the earliest and most common target. Skin infiltrating alloreactive lymphocytes causing keratinocyte cell death are pathophysiological hallmarks of GVHD. In search for a therapeutic approach targeting skin localized alloreactive lymphocytes in acute GVHD (aGVHD), near-infrared photoimmunotherapy (NIR-PIT) was established as a strategy that has not been yet introduced in the field of dermatology. NIR-PIT combines the systemic application of a monoclonal antibody labelled with a photosensitizer. Upon exposure to near-infrared light, the conjugated agent causes rapid cell death along with its fluorescence emission. Initially, the selectivity of this approach was demonstrated *in vitro* when targeting CD8 T cells. For studying the therapeutic value of NIR-PIT *in vivo*, a humanized mouse model of cutaneous aGVHD was established. Here, CD8 specific NIR-PIT caused the entire and selective ablation of CD8 T cells from human skin grafts in which aGVHD was induced. At the same time, inhibition of histopathological signs and expression of the disease specific biomarker anti-leukoprotease elafin were observed. These studies assigned important effector functions to CD8 T cells in the context of cutaneous aGVHD. Hence, NIR-PIT can be emphasized to serve as a novel skin-selective therapeutic approach for clinical use. Up to this point keratinocyte cell death that occurs downstream to allorecognition was believed to result from either apoptosis or unspecific necrosis. As an extension of the first part of these studies, the exact mode of keratinocyte cell death in aGVHD was examined. To this end, we compared lesional and non-lesional skin obtained from aGVHD patients and observed a strong upregulation of molecules of the necroptotic signaling pathway: nucleic-acid (NA) sensor Z-DNA-binding protein 1 (ZBP1), phosphorylated receptor interacting protein kinase 3 (RIP3) and phosphorylated mixed-lineage kinase like transcription profile (MLKL). The chief role of interferon gamma (IFN γ) for inducing the activation and *de novo* expression of the necroptotic signaling pathway was initially demonstrated in keratinocyte cultures. These findings were both confirmed in *ex vivo* skin organ cultures and *in vivo* in a humanized mouse model of experimental human aGVHD. Finally, inhibition of STAT1 and RIP3 activities using tofacitinib and GSK'872, respectively, could prevent necroptosis, thus confirming the results. These studies uncovered how IFN γ -mediated necroptosis and the necroptotic signaling pathway play a central role in aGVHD related keratinocyte cell death. While in the first part of these studies the important role of alloreactive CD8 T cells in aGVHD and a novel therapeutic approach for a targeted therapy of skin diseases was introduced, subsequent studies identified necroptosis as a novel cell death pathway executed by IFN γ producing alloreactive T cells.

Zusammenfassung

Die Spender-gegen-Wirt Erkrankung (GVHD) ist eine bedeutsame Komplikation, welche infolge einer hämatopoetischen Stammzelltransplantation auftreten kann. Hierbei ist die Haut eines der am frühesten und gleichzeitig häufigsten betroffenen Organe. Diagnostische Erkennungsmerkmale der kutanen akuten GVHD (aGVHD) sind die Infiltration von alloreaktiven Lymphozyten und die daraus resultierende Schädigung der Keratinozyten. Als Antikörper-vermittelte und hautselektive Therapiestrategie der kutanen aGVHD wurde die Nahinfrarot-Photoimmuntherapie (NIR-PIT) etabliert. Hierbei konnte zunächst in der Zellkultur gezeigt werden, dass NIR-PIT, unter Verwendung fluoreszenzmarkierter anti-CD8 Antikörper, zytotoxische T Zellen nach Belichtung effizient depletiert wurden und eine ungewollte Einflussnahme auf andere Leukozyten ausblieb. Im Anschluss daran wurde ein humanisiertes Mausmodell der kutanen aGVHD generiert, um die translationale Effizienz der NIR-PIT zu studieren. Durch die Behandlung mit NIR-PIT konnte eine gezielte CD8 T Zelldepletion selektiv im humanen, läsionalen Hauttransplantat erreicht werden. Infolgedessen wurde eine komplette Inhibition der histopathologischen Manifestationen sowie der Expression des krankheitsspezifischen Markers Elafin beobachtet. Diese Studien beschreiben eine essentielle pathologische Funktion der CD8 T Zellen in der kutanen aGVHD. Basierend darauf kann die NIR-PIT als neuer Therapieansatz für die klinisch-dermatologische Anwendung empfohlen werden. Der Keratinozytenuntergang infolge einer allogenen Erkennung ist beschrieben als Konsequenz von Apoptose oder unspezifischer Nekrose. Die hier präsentierten Daten zeigen jedoch, dass verstärkt programmierte Nekrose, genannt Nekroptose, in den Keratinozyten von kutanen aGVHD Patienten aktiviert ist. Pathomechanistische Untersuchungen in verschiedenen experimentellen Ansätzen haben gezeigt, dass Interferon gamma ($\text{IFN}\gamma$) die Expression von nekroptotischen Signalmolekülen induziert. Dies führt zu einem *mixed lineage kinase domain-like protein* (MLKL) abhängigen Zelltod. Weiterhin konnte gezeigt werden, dass $\text{IFN}\gamma$ -induzierte Keratinozytennekroptose von der Aktivierung des *signal transducer and activator of transcription 1* (STAT1) und der *de novo* Expression des Nukleinsäuresensors Z-DNA-bindendes Protein 1 (ZBP1) sowie der aufregulierten Expression der *receptor interacting protein kinase 3* (RIP3) abhängt. Im Hautorganmodell konnte dieser $\text{IFN}\gamma$ -abhängige Mechanismus, welcher dem klinischen Bild der *Interface* Dermatitis und dementsprechend der kutanen aGVHD gleich, rekonstruiert werden. Eine vergleichende Expressionsanalyse von nicht-läsionaler und läsionaler Patientenhaut konnte die beobachteten histologischen und transkriptionellen Veränderungen bestätigen. Durch den therapeutischen Einsatz von STAT1-Inhibitor Tofacitinib sowie dem RIP3 Kinaseinhibitor GSK'872 konnte jeweils die induzierte Nekroptose verhindert werden. Zusammenfassend belegen die hier präsentierten Ergebnisse die herausragende Bedeutung von CD8 T Zellen bei der Auslösung der aGVHD und demonstrieren zum ersten Mal die

Wirksamkeit einer zielgerichteten und hautspezifischen Photoimmuntherapie. Darüber hinaus ergaben die weiterführenden Untersuchungen zum Zelltod der Keratinozyten bei der aGVHD, erstmalig die Aktivierung des nekroptotischen Signalwegs, welcher für die Behandlung der kutanen aGVHD von direktem Wert sein kann.

List of Abbreviations

ADCC	antibody-dependent cellular cytotoxicity
aGVHD	acute graft-versus-host disease
APC	antigen presenting cell
ATP	adenosine triphosphate
CC	chemokine
CD	cluster of differentiation
cFLIP	cellular FLICE-inhibitory protein
cGVHD	chronic graft-versus-host disease
C _T	cycle threshold
CXC	CXC-motif chemokine
DAMPs	damage-associated molecular patterns
DNA	deoxyribonucleic acid
DR	death-receptor
EGFR	epidermal growth factor receptor
FADD	Fas-associated protein with death domain
GVL	graft-versus-leukemia
HCT	hematopoietic stem cell transplantation
HMGB1	high mobility group protein B1
IFD	interface dermatitis
IFN γ	interferon gamma
IL	interleukin
IR700	IRDye700DX
ISG	interferon-stimulated-genes
i.v.	intra venously
JAK	janus-kinase
KO	knock-out
LC	Langerhans cells
LTR	lichenoid tissue reaction
mAb	monoclonal antibody
MHC	major-histocompatibility
MLKL	mixed-lineage kinase like
NA	nucleic acid
NF κ B	nuclear factor kappa-light-chain-enhancer of activated B-cells
NHEK	normal human epidermal keratinocytes
NIR	near-infrared
nm	nanometer

NOD	non-obese diabetic
NSG	NOD.Cg-Prkdc ^{scid} Il2rg ^{tm1Wjl} /SzJ
PBS	phosphate buffered saline
PD	programmed cell death
PI	propidium iodide
PIT	photoimmunotherapy
PRR	pattern recognition receptors
RHIM	RIP homotypic interacting motif
RIP	receptor interacting protein kinase
RNA	ribonucleic acid
RT	room temperature
Smac	second mitochondria-derived activator of caspase
SCID	severe-combined-immunodeficiency disease
STAT	signal-transducer-and-activator-of-transcription
TBP	TATA-binding protein
TCR	T cell receptor
TLR	toll-like receptor
TNF α	tumor-necrosis-factor- α
TRIF	TIR-domain-containing adapter-inducing interferon- β
TUNEL	TdT-mediated dUTP-biotin nick end labeling
ZBP1	Z-DNA binding protein 1

Table of Figures

Fig. 1: Pathophysiology of cutaneous aGVHD.	19
Fig. 2: Scheme of NIR-PIT.	23
Fig. 3: Regulated cell death.....	25
Fig. 4: Skin manifestations of aGVHD.	38
Fig. 5: Characterization of CD8-tageted NIR-PIT.	39
Fig. 6: Skin xenograft mouse model.	41
Fig. 7: aGVHD mouse model.....	42
Fig. 8: Effects of localized CD8 NIR-PIT.	44
Fig. 9: Characterization of humanized cutaneous aGVHD.....	46
Fig. 10: Effects of CD8-IR700 or NIR light treatment alone.....	47
Fig. 11: Combination of CD8-IR700 and NIR light prevents cutaneous aGVHD.....	48
Fig. 12: Skin-selective CD8 depletion by NIR-PIT.....	49
Fig. 13: Delayed cutaneous aGVHD model of CD8 NIR-PIT.	51
Fig. 14: Incapability of isolated CD8 T cells to induce cutaneous aGVHD.	53
Fig. 15: Necroptotic signaling is activated in immunological type I cutaneous aGVHD.....	55
Fig. 16: Alloreactive leukocytes trigger necroptotic keratinocyte cell death.	56
Fig. 17: IFN γ induces keratinocyte necroptotic cell death.	59
Fig. 18: IFN γ -induced keratinocyte cell death is RIP3 dependent.....	60
Fig. 19: IFN γ mediates keratinocyte cytotoxicity via STAT1 signaling.	62
Fig. 20: ZBP1 is de novo expressed in IFN γ stimulated keratinocytes.	64
Fig. 21: IFN γ induces necroptosis in <i>ex vivo</i> skin organ cultures.	67
Fig. 22: Necroptotic signaling is activated in humanized aGVHD skin xenografts.	68
Fig. 23: Association between RIP3 levels and clinical GVHD.	69
Fig. 24: CD8 NIR-PIT for the treatment of cutaneous aGVHD.	84
Fig. 25: Hypothesized model of IFN γ -regulated keratinocyte necroptosis.....	85

1 Introduction

1.1 Immune system

The word immunity derives from the latin word “immunitas” meaning exemption from disease. The status of immunity is facilitated by our effective and highly adaptable immune system. Here, the main role of the immune system is to protect its host from potentially harmful invaders. Therefore, evolution formed two major branches, composed of innate and adaptive immunity. The innate immune system, a conserved defense apparatus, is shared in plants, invertebrates and vertebrates and is activated by germ-line encoded pattern-receptors causing rapid, but short-lived immunological responses. In contrast to that, clonal divers lymphocytes, as selective units in vertebrates, are equipped with antigen-specific receptors that represent central agitators of the adaptive immune system ^{1,2}. Generation and selection of those antigen-specific lymphocytes through somatic hypermutation are tightly regulated by the interaction with innate immune cells in lymphoid organs. Upon subsequent encountering, this cellular shaping provides antigen-specific, long-lived immunity which is able to cause immediate and robust responses tailored to a specific danger signal ³.

1.1.1 Innate immunity

Innate immune cells represent the first line of defense against invading pathogens. A subordinate simplified classification can be set to differentiate specialized phagocytic cells such as dermal macrophages and infiltrating neutrophils from professional antigen presenting cells (APCs) such as dermal dendritic cells or epidermal Langerhans cells (LC). The former ones are mainly for clearing the microenvironment from pathogens or destroyed tissue cells by unspecific uptake and digestion. In contrast, APCs are activated upon ligation of pattern recognition receptors (PRRs) inducing their migration into lymphoid tissues where these cells stimulate and shape the adaptive immune response. PRRs belong to a larger group of receptors that recognizes a diverse range of immune stimulators for such as bacterial, fungal or parasite derived components, viral nucleic acid (NA) or stress factors released by host cells. Upon ligation of PRRs, signal transduction induces the expression of major-histocompatibility (MHC) molecules and costimulatory factors like CD80/CD86 which are necessary for the activation of the adaptive immune system ^{4, 5, 6, 7}.

1.1.2 Adaptive immunity

Text book knowledge classifies CD4 T cells as promoters of the immune response and modulators of the infected tissue. Therefore, they are termed as helper T cells. On the other side, CD8 T cells are termed as cytotoxic cells, based on their ability to kill infected host cells ⁸. However, those classic termini blur with progressive research, often in the context of

diseases. In afferent lymphatics, activated APCs encounter naïve T cells which are comprised of CD4 and CD8 phenotypes. Through T cell-receptor's (TCR) interaction with MHC molecules that are loaded with a certain peptide in the presence of IL-2, these T cells differentiate into a mature T cell. Moreover, priming with different cytokines in the activation phase by IL-12, IL-4, IL-23 or IL-10, CD4/CD8 T cells mature into activated helper/cytotoxic T_H1/T_C1 , T_H2/T_C2 , T_H17/T_C17 or regulatory T_{Reg} cells, respectively. Derived from this nomenclature, immune responses are classified into type I ($T_{H/C1}$) reactions against intracellular bacteria, protozoa and viruses, type II ($T_{H/C2}$) reactions against helminths and allergens and type III ($T_{H/C17}$) reactions against extracellular bacteria and fungi⁷. The type of immune response is often determined by a central cytokine, such as interferon-gamma ($IFN\gamma$) for type I responses, IL-4 and IL-13 for Type II responses and IL-17 and IL-22 for Type III responses which are mainly produced by activated T cells or innate lymphoid cells^{9, 7}. After leaving the lymphoid organ, primed T cells patrol the circulation in order to immediately induce a strong immune response upon antigen recognition^{10, 3}.

1.1.3 Type I immune response

During type I immune responses against intracellular pathogens, activated $T_{H/C1}$ cells are recruited into peripheral tissues and infected sites. Here, these cells produce high amounts of $IFN\gamma$ as well as tumor-necrosis-factor- α ($TNF\alpha$) which then activate the downstream production of inflammatory cytokines by local adaptive and innate immune cells, respectively. By the secretion of IL-12, activated dendritic cells and macrophages induce the expression of transcription factors T-bet and Eomes in T cells which thereby mediate further $IFN\gamma$ secretion¹¹. $IFN\gamma$ signaling has pleiotropic immunomodulatory properties such as by increasing chemokine and MHC molecule expressions. In response to intercellular infections, $IFN\gamma$ signaling upregulates the expression of MHC molecules on the surface of infected cells, which facilitate the presentation of microbial components to the respective T cell or innate lymphoid cell. As a consequence, cytotoxic responses directed to infected cells, causes cell death and the destruction of the microbial reservoir¹².

1.2 Skin

The skin represents a natural border to protect its host from environmental influences. These parameters range from chemical and physical implications to harmful pathogens. Therefore, evolution formed a highly structured organ with a multifaceted cellular composition that differs both in function and origin. Anatomically, the skin can be divided into epidermis, dermis and subcutaneous adipose tissue. Lymph ducts, blood vessels, neurons and skin-associated lymphoid tissues are embedded in those structures and appendages such hair follicles and sweat glands form connectors to the outside world. On a cellular level, the

dermis mainly consists of connective tissue-forming fibroblasts and the epidermis is comprised of stratified keratinocytes ¹³.

1.2.1 Keratinocytes

A keratinocyte has basically two separate roads further develop after arising from a proliferating stem cell in the basal niche. Under healthy conditions, keratinocytes differentiate into denucleated corneocytes by trailing motion starting from the stratum basale passing the stratum -spinosum and -granulosum and transitioning to finally reach the most outer layer, the stratum corneum ^{14, 15}. On the other hand, upon stimulation for instance with components derived from injured cells, keratinocytes become activated which was historically described by the production of certain keratins. Here, the crosstalk between immune cells and keratinocytes facilitates an appropriate response according to a specific condition. Traditional inflammatory mediators such as Interleukin-1, TNF α or IFN γ were described to mediate keratinocyte wound healing, prolonged activation and contraction respectively ¹⁶. Apart from being simply epithelial cells, keratinocytes were further described to be part of the innate immune system. Keratinocytes themselves express several PRRs and are able to produce inflammatory cytokines such as IL-1 family member (IL-1, IL-33, IL-36) or TNF α , which promote a strong activation of the innate immune response. Essentially, through the production of chemoattractant molecules, keratinocytes determine the type of immune response upon activation. For instance, secretion of CXCL9 and CXCL10 induce a T_H1 influx, thymic stromal lymphoprotein, CCL17 and CCL22 a T_H2 tissue reaction or IL-17C and CCL20 in contrast a T_H17 response, each depending on the type of stimulation ¹⁷. Moreover, by the expression of MHC molecules class I and II in the combination with costimulatory molecule CD2 or CD80, keratinocytes might directly act as non-professional APCs ¹⁸.

1.2.2 Immune system of the skin

The different immune cells in the skin can be organized into the compartmentation of epidermis and dermis. In the epidermis, Langerhans cells of macrophage ontogeny represent the major APC population acting as sentinels for microbial invaders. The second major epidermal population consists of tissue-resident-memory CD8 T cells (T_{RM}). These long-lived cells are scattered in the epidermis ready to react upon recognition of its individual antigen that is independent of APC priming in lymphoid organs. CD4 T_{RM} and CD1c dendritic cells appear less frequently in the epidermis ^{5, 19}.

Generally, in comparison to the epidermis, the dermis is more diverse and frequently populated by immune cells. On the innate side, dermal dendritic cells are marked as professional APCs. However, extracellular matrix remodeling skin resident mast cells are able to equip APC functions. Resident macrophages present the major phagocytic

population. Although CD4 and CD8 T_{RM} or effector memory T_{EM} cells are scattered in the dermis, they cluster in perivascular skin-associated lymphoid tissues where adaptive immune cell priming occurs¹⁹. Upon inflammation, high numbers of granulocytic neutrophils, inflammatory monocytes (sIaMo) and T cells are recruited and accumulate in the skin, ready to eliminate a potential infection. In addition, inflammatory factors mediate an increase of endothelial vascular permeability allowing high-molecular-weight proteins such as antibodies to pass and penetrate⁴.

1.2.3 Biology of IFN γ

As a broadly expressed pro-inflammatory cytokine, produced in large amounts by activated lymphocytes, IFN γ shows diverse downstream functions depending on the responding cell and microenvironment. Immunologically, IFN γ is important for the differentiation of naïve CD4 T cells to T_H1 T cells as it stimulates the expression of transcription factor T-bet and thus feed-forward stimulates the expression of IL-12R and consequently T_H1 differentiation^{20, 21}. Moreover, IFN γ regulates T cell homeostasis and immunological overreaction through the induction of indoleamine-2,3-dioxygenase and programmed cell death ligand-1 (PD-L) expression by T_{Reg} cells and stromal cells²². The IFN γ R is a heterodimeric receptor composed of IFN γ R1 and IFN γ R2 (α and β chain) with IFN γ as its exclusive ligand. In principle, IFN γ R1 is expressed on every nucleated cell, whereas IFN γ R2 is rather expressed on myeloid cells, B cells and T cells of specific developmental stages. Since it has been described as an inhibitor for viral intracellular replication, IFN γ is known to regulate many different processes in response to its receptor ligation²³. Taking a closer look, intracellular janus-kinase-1/2 (JAK1/2) activation leads to phosphorylation and dimerization of transcription factor signal-transducer-and-activator-of-transcription-1 (STAT1). Upon translocation to the nucleus, STAT1 then binds to interferon-gamma-activated-sequence promoters and thereby increases the expression of interferon-stimulated-genes (ISG) mediated by interferon regulatory factors²⁴.

IFN γ is a strong modulator of skin immunology and inflammatory responses. It was shown that intradermal injections of IFN γ into healthy skin upregulated CXCL9, CXCL10 and CXCL11 chemokine expression. These chemoattractant molecules are crucial for a peripheral immunological type I response, facilitated by the recruitment of CXCR3 expressing T cells. Moreover, IFN γ administration induced expression of myeloid chemoattractant molecules CCL2 and CX3CL1, causing recruitment of dendritic cells and monocytes. In line with that, skin localized APCs showed an upregulated expression of IL-12, thereby promoting the T_H1 immune response in a feed-forward loop²⁵.

1.3 Hematopoietic stem cell transplantation (HCT)

Hematopoietic stem cell transplantation (HCT) as a curative treatment procedure was first performed in 1957 by E. Donnall Thomas and has currently raised to more than 70.000 performances annually ^{26, 27}. Clinical necessity of HCT originates most often from life-threatening hematologic disorders such as multiple myeloma or leukemia. The purpose of HCT is to reconstitute hematopoiesis and immunity upon conditioning with different regimes of chemotherapy, radiotherapy and immunotherapy. The beneficial effects of tumor cell elimination by conditioning regimes comes along with harmful side effects such as direct toxicity and immunosuppression due to clearance of normal immune cells ²⁸. Therefore, opportunistic infections, as a consequence of immune suppression, remain a steady risk for patients undergoing HCT and display one major cause of non-relapse mortality. However, the major cause of post-HCT death by far remains to be relapse of the primary tumor. Therefore, reconstitution of immunity to evoke an effective anti-tumor response (graft-versus-leukemia, GVL) and to protect from opportunistic infections are significant concerns of HCT in addition to reconstitution of normal hematopoiesis ²⁷. Hematopoietic stem cells can be isolated either from peripheral blood, umbilical cord or directly from the bone marrow which obtained from auto-(from Greek “*autos*” meaning “self”)logous or allo-(from greek “*allos*” meaning “different”)genic donors. The allogeneic grafts are obtained from related or unrelated donors that are matched for 10 MHC loci. Mismatches in those constellations can activate donor T cells leading to harmful reactions, such that these cells attack the allogeneic recipient, thereby causing graft-versus-host disease (GVHD) ²⁹.

1.3.1 Allogeneic activation

Central event in the initiation phase of GVHD is the allogeneic activation of mature donor T cells. Alloantigens are MHC molecules or species-specific, human-leukocyte-antigen (HLA) molecules which are immunogenic and therefore potentially cause GVHD. Apart from MHC molecules, minor histocompatibility complexes such as male Y-chromosomal derived antigens can play a role during alloactivation ³⁰. In the context of normal immunological conditions, MHC molecules are loaded with peptides at the protein-binding site, which are presented to the T cell-receptor on the corresponding lymphocyte. Hereby, CD8 coreceptors interact with MHC-I molecules and CD4 coreceptors with MHC-II molecules. Basically, class-I molecules are expressed by all nucleated cells in contrast to class-II molecules which are only expressed by the APC ³¹. Mechanistically, cytosolic peptides are loaded on class-I types MHC-A, -B or -C, whereas peptides derived from the phago-endosome entry, a feature of sentinel cells, are presented by class-II types MHC-DR, -DQ or -DP. Nevertheless, cross-presentation facilitates oppositional T cell activation ³². Depending on the immunogenetic

nature, in European transplantation medicine, preferentially 10 loci are matched prior to HCT, accounting for HLA-A, -B, -C and DRB1 and DQB1 (codominant expression)³³.

Basically, there are two ways of allogeneic activation, direct and indirect. The indirect pathway is parallel to the normal priming of the adaptive immune response. Donor derived APCs process allogeneic MHC molecules derived from damaged host cells and present the immunogenic peptides to the donor derived T cells. During direct activation T cell recognize allogeneic MHC molecules expressed on the surface of host cells. The frequency of potential alloreactive peripheral T cells ranges from 1-10% depending on the compatibility³⁴.

1.4 Graft-versus-Host Disease (GVHD)

GVHD is a systemic inflammatory disease occurring upon allogeneic HCT and is classified into acute and chronic manifestations. The cut off for the differentiation between the two variants is the onset of disease before or after 100d post transplantation. The prevalence of aGVHD varies between 30 to 60% with an overall mortality between 15 and 30% and a higher incidence among unrelated donors. The main targeted organs during aGVHD are intestine, skin and liver³⁵. The prevalence for cGVHD is around 50% with a mortality rate of 25% in severe progressions, whereas mild courses might be beneficial for the GVL effect. In principal, any organ can be affected during cGVHD; however, skin, mucosal sides, intestine, liver and lung show the highest incidence^{36, 37, 38}.

1.4.1 Pathomechanisms of aGVHD

The pathophysiology of aGVHD can be separated into three periods. In the first phase, damage-associated molecular patterns (DAMPs) and alloantigens are released from host tissues due to harmful conditioning regimes. In the second phase, APC mature and home to lymphatic organs where they activated allogeneic T cells. In the third phase, those alloreactive T cells infiltrate target organs, inducing subsequent tissue destruction. The second phase is frequently accelerated due to impaired barrier function of epithelial tissues such as the intestinal tract, skin or lung. Here, microbes or their derived components translocate into the circulation, thereby leading to a strong PRR-dependent innate immune cell activation^{39, 35}. It is thought, that initial IFN γ signaling and bacterial toxins activate tissue resident phagocytes which produce TNF α , thereby polarizing a type I immune response. The subsequently, activated allogeneic T cells are recruited into target organs where they produce in turn high amounts of IFN γ in combination with cytotoxic molecules. Intestine, skin and liver as primary target organs show a strong tropism for alloreactive T cells. It is assumed, that high turnover rates and consequently increased cell death in combination with conditioning regime resistant APCs in the target organs may lead to a strong innate immune cell activation³⁷.

1.4.2 Cutaneous aGVHD

During aGVHD progression, the skin presents the earliest and most frequently affected organ. Therefore, cutaneous manifestations correlate with overall severity and disease progressions which can be used as a prognostic tool. In the acute form, symmetrical maculopapular rashes, erythema and in severe cases formation of bullae and epidermal necrosis are the major macroscopical phenomena. Whereas in chronic manifestations, lichenoid or sclerodermatous changes are commonly occurring in the epidermis or dermis, respectively ⁴⁰.

Histopathological hallmark of cutaneous aGVHD is the presence of a perivascular band-like lymphocytic infiltrate at the dermal-epidermal interface. The morphological changes induced by infiltrating alloreactive cells are mainly affecting the keratinocytes such as basal cell necrosis, acanthosis, parakeratosis hyperkeratosis and -granulosis. Stages of cutaneous GVHD are categorized into vacuolization of the basal layer (grade I), satellite cell necrosis (grade II), pyknotic nuclei and eosinophilic cytoplasm often with subepidermal clefts (grade III), and finally complete loss of the epidermis (grade IV) ⁴¹.

The cellular infiltrate is mainly composed of activated subsets of CD4 and CD8 T cells. Generally, cutaneous aGVHD is described as a Type I immune response with high numbers of T_H1 and T_C1 positive cells. In addition, infiltration of T_H2 and T_H17 cells was detected in acute and chronic manifestations. Overall, both CD4 and CD8 T cells show a dominant IFN γ expression in cutaneous lesions ⁴². The cell mediated cytotoxic pathways against allogeneic target cells are mainly CD95 or perforin/granzyme mediated, preferentially expressed by CD4 and CD8 T cells, respectively. Moreover, soluble factors such TNF α , TNF-related apoptosis inducer ligand (TRAIL) and IFN γ were described to mediate cellular cytotoxicity. All factors were reported to activate or upregulate the caspase machinery and downstream of apoptotic cell death ⁴³. However, evidence for the activation of the apoptotic machinery for instance by cleaved caspase 3 remains absent. Solely TdT-mediated dUTP-biotin nick end labeling (TUNEL) positive keratinocytes, as indicator for regulated cell death were described in the epidermis of aGVHD patients. These results were correlated with downregulation of anti-apoptotic factors in keratin 15 positive basal cells ^{44, 45}. In response to IFN γ signaling, keratinocytes secrete chemoattractant molecules CXCL9-11, thereby recruiting CXCR3 positive alloreactive T cells. Moreover, CXCL9 and CXCL10 were proposed as biomarkers for GVHD ^{46, 47}. In line with that, it was shown that recipients of IFN γ R knock-out (KO) donor T cells were protected from aGVHD including cutaneous manifestations ⁴⁸. IL-33, which is predominantly expressed by epithelial cells such as keratinocytes, was shown to augment IFN γ signaling by the activation and mobilization of suppressor of tumorigenicity (ST2) expressing T cells which is another important biomarker for aGVHD ⁴⁹. Recruited alloreactive T cells localize to the dermal-epidermal junction with a

divergence of dermal CD4 T cells and intra-epithelial CD8 T cells. Those activated cells surround and attack MHC high expressing keratinocytes, known as satellite cell necrosis. In response to inflammatory cytokines such as $TNF\alpha$, keratinocytes produce the skin-derived antileukoproteinase (Elafin) which is the best-established biomarker for cutaneous GVHD. Differential expression in respect to GVHD is defined by 50% positive keratinocytes in depth 50, 51.

On the innate cellular side, LC were described as possible inducers of cutaneous GVHD. On account of their radio-resistant properties, LC are activated upon conditioning regime-mediated tissue damage leading to downstream priming of allogeneic T cells in afferent lymphatics ⁵². Moreover, tissue resident macrophages together with dermal dendritic cells amplify the inflammatory microenvironment in the skin.

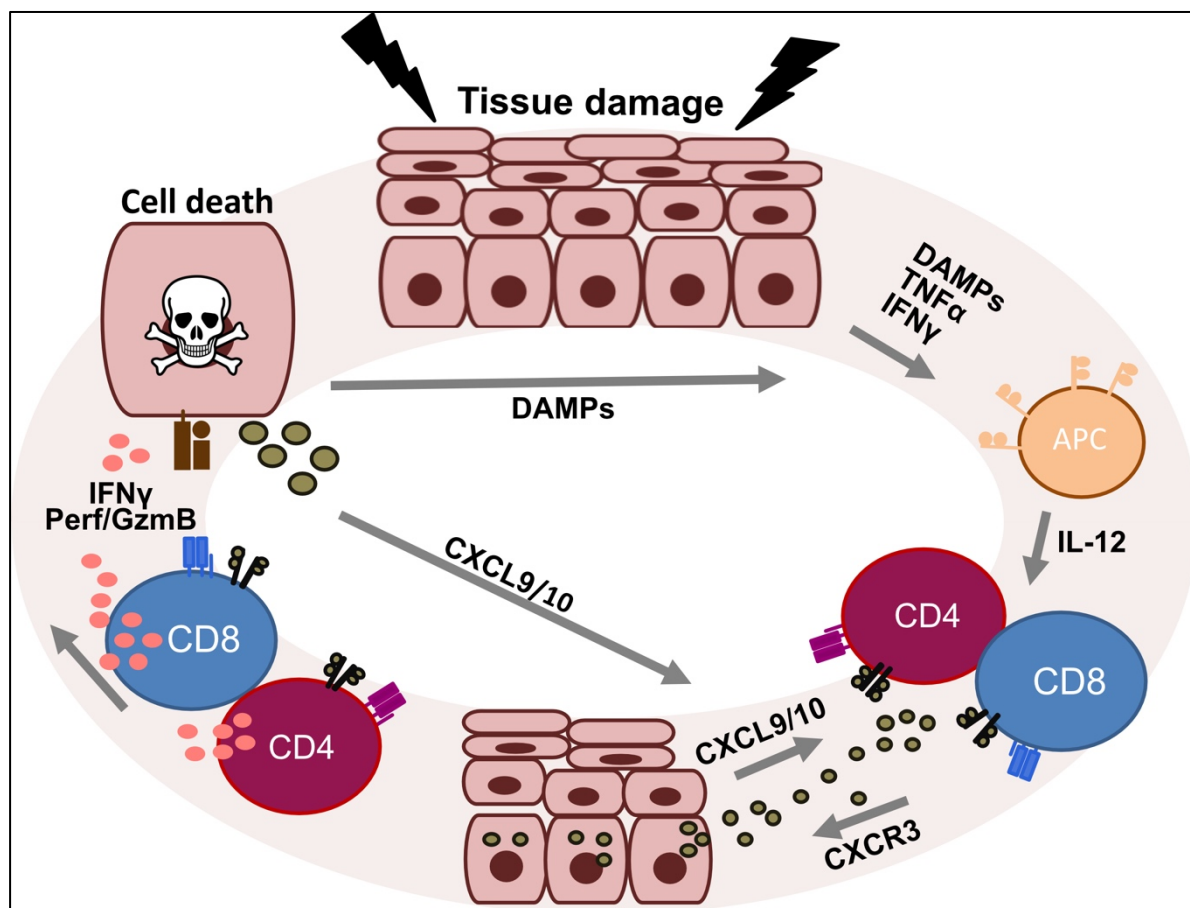


Fig. 1: Pathophysiology of cutaneous aGVHD. Conditioning regime induces the release of DAMPs and inflammatory mediators thereby activating tissue resident innate immune cells. Those APCs prime allogeneic donor T cells which are recruited into the skin by chemoattractant molecules. Infiltrating alloreactive CD4 and CD8 T cells attack keratinocytes through the release of inflammatory cytokines and cytotoxic molecules. Damage and activation further stimulate disease progression by the release of DAMPs and chemokines.

1.4.3 Management of GVHD

The European Society of Blood and Marrow Transplantation (EBMT) updated their recommendations in 2019 for the prophylaxis and management of GVHD after HCT considering matched related or matched unrelated allogeneic donors⁵³. Primarily, calcineurin inhibitor (ciclosporin) plus anti-metabolite (methotrexate) should be used as prophylaxis against the occurrence of GVHD starting one day before graft infusion⁵⁴. In addition, anti-T-lymphocyte globulin (ATG) can be used for patients with high risk of GVHD⁵⁵. The initial treatment of acute or chronic GVHD is based on clinical signs or biopsies; systemic treatments are started from grade II or higher for aGVHD. First-line treatment for a/cGVHD is the administration of glucocorticoids such as methylprednisolone or prednisone with lower doses for isolated cutaneous GVHD, whereas topical steroids can be applied for grade I cutaneous aGVHD. If patients are refractory for steroid therapy, different second-line drugs are approved and recommended such as cellular therapies (T_{reg}), extracorporeal photopheresis (ECP) or JAK 1/2 inhibitor Ruxolitinib^{53, 56}.

1.4.4 Experimental models to study cutaneous aGVHD

Depending on the scientific question, different preclinical models with diverse complexity can be used to investigate alloreactive interactions including upstream and downstream consequences. A very basic experimental setup is the mixed-leukocytes-reaction in which PBMCs of two mismatched donors are co-cultured to detect proliferative and alloreactive properties, generally used to study graft failure. Similar to that, stimulated co-cultures of non-hematopoietic cells such as keratinocytes in combination with mismatched PBMCs can be used to study peripheral aGVHD^{57, 58, 59}. A higher level of complexity can be achieved by the usage of *ex vivo* organ cultures. For instance, to predict alloreactivity and outcome before performing allogeneic HCT, mixed-leukocytes-reactions and skin explants are co-cultured and analyzed by histopathology^{60, 61}. Those skin explant models or similar three-dimensional organotypic-skin models can be further used to study therapeutic approaches^{62, 63}. Of importance in those *ex vivo* skin culture models is the establishment of an air-medium interface to generate physiological conditions that reflect the human situation⁶³. As being a “gold standard” for immunologists, mouse models are indispensable for basic and translational research. Here, mimicry of human pathological conditions provides a platform to test novel drugs or investigate pathomechanisms by genetic modifications. However, those *in vivo* models clearly have their shortcomings and the prediction cannot always be transferred into the clinical situation⁶⁴. To overcome species disparities combined with physiological whole-organism conditions, human to mouse skin-xenograft models were performed after the generation of immunodeficient mice⁶⁵. A perfect mouse strain to study human skin biology are NOD.Cg-Prkdc^{scid} Il2rg^{tm1Wjl}/SzJ (NSG) mice. Based on their genetic background, non-

obese-diabetic (NOD) mice have no hemolytic complement, a reduction in dendritic and NK cell function as well as defective macrophages. The severe-combined-immunodeficiency disease (SCID) mutation prevents maturation of T and B lymphocytes. Finally, the IL-2R γ chain knockout eliminates signaling from six different interleukins, such as IL-2, IL-4, IL-7, IL-9, IL-15 and IL-21 which are key signaling molecules for the function and maturation of dendritic cells, neutrophils as well as T, B and NK lymphocytes⁶⁶. Therefore, NSG mice are optimal to engraft human solid organs such as skin grafts, based on the missing graft rejection mediated by xenogeneic recognition. Additional depletion of murine Ly6G expressing granulocytes can be performed to prevent inflammatory reactions that might reduce engraftment quality of solid organs⁶⁷. Moreover, genetic studies have demonstrated that NOD mice harbor a polymorphic Sirp α allele which allows the recognition of human CD47 therefore, this protects transferred human leukocytes from phagocytic engulfment⁶⁸. The combination of this complexity permits the possibility to study fully human cutaneous aGVHD by using skin and PBMCs from two independent donors^{69, 70}.

1.5. Immunotherapy

Paul Ehrlich described over a century ago, that every antigen has a complementary antibody and is neutralized simply by the presence of the antibody⁷¹. Since then, antibody-based therapy, known as immunotherapy, became an important and widely used tool in research and clinical context⁷². Monoclonal antibodies (mAb) have multifaceted properties which might show undesirable side effects in clinical settings⁷³. A perfect example is the first clinical mAb targeting CD3-muromunab (OKT3), approved in 1985 for cellular transplant rejection. Apart from the desired immunosuppressive effects by the depletion of reactive T cells, some patients showed a strong cytokine storm due to the activation and signal transduction of CD3 by muromunab⁷⁴. In context of cellular depletion, mAb either interfere with cellular functions, opsonize and activate the complement cascade or induce cell death via antibody-dependent cellular cytotoxicity (ADCC)⁷⁵. However, systemic ablation of immune cells such as T cells leads to immunosuppression. In the context of HCT, this ablation could favor relapse of primary tumors or opportunistic infections⁷⁶.

1.5.1 Near-infrared photoimmunotherapy (NIR-PIT)

A novel method for localized immunotherapy was demonstrated in 2011 by the introduction of near-infrared photoimmunotherapy (NIR-PIT). Here, the authors conjugated a clinically established mAb targeting epidermal growth factor receptor (EGFR, cetuximab) with a photoactivating chemical, called photosensitizer. The used photosensitizer IRDye700DX (IR700) has an excitation optimum wavelength of 690 nm in the near-infrared (NIR) spectrum. NIR light is nonionizing; causing no damage to DNA; therefore, this light is harmless to normal cells and penetrates several centimeters deep into irradiated tissues⁷⁷.

Upon NIR light exposure, mAb-bound IR700 undergoes photochemical ligand reactions. In brief, hydrophilic side chains are released from the activated photosensitizer, leaving not only a hydrophobic protein structure behind, but also a quenched fluorescence signal. The hydrophobic molecules form aggregates with the antigen-antibody complex, thereby reducing cell membrane integrity of transmembrane proteins. This modification causes water influx leading to rapid cell swelling and downstream necrotic cell death ⁷⁸.

Photosensitizing drugs are commonly used in the field of dermatology such as aminolevulinic acid or methyl aminolevulinate which are both used for photodynamic therapy (PDT). On the other side, methoxypsoralen is applied for ultraviolet A therapy (PUVA) and ECP ⁷⁹⁻⁸⁰. Apart from the efficiency from those photosensitizers to induce cell death upon cellular penetration and light activation, these drugs suffer from specificity, since healthy and unwanted cells are equally targeted by those therapies. In comparison to that, mAb bound IR700 is membrane impermeable and due to the specificity of mAb, this is only directed against a certain antigen and according to that a specific cell type. Importantly, this cellular depletion is selective for the mAb targeted cell, whereas adjacent cells remain unaffected ⁸¹.

1.5.2 NIR-PIT in clinical context

In clinical contexts, NIR-PIT is currently undergoing a phase 3 clinical trial for the proposal of EGFR-targeted NIR-PIT as a second-line treatment of recurrent head and neck cancer. Moreover, different R&D studies showed ablation efficiency in the context of cancer, against CD25 expressing T_{reg}, CD20 expressing B-cells and different tumor cells such as CD44 and CD133 in breast cancer and glioblastoma, respectively ⁸¹.

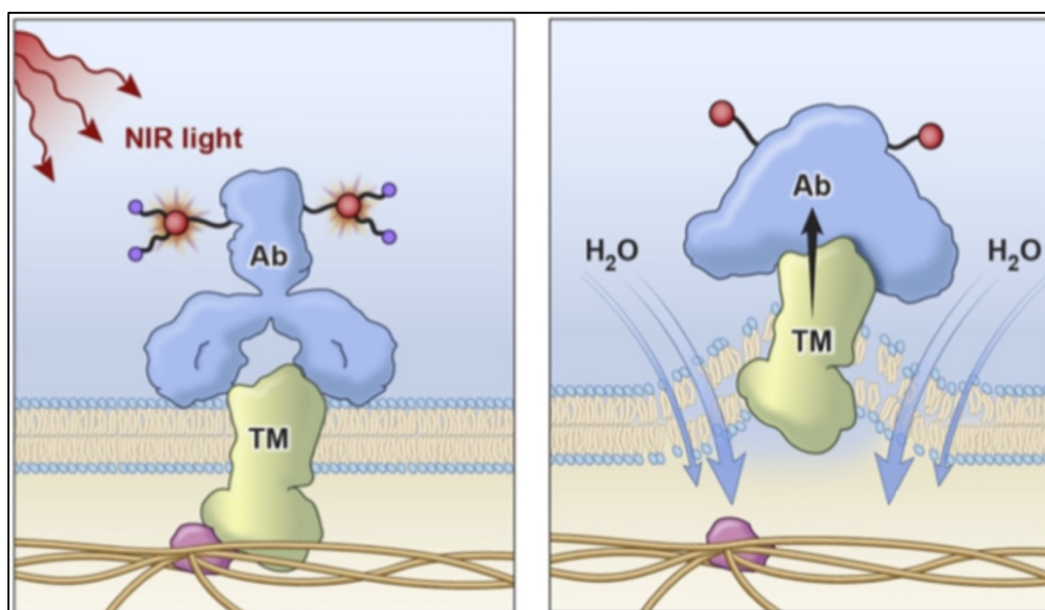


Fig. 2: Scheme of NIR-PIT. Upon antibody binding to its specific target and subsequent activation by NIR light, photochemical ligand reactions diminish the integrity of membrane proteins. This reaction causes water influx and consequently necrotic cell death. Adapted from Kobayashi and Choyke ⁸¹.

1.6 Regulated cell death

For a long period of time, regulated apoptosis and unregulated accidental necrosis were the only established forms of cell death. However, a form of regulated necrosis, called necroptosis represents a novel form of cellular destruction. Regulated cell death can be defined by the circumstance of intrinsic signaling in developmental cellular stages or induced by extracellular signal transduction. Moreover, due to genetic modification or pharmacological inhibition, those signalling pathways can be modified to interfere with regulated cell death. Cellular death that is not associated with development often indicates stress, injury or infections. As the compositional word already implies, necroptosis shows phenomena of necrosis and apoptosis which is similar to other forms of regulated necrosis, pyroptosis and ferroptosis. Here, apoptosis denotes the regulation and necrosis the immunogenicity of the cell death ^{82, 83}.

Apoptosis can be either induced intrinsically through the mitochondrial pathway and a differential expression of apoptotic regulators of the Bcl-2 family or extrinsically by death-receptor (DR) signaling. In case of the latter, TNFR1 (TNF α) and CD95 signaling are the best studied DR in the context of regulated cell death. Upon ligation, Fas-associated protein with death domain (FADD) complexes with caspase-8 at the intracellular death-domain of the DR. Following dimerization, caspase-8 cleaves and activates executioner of apoptosis caspase-3 and caspase-7 which leads to DNA fragmentation and apoptotic body formation ^{84, 85}.

1.6.1 Necroptosis

Necroptosis was first described in 2005 by the observation that pan-caspase inhibitor zVAD did not prevent cell death upon DR-signaling. However, this alternative cell death was blocked by a small-molecule inhibitor necrostatin-1, which prevented phenotypical necrotic but not apoptotic cell death in a receptor interacting protein kinase 1 (RIP1) dependent fashion ⁸⁶. This novel pathway was then verified by the reports of phosphorylated RIP1 interaction and recruitment of receptor interacting protein kinase 3 (RIP3), forming the necrosome complex as a key event in cell death induction downstream to TNF α signaling ⁸⁷. RIP homotypic interacting motif (RHIM) was described as an essential domain for the interaction between RIP1 and RIP3. A few years later, the mixed-lineage kinase like (MLKL) pseudokinase a substrate of RIP3 was shown to finally execute necroptotic cell death in response to TNF α ⁸⁸. Mechanistically, upon oligomerization and autophosphorylation of

RIP3, MLKL is phosphorylated and in turn oligomerizes. This activation induces conformational changes of MLKL and mediates the interaction of 4-helical bundle domain with membrane bound phosphatidylinositolphosphate that consequently lead to lytic pore formation. Thereby, the transportation of MLKL to the plasma membrane is regulated by endosomal sorting complexes which is required for transport III (ESCRT III). ESCRT III itself repairs plasma membrane damage and is triggered by Ca^{2+} influx, which is induced by MLKL-dependent pore formation. Thus, a certain threshold of membrane damage needs to be overcome to finally result in cellular death ⁸⁹.

As described before, apart from NF- κ B dependent activation and inflammation, pleiotropic TNF α -dependent DR signaling can lead to apoptotic or necroptotic cell death. Therefore, downstream signaling must be tightly regulated. Here, caspase-8, in complex with cellular FLICE-inhibitory protein (cFLIP), functions as a central regulator as it cleaves RIP1 and RIP3 to prevent necroptotic cell death ⁹⁰.

So far there are four known signaling proteins with an encoded RHIM domain that induce RIP3-mediated necroptotic cell death. Apart from RIP1, TIR-domain-containing adapter-inducing interferon- β (TRIF) downstream to toll-like receptor (TLR) signaling and Z-DNA binding protein 1 (ZBP1) are able to interact and activate RIP3 ⁹¹. The latter is hypothesized to be a sensor of double-stranded, left-handed Z-DNA and Z-RNA, a conformational distinct form of activated nucleic acids (NA). Originally, ZBP1 was described to induce PANoptosis (apoptosis/necroptosis/pyroptosis) upon viral infection with influenza A and the recruitment of RIP1 and RIP3. However, recent publications demonstrated that when RIP1 is genetically modified, spontaneous activation of ZBP1 leads to necroptosis and inflammation in the skin and intestine under sterile conditions. It is proposed that this activation results from interferon (Type I or II) dependent *de novo* expression and recognition of endogenous retroviruses ⁹². As described before, necroptosis results in a “loud” necrotic, immunogenic cell death. It was shown that necroptotic cells release DAMPs such as high mobility group protein B1 (HMGB1), adenosine triphosphate (ATP), mitochondrial DNA, or IL-1 family members, IL-1 α and IL-33. Those DAMPs then activate innate immune responses via TLR signaling, leading to adaptive immune priming and inflammation ^{93, 94, 95}.

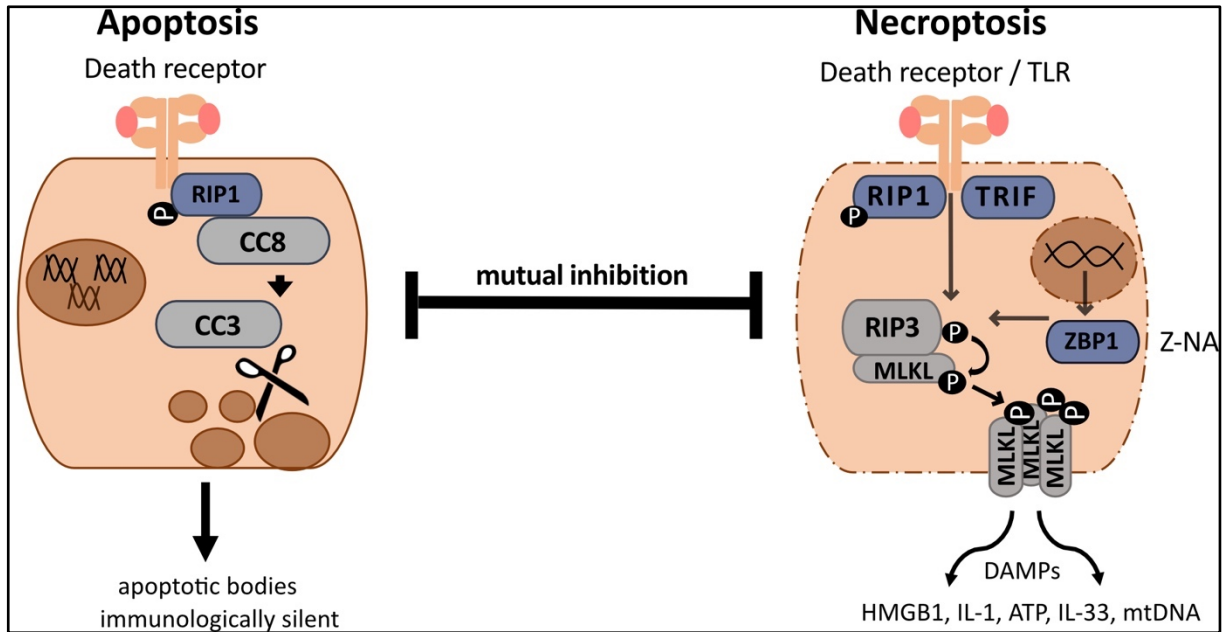


Fig. 3: Regulated cell death. The left panel displays extrinsic apoptotic cell death induced by death receptor signaling. Receptor ligation induces recruitment and interaction of RIP1 and caspase-8. Cleaved caspase-8 in turn cleaves caspase-3 which mediates apoptotic body formation and immunologic silent cell death. The right panel shows the different pathways of necroptotic cell death. Ligation of death receptors and certain TLRs recruit RIP1 and TRIF adaptor molecules respectively, while cytoplasmic double-stranded Z-NA causes dimerization and activation of ZBP1. RIP1, TRIF and ZBP1 contain a RHIM domain that interacts and activates RIP3. Upon autophosphorylation, RIP3 activates MLKL which leads to channel formation by oligomerization causing immunogenic cell death.

1.7 Aim of this study

After decades of intensive investigations, clinicians are still fighting and balancing on the tightrope walk between GVL and GVHD. Although, by far relapse is the major cause of death following HCT, treatment with systemic immunosuppression remains the gold standard for the treatment of GVHD thereby favoring the recurrence of primary tumors. However, without immunosuppression 100% of allogeneic graft recipients would develop GVHD. Therefore, a better understanding of the pathomechanisms of GVHD enables the development of new therapeutic strategies to bundle the efforts towards GVL. Moreover, because patients frequently become resistant to first-line treatment, which accounts for severe GVHD morbidity and mortality, development of new therapeutic strategies to shape the immunological response remains a major goal.

In line with those fundamental issues, we claimed two central objectives for this project:

- I) To modulate the allogeneic immune response in targeted skin tissue by circumventing systemic immunosuppression.
 - a. Developing a CD8 T cell specific depletion strategy by using near-infrared photoimmunotherapy.
 - b. Establishing a humanized mouse model of cutaneous aGVHD.
 - c. Localized ablation of CD8 T cells from aGVHD skin grafts, considering functionality and pathology.

- II) To investigate the pathomechanistic occurrence of necroptosis during cutaneous aGVHD.
 - a. Showing necroptotic signaling in aGVHD patients.
 - b. Unrevealing the extrinsic and intrinsic necroptotic signaling pathways in affected keratinocytes.
 - c. Prevention of cell death by therapeutical interference.

2 Material and Methods

2.1 Material

2.1.1 Antibodies for flow cytometry

Specificity	Host	Clone	Conjugation	Company	Dilution
CD3	Mouse	UCHT1	FITC	Beckman Coulter	1:50
CD4	Mouse	RPA-T4	BV452	BD Bioscience	1:50
CD8	Mouse	RPA-T8	APC-Fire	Biolegend	1:50
HLA-ABC	Mouse	PN IM1838	FITC	Beckman Coulter	1:20
HLA-DR	Mouse	L243	PE-Cy7	Biolegend	1:50

2.1.2 Reagents for flow cytometry

Product	Company	Catalogue	Dilution
Propidium Iodide	BD Pharmingen	51-66211E	1:100
Apotracker green	Biolegend	427402	1:200
Counting Beads	Thermo Fisher	C36950	50 µl/sample

2.1.3 Antibodies for depletion and neutralization

Specificity	Host	Clone	Company	Dilution
Gr1	Rat	RB6-8C5	Biolegend	100 µg/mouse
CD8	Mouse	HIT8 α	Biolegend	3 µg/ml
IFN γ	Mouse	B133.5	BioXCell	25 µg/ml

2.1.4 Antibodies for histology

Specificity	Host	Clone	Company	Dilution
Ki67	Mouse	MIB-1	Dako	1:70
CD31	Mouse	H-3	Santa Cruz	1:250
CD45	Mouse	HI30	Biolegend	1:250
CD4	Rabbit	EPR6855	Abcam	1:400
CD8	Rabbit	EP1150	Abcam	1:400
Elafin	Rabbit	Polyclonal	Novus Biologicals	1:400
Granzyme B	Mouse	2C5	Santa Cruz	1:300
T-bet	Rabbit	D6N8B	Cell Signaling	1:1000
pStat1	Rabbit	58D6	Cell Signaling	1:800
ZBP1	Rabbit	Polyclonal	Atlas Antibodies	1:1500
MLKL	Rabbit	EPR17514	Abcam	1:400
pMLKL	Rabbit	EPR9514	Abcam	1:250
Anti-mouse AF488	Donkey	Polyclonal	Dianova	1:400

Anti-rabbit AF647 Donkey Polyclonal Dianova 1:400

2.1.5 Histology kits and reagents

Product	Company	Catalogue
Dako REAL detection system	Dako	K5005
TUNEL assay kit	Abcam	ab206386
DAPI	Sigma Aldrich	10236276001
Roti-Histol	Carl Roth	6640.5
Target retrieval solution	Dako	S1699
EDTA	Appllichem	A2937
Eosin	Sigma Aldrich	E4009
Mayer's Hemalum	Merck	109249
Hematoxylin Gill 3	Thermo Scientific	6765009
Aqueous mounting medium	Merck	108562
Xylene based mounting medium	Consul Mount	9990440
Tween 20	Gerbu Biotechnik	2001,0500

2.1.6 Antibodies for western blot

Specificity	Host	Clone	Company	Concentration
β -actin-HRP	Mouse	sc-47778	Santa Cruz	1 μ g/ml
GAPDH	Mouse	sc-47724	Santa Cruz	1 μ g/ml
ZBP1	Rabbit	60968	Cell Signaling	1 μ g/ml
STAT1	Rabbit	D1K9Y	Cell Signaling	1 μ g/ml
pSTAT1	Rabbit	58D6	Cell Signaling	1 μ g/ml
RIP1	Rabbit	E8S7U	Cell Signaling	1 μ g/ml
pRIP1	Rabbit	E9K2A	Cell Signaling	1 μ g/ml
RIP3	Rabbit	D4G2A	Cell Signaling	1 μ g/ml
pRIP3	Rabbit	D6W2T	Cell Signaling	1 μ g/ml
MLKL	Rabbit	D2I6N	Cell Signaling	1 μ g/ml
pMLKL	Rabbit	EPR9514	Abcam	1 μ g/ml
CC3	Rabbit	5A1E	Cell Signaling	2 μ g/ml
Anti-rabbit-HRP	Goat	Polyclonal	Dianova	0,2 μ g/ml
Anti-mouse-HRP	Goat	Polyclonal	Dianova	0,13 μ g/ml

2.1.7 Western Blot kits and reagents

Product	Company	Catalogue
BCA Protein Assay	Thermo Fisher Scientific	23225
Qproteome Cell Compartment Kit	Qiagen	37502
ProSieve Color Protein Marker	Lonza	830537

Protease Inhibitor	Sigma Aldrich	11836153001
Phosphatase inhibitor	Sigma Aldrich	4906845001
ECL Substrate	GE Healthcare	RPN2235

2.1.8 Enzyme-linked Immunosorbent Assay (ELISA) kits

Product	Company	Catalogue
IFN γ ELISA Set	BD Bioscience	555142
RIP3 ELISA Kit	Cusabio	CSB-EL019737HU

2.1.9 Cell lines

Name	Organism	Cell type	Properties	Media	Provider
NHEK	Homo sapiens, Juvenile pooled	Keratinocytes	Adherent	Keratinocyte Growth Media 2	PromoCell

2.1.10 Media

RPMI w/ and w/o phenol:	RPMI 1640 Media, 2 mM L-glutamine, 1% Penicillin/Streptomycin, 1x MEM amino acids, 1 mM sodium pyruvate (Life Technology)
DMEM	20 mM L-Glutamin, 1 mM Na-Pyrovat, 10 mM Hepes, 1% Penicillin/Streptomycin (Life Technology)

2.1.11 Cell culture reagents

Product	Company	Catalogue
Fetal calf serum	Sigma	F7524
Phosphate buffered saline (PBS)	Thermo Fisher	14190144
Biocoll separation solution	Biochrom	L6115
Penicillin/Streptomycin	GE Healthcare	P11-010
Trypan Blue	Thermo Fisher	15250-061
Cryomedium (Cryo-SFM)	PromoCell	C-29912
Hepes BSS	PromoCell	C40010
0.04% Trypsin/0.03% EDTA	PromoCell	C-41010
0.05% Trypsin Inhibitor, 0.1% BSA	PromoCell	C-41110

2.1.12 Magnetic activated cell sorting (MACS)

Product	Company	Catalogue
LS columns	Mitenyi	130-042-401
CD8+ T cell isolation kit	Mitenyi	130-096-495

2.1.13 Oligonucleotides

Gene	Forward Sequence	Reverse Sequence
hSTAT1	AGCTTGACTCAAATTCCTG	CCAGTCTTGCTTTTCTAACC
hZBP1	GATTCTGGAAGAAGAGCAAAG	GAGACTGTCTGTCTTGTAAATG
hRIPK1	TGATAATACCACTAGTCTGACG	ACAGTTTTTCCAGTGCTTTC
hRIPK3	AACTTTCAGAAACCAGATGC	GTTGTATATGTTAACGAGCGG
hMLKL	GTGAAGAATGTGAAGACTGG	AAGATTTTCATCCACAGAGGG
hCXCL9	AGGGTCAGCCAAAAGAAAAG	TGAAGTGGTCTCTTATGTAGTC
hCXCL10	AAAGCAGTTAGCAAGGAAAG	TCATTGGTCACCTTTTAGTG
hCASP3	AAAGCACTGGAATGACATC	CGCATCAATTCCACAATTTTC
hCASP8	CTACAGGGTCATGCTCTATC	ATTTGGAGATTTCTCTTTC
hTBP	AGTGAGGTCGGGCAGGTT	AGAAACAGTGATGCTGGGTC

2.1.14 qRT-PCR Kits and reagents

Product	Company	Catalogue
QuantiTect Reverse Transcription Kit	Qiagen	205311
QantiRect SYBR Green PCR Kit	Qiagen	204145
pegGOLD TriFast	VWR	30-2010

2.1.15 Biological compounds

Product	Company	Catalogue
Ketamin/Xylazin	Sigma Aldrich	1002702317
Ringer Solution	B. Braun	3570010
NHS-700DX	Li-Cor Biosciences	P/N 92970010
Recombinant IFN γ	Immunotools	11343536
Recombinant TNF α	Immunotools	11343015
Z-VAD(OMe)-FMK	Santa Cruz	187389-52-2
Staurosporin	Santa Cruz	sc-3510
GSK'872	Sigma Aldrich	530389
Tofacitinib citrate	Sigma Aldrich	PZ0017
Normal donkey serum	Dianova	017-000-121
Fetal bovine serum	Sigma Aldrich	F7524

2.1.16 Buffers and solutions

Buffer	Composition
PBS	137 mM NaCl, 2.7 mM H ₂ PO ₄ , pH 7.4
TBS	50 mM Tris, 150 mM NaCl, pH 7.5
TBS-Tween (TBS-T)	TBS + 0.05% Tween 20
PBS/EDTA	PBS + 2 mM EDTA

MACS buffer	PBS + 2.5% human albumin + 2 mM EDTA
FACS buffer	PBS + 2.5% human albumin + 2 mM EDTA + 0.1% sodium azide
K ₂ HPO ₄	1 M Potassium Phosphate buffer, pH 9
Blocking buffer (IF/(IHC))	TBS + 0.5% (v/v) donkey or goat serum
Blocking buffer (WB)	TBS + 5% (w/v) BSA / 5% (w/v) non-fat milk powder
RIPA lysis buffer	50 mM Tris, 150 mM NaCl, 2 mM EDTA, 0.5% (v/v) Na deoxycholate, 1% (v/v) NP-40, 0.1 (v/v) SDS, pH 8, Protease/Phosphatase inhibitors
SDS sample buffer	0.15 M Tris, 1.2% (v/v) SCS, 4 mM glycerol, 2 mM β-mercaptoethanol, 0.02 μM bromphenolblue, pH 6.8
SDS running buffer	2.5 M Tris, 192 mM glycine, 0.1% (v/v) SDS
Transfer buffer	47 mM Tris, 20% (v/v) methanol, 1.3 mM SDS, 34 mM glycine
Stripping buffer	2 % (w/v) SDS, 6.3% 1M Tris (pH 6.7), 0.7% (v/v) β-mercaptoethanol

2.1.17 Laboratory instruments

Instrument	Commercial Name	Company
Centrifuge	Z233 MK-2	Hermle
Centrifuge	Rotina 420R	Hettich
Centrifuge	Multifuge 3S-R	Heraeus
Counting chamber	Neubauer Improved	Neolab Migge
Incubator	MCO-20AIC	Sanyo
Multiplate ELISA Reader	Multiskan EX	Thermo Fisher
Flow Cytometer	Gallios 4L	Beckman Coulter
Microtome	Slide 2003	Pfm medical
Brightfield microscope	Axioskop 40	Zeiss
Brightfield microscope	Leica DM IRB	Leica
Fluorescence microscope	Leica DM 5500 B	Leica
Imaging System	iBright FL 1500	Invitrogen
Standardized Light-Emitting Diode for PIT		Kindly provided by Prof. Dr. Rodewald
Thermocycler	T Gradient	Biometra
Real Time PCR System	StepOnePlus System	Applied Biosystems
Blot Modul	XCell Sure Lock	Invitrogen
Tissue homogenizer	TissueLyser LT	Qiagen
Nanodrop	DS-11 FX+	DeNovix

2.2. Methods

2.2.1 Study approval

The present study was approved by the ethics committee of the University of Heidelberg and conducted according to ethical principles stated in the Declaration of Helsinki (S-305/2010 and S-306/2010). Included animal studies were performed according to ethical guidelines applied by the Heidelberg Interfaculty Biomedical Faculty (G-47/19).

2.2.2 Antibody conjugation

Antibody conjugation was performed as instructed by the manufacturer. The commercial mAb targeting CD8 (HIT8 α) was dialyzed in PBS to remove containing sodium azide and BSA. Therefore, mAb solution was transferred into a dialysis tube (exclusion 10 kDa) and incubated in 5 l rotating PBS at 4°C. The buffer was exchanged twice after 4 h and then dialyzed overnight. Due to potential volume increase following dialysis, protein concentrations were measured by BCA. To obtain optimal conjugation efficiency, the pH value was increased from 7.5 to 8.5 by the addition of 10% (v/v) K₂PO₄ (pH 9). Purified CD8 mAb was conjugated with 4 mol NHS-700DX photosensitizer (per mol mAb at 4°C overnight). Following conjugation, repeated purification steps were performed by dialysis, as described above. Conjugated mAb is referred as CD8-IR700.

2.2.3 Blood samples

Sera from HCT patients and healthy donors were purified from peripheral blood whereas peripheral blood mononuclear cells (PBMCs) were isolated from buffy coats of healthy donors. For the latter, blood samples were layered on Biocoll solution and separated by gradient centrifugation. Following withdrawal of the PBMCs-containing interface and repeated washing steps (twice with PBS/EDTA), PBMCs were quantified and transferred to cell culture medium⁹⁶.

2.2.4 *In vitro* depletion

Ablation efficiency and specificity of NIR-PIT was determined by using CD8 T cell targeted PBMC. For this purpose, 0.5x10⁶ petri dish-plated leukocytes were stained with CD8-IR700 (3 μ g) for 30min at 37°C in RPMI phenol-free medium. Following incubation, PBMCs were irradiated with 22 J/cm² (60s) NIR light by using a NIR light-emitting diode. Upon treatment, cell numbers were compared to untreated control by flow cytometry^{97, 77}.

2.2.5 Flow cytometry

PBMCs were surface stained in FACS buffer for 15min at 4°C with an antibody cocktail and washed afterwards. Shortly before measuring, propidium iodide (PI) and counting beads

were added to the cell suspension in the context of NIR-PIT experiments. Keratinocytes were antibody surface stained in PBS for 15min at 4°C or by apotracker green for 20min at RT and subsequently washed. Again, PI was added shortly before measuring.

2.2.6 Skin samples

Formalin-fixed and paraffin embedded skin punch biopsies from aGVHD patients were provided by the Institute of Pathology of the University Hospital Heidelberg and were used for histopathological analysis. Leftover healthy human split skins of autologous skin transplantation were obtained from residential operations and were used for mouse transplantation and *ex vivo* experiments. Fresh skin punch biopsies (6 mm diameter) from aGVHD patients were taken under local anesthesia at the Department of Hematology and Oncology of the University Hospital Heidelberg. Half of the sample was fixed in formalin and used for histopathological analysis. The other half of a tissue was snap frozen in liquid nitrogen for subsequently RNA extraction.

2.2.7 Mouse model

NOD.Cg-Prkdc^{scid} Il2rg^{tm1Wjl}/SzJ (NSG) mice originally purchased from Charles River Laboratories (France) were in house bred at the Heidelberg Interfaculty Biomedical Faculty (Breeding line 2257). Healthy human split skins were transferred into RPMI medium (serum free) containing antibiotics and cut into pieces of 1 cm². Transplantations were performed under sterile conditions. Therefore, NSG mice were anesthetized with ketamine/xylazine shaved and disinfected. Back skin of similar size as the human graft was removed by surgery and replaced by the human skin. Human skin grafts were fixed by sutures and covered with gauze for 7d protected by a skin fold. Subsequently, 3x10⁷ mismatched PBMCs, obtained from healthy buffy coats, were adoptively transferred intravenously (i.v.) on day 7 post transplantation. Following skin engraftment for 13d or 20d in the delayed GVHD model, mice were injected with 100 µg Gr1 mAb intra peritoneal (i.p.) to deplete mouse inflammatory Ly6C monocytes and Ly6G neutrophils. This depletion prevents possible FcR-dependent ADCC.

One day after Gr1 injection, mice received conjugated CD8-IR700 (3 mg/kg) i.v.. Following systemic distribution for 24h, mice were anesthetized and irradiated with 100 J/cm² (252s) NIR light (690 nm), which was restricted to the human skin graft. During irradiation mice were cooled with conventional ventilation. NIR light treatments were repeated 48h and 72h after CD8-IR700 injection (each time 100 J/cm²). Terminally, skin grafts and spleens were dissected three days following the final light treatment that were processed for further analysis.

2.2.8 CD8 T cell transfer experiments

For transfer experiments, CD8 T cells were isolated from healthy PBMCs using negative MACS purification. Cells were handled according to manufacturer's instructions. The state of purity of isolated T cells was controlled by flow cytometry. According to the CD8 T cell frequency among PBMCs⁹⁸, 7×10^6 isolated cells were transferred i.v. to human skin graft NSG mice 7d after transplantation. Spleen and skin were dissected 20d after skin transplantation and analyzed by histology.

2.2.9 Histology

Skin and spleen samples were fixed in 4% formalin for 24h following dissection and subsequently embedded in paraffin. For immunofluorescence (IF) and immunohistochemistry (IHC) 2 μm and for hematoxylin and eosin (H&E) 7 μm thick sections were sliced and dried for 15min at 90°C. Deparaffination was achieved by repeated xylene incubation. Rehydration was performed with decreasing concentrations of ethanol (100%, 96%, 70%) with a final incubation in demineralized (VE) water. Heat-induced epitope retrieval was performed in citrate buffer (pH 6) or EDTA buffer (pH 9) for 25min in a conventional steamer. Lukewarm slides were briefly washed in VE water and incubated with blocking buffer (goat for IHC, donkey for IF) for 30min (every incubation step from here in a humidified chamber). Following blocking, sections were incubated with primary antibodies, diluted in blocking buffer over night at 4°C. For IHC staining, sections were processed with Dako Real™ Detection System Alkaline Phosphatase/RED Rabbit/Mouse including incubation steps with biotinylated secondary antibody, streptavidin-alkaline phosphatase and substrate-chromogen and handled according to the manufacturer's protocol. Following signal production, slides were then counterstained with hemalum in running tap water and mounted in water-based mounting medium. For IF staining, sections were incubated with fluorescence conjugated secondary antibodies for 30min at RT. Nuclei were stained with DAPI before mounting. For H&E staining, slides were deparaffinized and rehydrated as described above. Next, slides were incubated in hematoxylin and differentiated in a respective buffer. Following development in running tap water, slides were stained in eosin followed by dehydration with increasing concentrations of ethanol (70%, 96%, 100%) and xylene. Mounting was performed with a xylene based mounting medium. The images were captured with a Leica 5500 B microscope (Leica). Scale bars indicate 100 μm for 200 x, 25 μm for 400 x and 30 μm for 630 x magnification.

2.2.10 Cell culture

For *in vitro* experiments, normal human epidermal keratinocytes (NHEKs) were used up to passage ten. Therefore, cells were seeded (1×10^5 per well) in a 12-well plate in 2 ml of

KGM2 medium until they reached semi-confluence. For co-culture experiments, NHEK were stimulated with IFN γ (50 ng/ml) for 24h. Following pre-activation, NHEKs were washed twice (PBS) and cultured for 72h in a fresh medium (KGM2) containing 1×10^6 mismatched PBMCs per well (Ratio 1:10). Cultured NHEKs were washed twice (PBS) and collected using trypsin for viability assay or western blot analysis. To study cell death inhibition experiments, co-cultures or keratinocytes, treated with IFN γ (50 ng/ml) alone for 72h, were manipulated as followed: using 25 μ M Z-VAD(OMe)-FMK, different concentrations of GSK'872, tofacitinib or 25 μ g/ml IFN γ blocking antibody. Viability of NHEKs was measured by flow cytometry using apotracker/propidium iodide double staining.

2.2.11 Subcellular fractionation

Keratinocytes from *in vitro* experiments stimulated with IFN γ (50 ng/ml) were collected as described before and fractionized using a cell compartment kit and handled according to manufacturer's instructions. In brief, different solutions were used to destruct membrane integrity which ultimately separate cytosolic from membrane bound proteins. The different fractions were precipitated using ice-cold acetone and resuspended in RIPA buffer for further protein analysis.

2.2.12 Western Blot

Total proteins were isolated by incubation with RIPA buffer, containing protease and phosphatase inhibitors for 20min on ice. Upon lysis and centrifugation, protein yield was quantified by BCA from supernatants. Proteins were then diluted in sample buffer (1:5) and heated for 5min at 95°C before loading. Size separation was performed by gel electrophoresis using 8-12% resolving gel, depending on the protein of interest. Following separation, proteins were blotted on a methanol-activated nitrocellulose membrane and subsequently blocked with an appropriate buffer for 30min at RT. Thereupon, the membrane was incubated with primary antibody over night at 4°C. Upon secondary antibody incubation for 1h at RT, luminescence was developed using ECL-solution and detected by an iBright system. Loading control was assessed by 1h incubation using primary β -actin or GAPDH antibody.

2.2.13 Expression analysis

Snap frozen skin samples were thawed on ice and homogenized in TriFast using TissueLyzerLT and metallic beads for downstream RNA isolation. RNAs from cultured keratinocytes were directly isolated from TriFast. The purity and quantity of isolated RNA were measured by spectrophotometry. cDNA Reverse Transcription Kit was used to perform

reverse transcription from RNA to cDNA using random hexamers. The reactions were amplified and quantified by a SYBR green assay on an Applied Biosystem. The housekeeping human TATA-binding protein (*TBP*) gene was used to normalize the target genes. Datasets were analyzed by comparative ΔC_T , $\Delta\Delta C_T$ and $2^{-(\Delta\Delta C_T)}$ method with *TBP* as reference gene relative to healthy human skin, *in vitro* cultured keratinocytes or *ex vivo* cultured control skin depending on the experiment.

2.2.14 Enzyme-linked immunosorbent assay

Protein quantities of secreted IFN γ and extracellular RIP3 were measured from *in vitro* supernatants or serum samples from healthy controls and aGVHD patients using commercial kits. ELISA experiments were performed by Stefan Meisel according to the manufacturer's protocol. Here, target proteins were captured by plate bound antibodies and visualized by detection antibodies. Protein quantities were measured by photometry.

2.2.15 *Ex-vivo* organ culture

Human split skin was washed twice in PBS containing penicillin/streptomycin and cut in pieces of 1cm² size. Those pieces were sewed on a reversed strainer and inserted into a 6-well plate. Next, the wells were filled with DMEM medium (containing 10% bovine serum) to create an air-medium interface. The *ex-vivo* organ cultures were cultured for 72h in an incubator at 37°C containing 5% CO₂. To induce or prevent necroptotic signaling, IFN γ (500 ng/ml) and tofacitinib (10 μ M) were added to the culture medium immediately after start of the culture. Following culturing, samples were either formalin-fixed and paraffin embedded for histological analysis or snap-frozen for gene expression analysis.

2.2.16 Statistics

For *in vitro* CD8 depletion efficiency, cell numbers/ μ l of 6 independent PBMCs donors were compared using paired t-test analysis. For *in vivo* analysis, 5 independent experimental groups were used to quantify the depletion efficiency by immunofluorescence. Positive cells were counted in 3 visual fields (200x) per condition by 2 independent investigators in a blinded manner. Measurements were compared using one-way ANOVA followed by Kruskal-Wallis post-test and presented as mean \pm SEM. Viability of keratinocytes and serum levels of RIP3 following ECP treatment were compared using paired t-test analysis. Significance levels were defined as *p<0.05; **p<0.01; ***p<0.001. Western blot analysis from stimulation assays and co-culture experiments were performed and analyzed using a minimum of three experimental setups and independent PBMC donors.

3 Results

3.1 Characterization of cutaneous aGVHD

Upon allogeneic HCT, T cells preferentially infiltrate epithelial and sub-epithelial sides such as the epidermis and dermis in the skin, causing aGVHD. Due to their high expression of MHC-I and the secretion of chemoattractant molecules, keratinocytes are favorably attacked by infiltrating alloreactive T cells. Therefore, histopathological hallmarks of aGVHD and lichenoid cGVHD are mainly associated with keratinocyte cell death^{40, 99}. In comparison to healthy skin, aGVHD biopsies show typical manifestations of interface dermatitis with basal cell vacuolization, satellite necrosis, acanthosis and parakeratosis (Fig. 4a). It is well accepted that aGVHD is a T cell-driven disease due to its interaction with allogeneic MHC molecules. To confirm this, infiltrating T cells were marked in sections of aGVHD. Here, high numbers of activated CD8 T cells were found, preferentially located in the epidermis. The activation status of those dermal and intraepithelial CD8 T cells were highlighted by increased granzyme B production with polarized vesicles at the inner and outer cell membrane, indicating lytic granule exocytosis (Fig. 4b). In addition, high numbers of CD4 T cells were found preferentially located at subepidermal sites (Fig. 4b). As a consequence of the cytotoxic and inflammatory response by the infiltrating alloreactive leukocytes, increased numbers of dead keratinocytes could be detected in those skin lesions (Fig 4c). Moreover, expression of elafin, as the accepted biomarker of cutaneous aGVHD, was detectable in great depth of lesional keratinocyte layers (Fig 4c).

3.2 NIR-PIT in cutaneous aGVHD

3.2.1 Targeting CD8 T cells by NIR-PIT

Due to the pathological importance of CD8 T cells, mediated by their cytotoxic and inflammatory reactivity directed against allogeneic MHC-I-expressing keratinocytes, CD8 T cells were targeted by NIR-PIT. Therefore, a non-depleting mAb targeting human CD8 was conjugated to a NIR-reactive photosensitizer called IRDye-700DX. Followed by binding of CD8-IR700 to its unique antigen, detection of CD8 T cells by RPA-T8 was still possible under saturated conditions, ensuring depletion efficiency (Fig 5b). Next, CD8 T cells were depleted from a cellular conglomerate of PBMCs. Therefore, culture plate seeded PBMCs were incubated with CD8-IR700, followed by exposure to 22 J/cm² NIR light *in vitro* (Fig. 5c). Unbound cells such as CD4 T cells, which are in close proximity to the targeted CD8 T cells, remained unchanged (Fig. 5d). Noteworthy is the efficiency of absolute ablation of targeted CD8 T cells by NIR-PIT. Moreover, T cell toxicity by NIR light irradiation can be excluded since CD4 T cell numbers remained unchanged (Fig. 5 a-d).

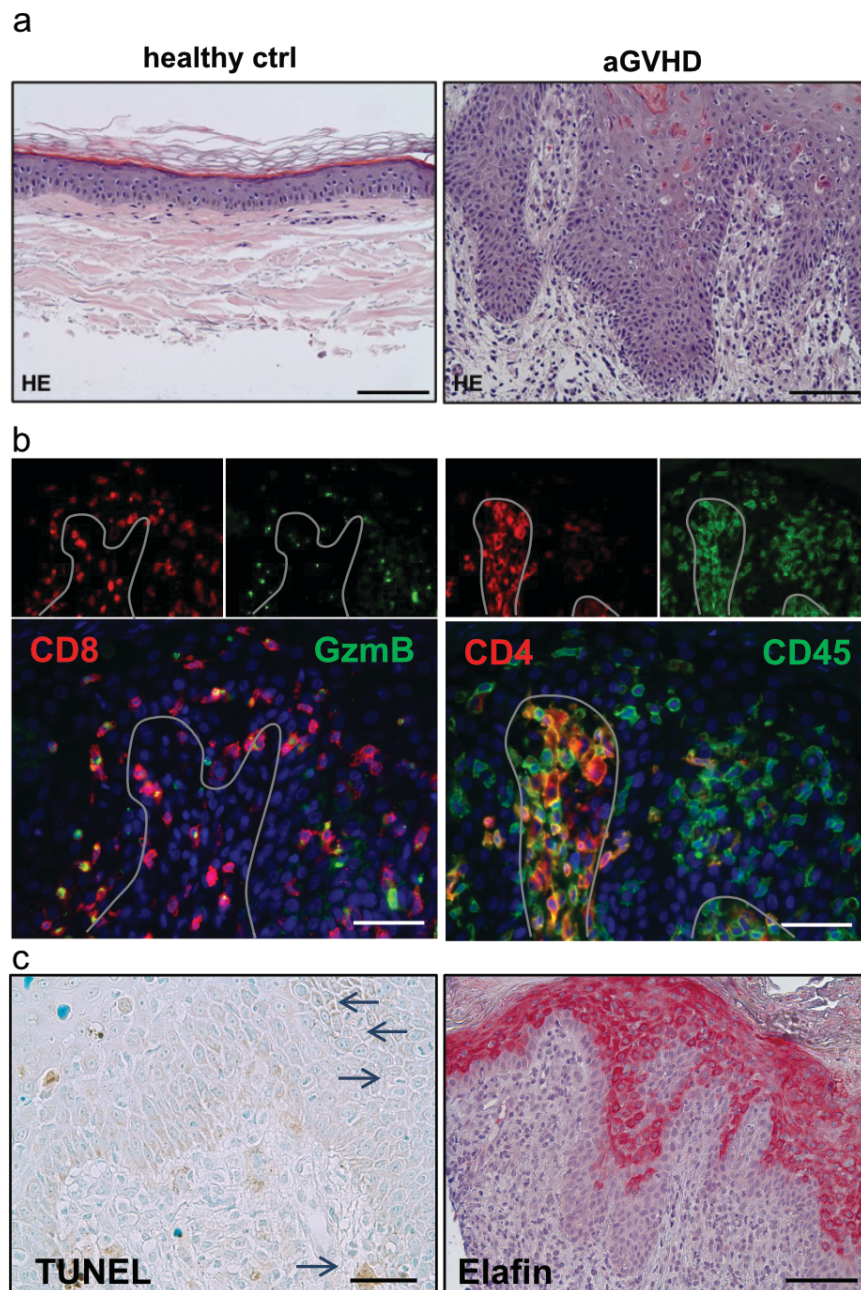


Fig. 4: Skin manifestations of aGVHD. **a)** Shows H&E staining of FFPE skin biopsies from healthy donor and aGVHD patient. **b-c)** Skin sections of a representative aGVHD patient (grade II-III) were analyzed by IF double staining targeting CD8 combined with granzyme B and CD4 together with CD45 (**b**) and by IHC targeting elafin as well as by TUNEL-assay (**c**). (Published and modified from Freund et al. 2019¹⁰⁰)

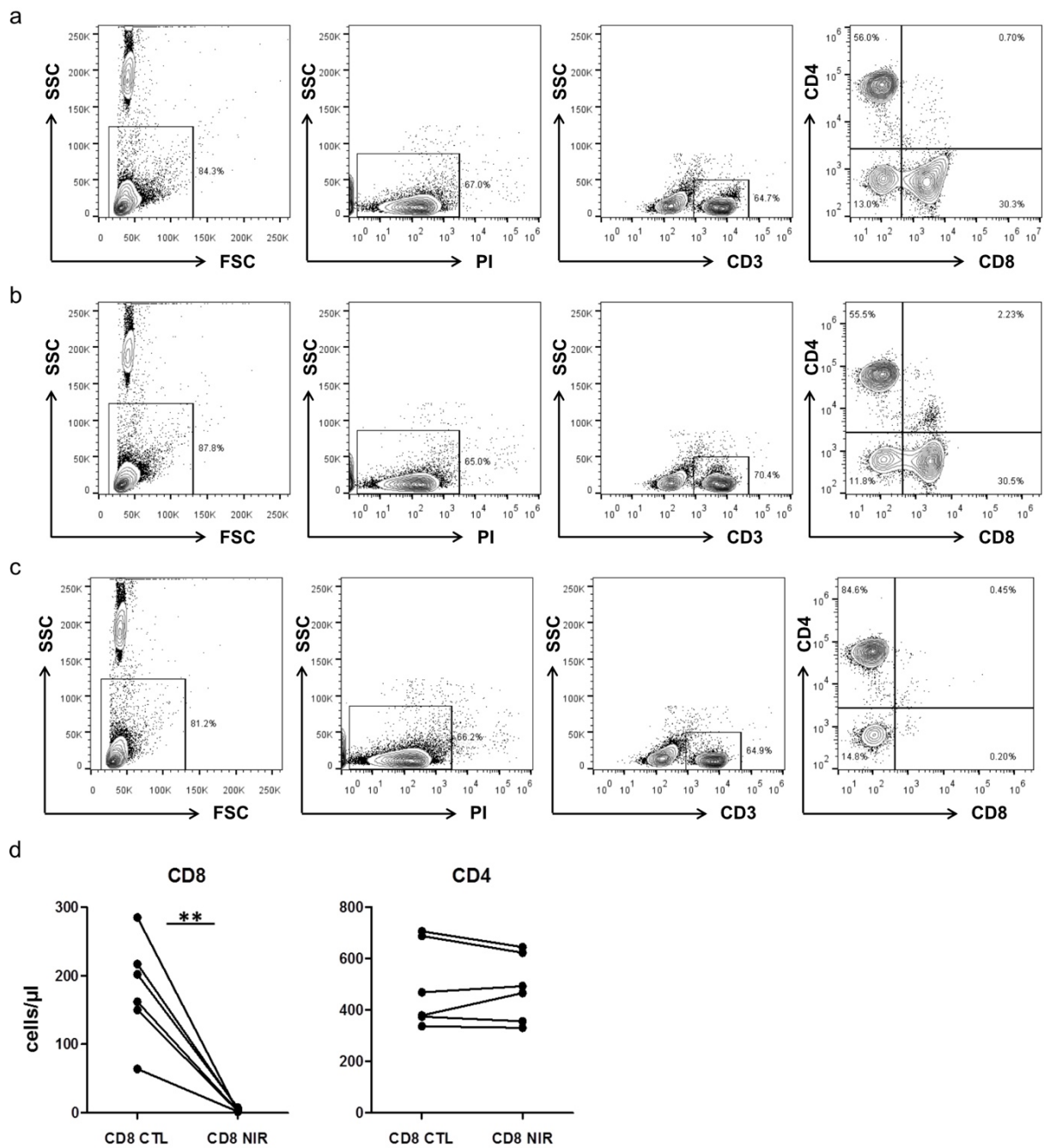


Fig. 5: Characterization of CD8-targeted NIR-PIT. a-d) PBMCs isolated from buffy coats were surface stained with the antibody mix as indicated and analyzed by flow cytometry. a) Shows control staining of PBMCs revealing reference frequencies and cell numbers of targeted populations in comparison to PBMCs that were stained b) with CD8-IR700 in addition and c) stained with CD8-IR700 and treated with 60s NIR light in addition. d) Displays absolute cell numbers of CD8-IR700 stained PBMCs showing CD3 CD8 T cells and CD3 CD4 T cells detected by counting beads before and after treatment with NIR light. (Published and modified from Freund et al. 2019¹⁰⁰)

3.2.2 Mouse model of humanized cutaneous aGVHD

The usage of a humanized cutaneous aGVHD mouse model enabled the investigation and suitability of NIR-PIT in the context of inflammatory skin diseases and moreover by targeting CD8 T cells to study their pathogenetic role in cutaneous aGVHD. In this context, immunodeficient NSG mice were reported to engraft human PBMCs and solid organs; therefore, they represent an ideal experimental model to answer the stated objectives (Fig. 6a). Kinetic investigations revealed that human split skin transplants (300-500 μm thickness) were fully engrafted within 14d, thereby showing human epidermal/dermal structures with murine sub-cutaneous connection. Moreover, proliferating basal keratinocytes (Ki67), revascularization by endothelial cells (CD31) and scattered engrafted leukocytes (CD45) were detectable 14d after transplantation by human-specific antibodies (Fig. 6b).

To minimize the inflammatory effects induced by infiltrating murine leukocytes, neutrophils were depleted by injection of Gr1 mAb targeting Ly6G-expressing granulocytes and Ly6C-expressing monocytes one day before therapy initiation⁶⁷ (Fig. 7a). Kinetic studies revealed that prominent cutaneous aGVHD manifested already one week after mismatched PBMCs injection. Exemplary, on day 15 post skin transplantation, tissue sections showed phenotypical signs of interface dermatitis (IFD) with a band-like infiltration, satellite structures, basal-cell vacuolization, pyknotic and dead keratinocytes (Fig. 7b and c). Moreover, strong expression of elafin in the suprabasal keratinocyte layers indicate inflammatory reactions reflecting cutaneous aGVHD (Fig. 7c). The cellular composition of infiltrating cells mainly consisted of human CD8 and CD4 T cells. Here, CD8 T cells showed a strong activation status through enriched cytotoxic granules with polarized membrane structures, indicating perforin/granzyme B exocytosis (Fig. 7d). In comparison, these histopathological observations reflect the described features seen in aGVHD sections from HCT patients (Fig. 4). Similarly, on day 14, 16 and 17, phenotypical aGVHD could be detected in the respective transplants (data not shown), thus confirming the described observations.

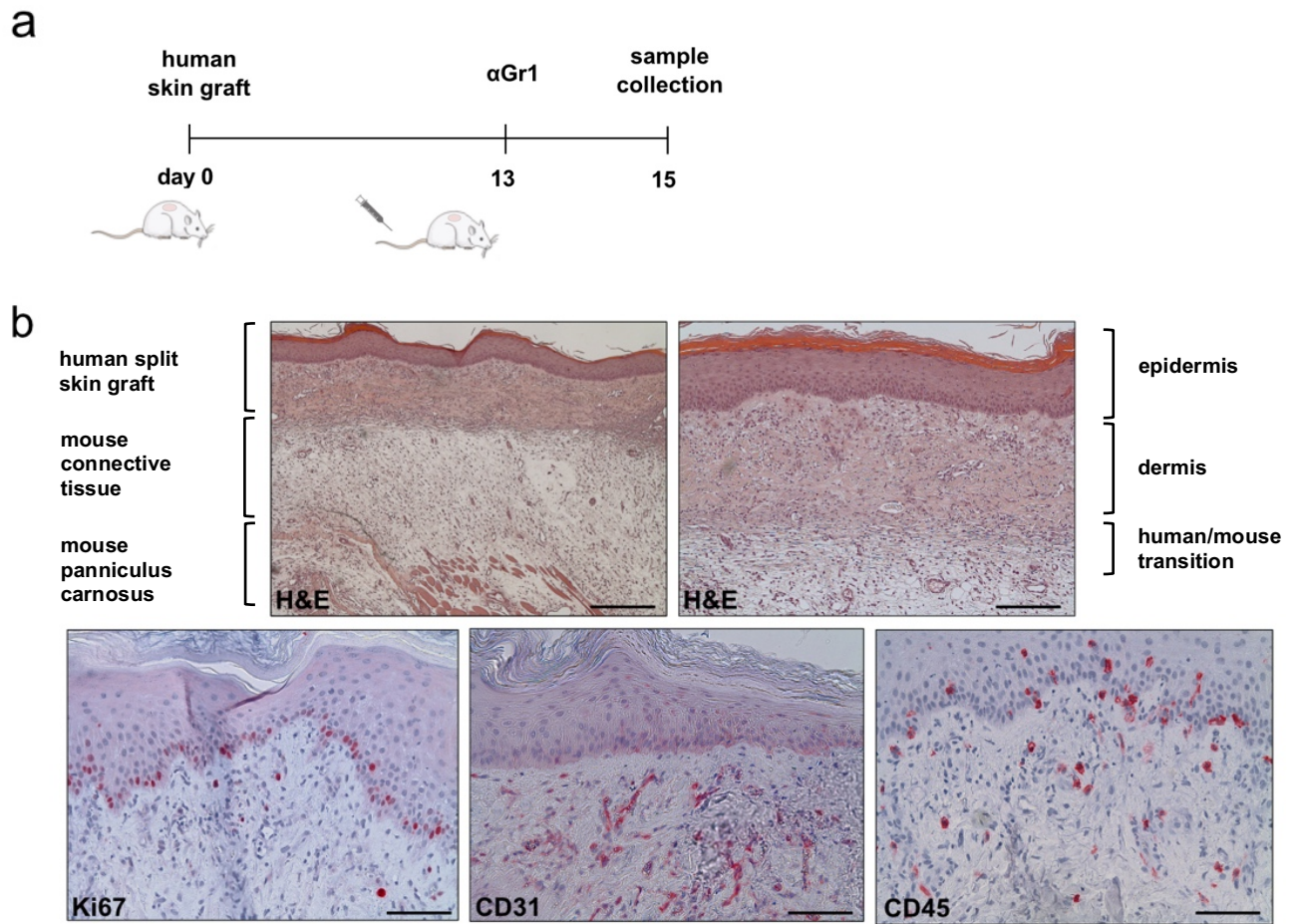


Fig. 6: Skin xenograft mouse model. a) Schematic depiction of experimental humanized skin graft mouse model. b) Sections of skin xenografts from day 14 post transplantation were analyzed in by H&E staining (upper row) and IHC staining for human Ki67, CD31 and CD45 (lower row).

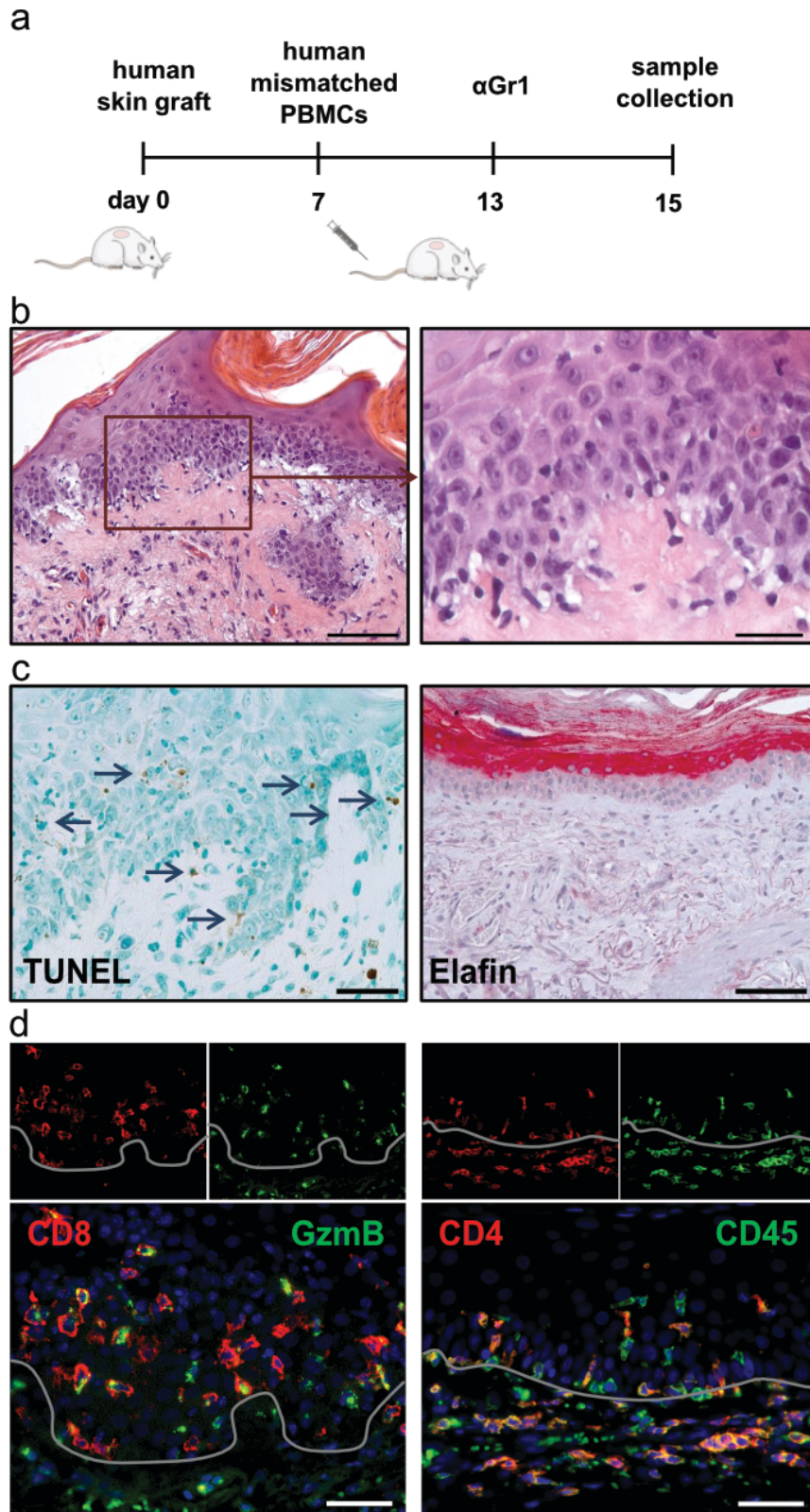


Fig. 7: aGVHD mouse model. **a)** Schematic depiction of experimental humanized aGVHD mouse model treated with anti-CD8 NIR-PIT. **b-c)** Sections of cutaneous aGVHD xenografts from day 15 post skin transplantation were analyzed in **b)** by H&E staining, **c)** by TUNEL-assay and IHC targeting elafin expression and **d)** by IF double staining targeting CD8 combined with granzyme B and CD4 together with CD45. (Published in Freund et al. 2019 ¹⁰⁰)

3.2.3 CD8 NIR-PIT prevents histopathology of cutaneous aGVHD

Based on the pathological manifestations seen one week after injection of mismatched PBMCs in the skin, CD8-directed NIR-PIT therapy (100 J/cm^2) was started on day 15 post skin transplantation with initial CD8-IR700 injection on day 14. Repeated irradiations with NIR light on day 16 and 17 (each 100 J/cm^2) post skin transplantation aimed to efficiently deplete skin-localized CD8 T cells. Therapeutical efficiency was assessed following three resting days (day 20 post skin transplantation) (Fig. 8a). First, histopathology of transplanted control and aGVHD skin grafts were evaluated by H&E staining. Mice that received skin grafts without aGVHD induction, depicting reference skin grafts, showed phenotypical normal histology comparable to normal healthy skin (Fig 8b, ctrl). In contrast, mice with cutaneous aGVHD (skin graft plus PBMCs) that received a non-depleting CD8-IR700 displayed phenotypical disease specific histopathology. Hallmarks of aGVHD including interface dermatitis with band-like infiltrations, basal cell vacuolization, satellite structures, pyknotic keratinocytes, acanthosis and parakeratosis were all clearly visible (Fig 8b, GVHD α CD8). In relation, mice that received CD8-IR700 and were treated with NIR light additionally showed completely abolished histopathology in the respective skin sections, reflecting those from control skin grafts (Fig 8b, GVHD α CD8 NIR). Of note, these results indicated that CD8-IR700 alone without NIR light treatment did not inhibit phenotypical cutaneous aGVHD, but the combination did.

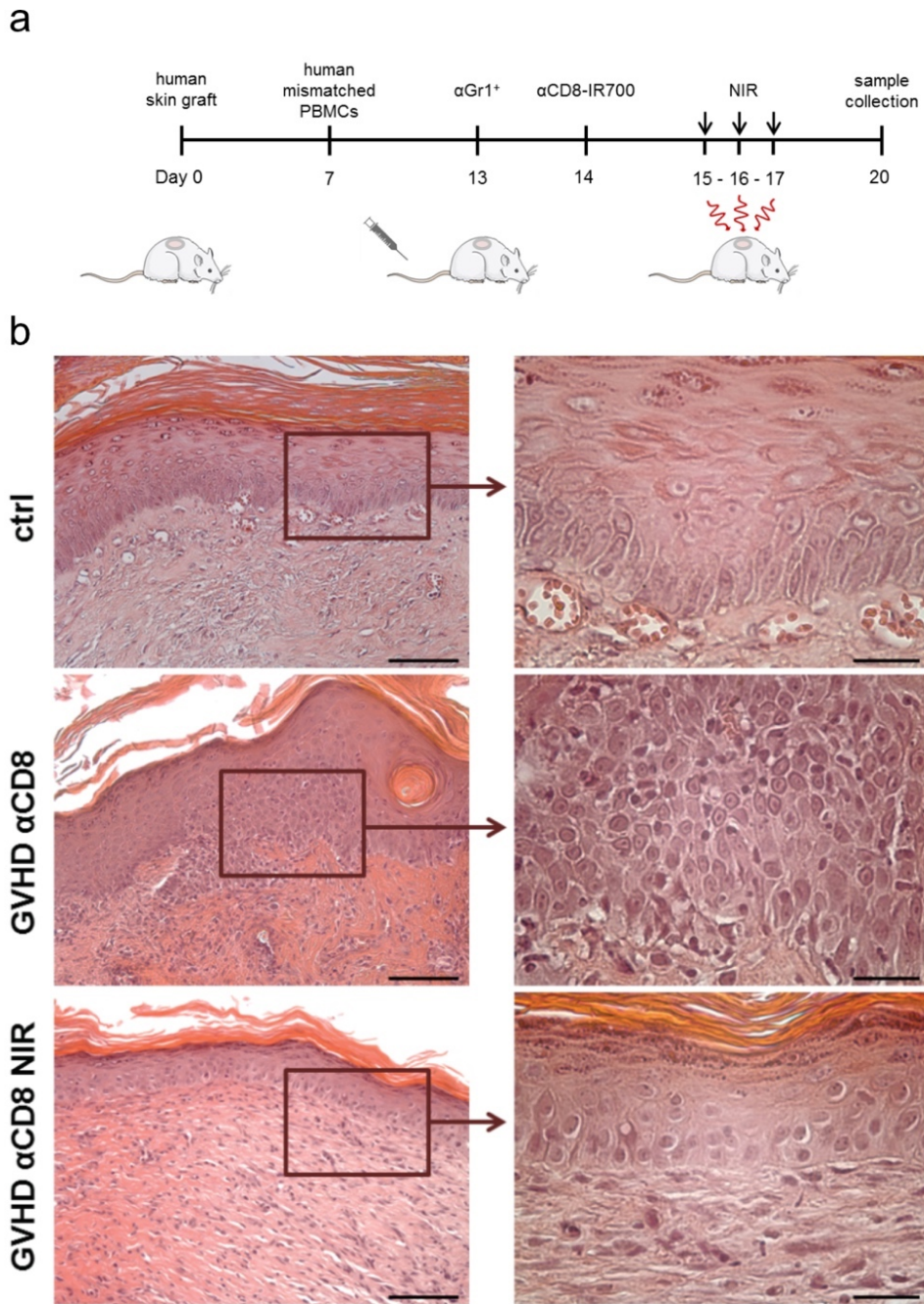


Fig. 8: Effects of localized CD8 NIR-PIT. **a)** Schematic depiction of experimental humanized skin graft mouse model. **b)** Displays representative tissue images from skin xenograft mice alone (ctrl), mice with cutaneous aGVHD that received CD8-IR700 (GVHD α CD8) as a control and of cutaneous aGVHD mice that were treated with CD8 NIR-PIT (GVHD α CD8 NIR). Skin sections were stained using H&E method. (Published in Freund et al. 2019¹⁰⁰)

3.2.4 NIR-PIT ablates targeted skin CD8 T cells thereby inhibiting cutaneous aGVHD

Based on the results seen by H&E staining (Fig. 8), cellular analysis of infiltrating allogeneic T cells and downstream response markers were assessed in the transplanted human skin grafts. Skin grafts of mice without cutaneous aGVHD that did not receive mismatched PBMCs served as base-line references. These skin grafts presented only few numbers of skin localized human CD45-expressing CD8 and CD4 T cells, distributed in dermis and epidermis. In these mice, CD8 T cells displayed only little cytoplasmic granzyme B staining, indicating low numbers of lytic granules and cytotoxic activity (Fig. 9a). Hence, engrafted keratinocytes appeared vital and did not express elafin (Fig. 9b). Comparing these results to skin grafts of mice that received mismatched PBMCs showed increased numbers of infiltrating human CD45-expressing CD8 and CD4 T cells, localizing at the dermal-epidermal junction. Moreover, CD8 T cells showed high reactivity by increased expression of granzyme B-containing cytotoxic granules. Furthermore, their polarized granule structures indicated lytic exocytosis (Fig. 9c). Viability analysis revealed that numerous cells in the basal and suprabasal layers showed DNA fragmentation demonstrating increased keratinocyte cell death (Fig. 9d). In addition, elafin, as the response marker to inflammation, was strongly produced by the affected keratinocytes, several layers in depth (terminally differentiated corneocytes to less differentiated keratinocytes) (Fig. 9d). Similar results were obtained from mice with aGVHD that received CD8-IR700 alone or which were treated with NIR light alone, both for control. In the experimental setups, cellular phenotyping revealed a strong unchanged infiltration and reactivity of CD8 T cells and CD4 T cells (Fig. 10a and c). In addition, increased cell death and elafin expression were detectable in several epidermal layers, comparable to those of untreated cutaneous aGVHD mice (Fig. 10b and d). These results obtained from IF data confirmed the previous observations by histology. CD8-IR700 alone does not deplete and thereby inhibit cutaneous aGVHD. Moreover, NIR light treatment alone appears to be harmless to the skin neither by induction of increased cell death or inflammation nor does it cause unspecific CD8 T cell depletion.

Finally, when cutaneous aGVHD mice were treated with NIR-PIT, CD8 T cells were completely absent in human skin grafts, demonstrating efficient and sustainable depletion. In addition, lytic granules that regularly co-localize with cytotoxic CD8 T cells were highly reduced or absent in the respective skin sections (Fig. 11a). Again, to exclude antigen masking by CD8-IR700, phenotyping of CD4 T cells revealed that all skin-localized human CD45 expressing leukocytes co-expressed CD4, in turn demonstrating complete absence of CD8 T cells. Interestingly, CD8 T cell ablation led to an altered dermal infiltration of CD4 T cells (Fig. 11a and c). Consequentially, due to the alterations mediated by CD8 T cell ablation, epidermal cell death and elafin expression were reversed, resembling normal

keratinocyte physiology and therefore comparable to those of skin grafts from control mice without cutaneous aGVHD (Fig. 11b).

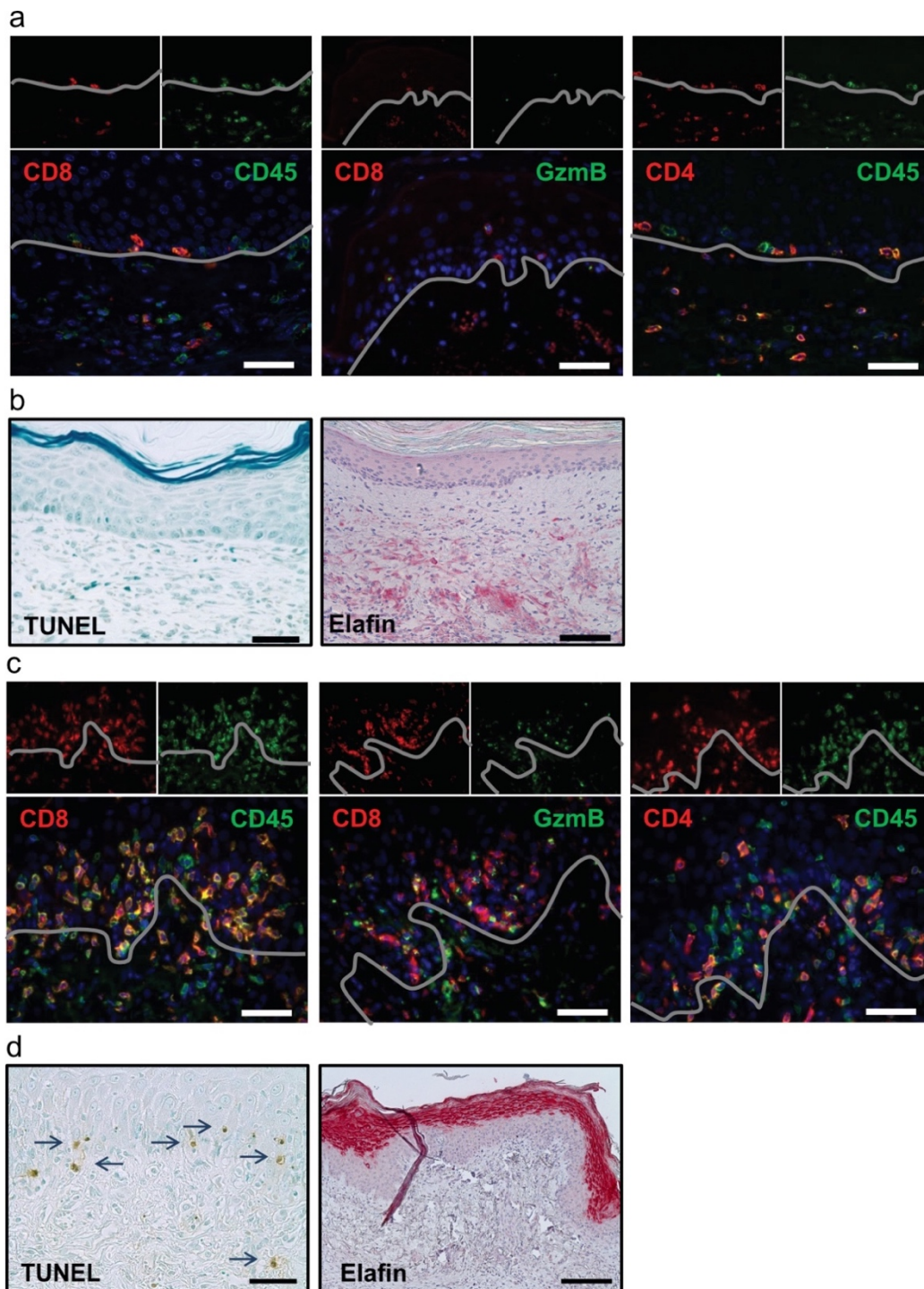


Fig. 9: Characterization of humanized cutaneous aGVHD. a-d) Displays representative skin images from skin xenograft mice alone (a-b) and skin xenograft mice with cutaneous GVHD (c-d) all from day 20 post skin transplantation (n=5). a and c) Skin sections were stained by IF double staining targeting CD8 or CD4 combined with CD45 or granzyme B. b and d) Skin sections were stained by IHC using anti-elafin and processed by TUNEL-assay. (Published and modified from Freund et al. 2019¹⁰⁰)

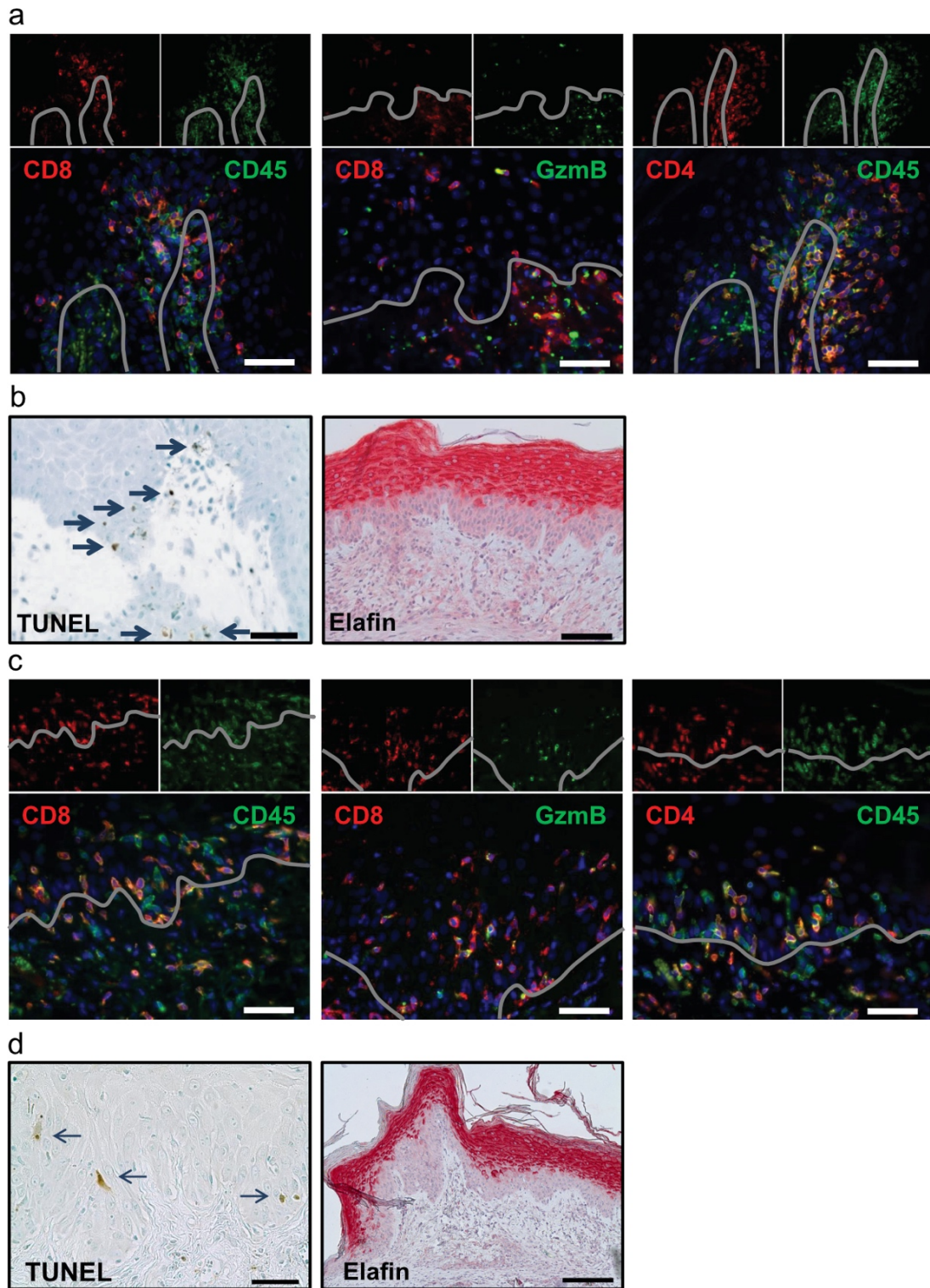


Fig. 10: Effects of CD8-IR700 or NIR light treatment alone. a-d) Shown are representative skin images from cutaneous aGVHD skin xenograft mice treated with CD8-IR700 (n=5) (a-b) or NIR light (n=3) (c-d) all from day 20 post skin transplantation. **a and c)** Skin sections were stained by IF double staining targeting CD8 or CD4 in combination with CD45 or granzyme B. **b and d)** Skin sections were stained by IHC using anti-elafin and processed by TUNEL-assay. (Published and modified from Freund et al. 2019¹⁰⁰)

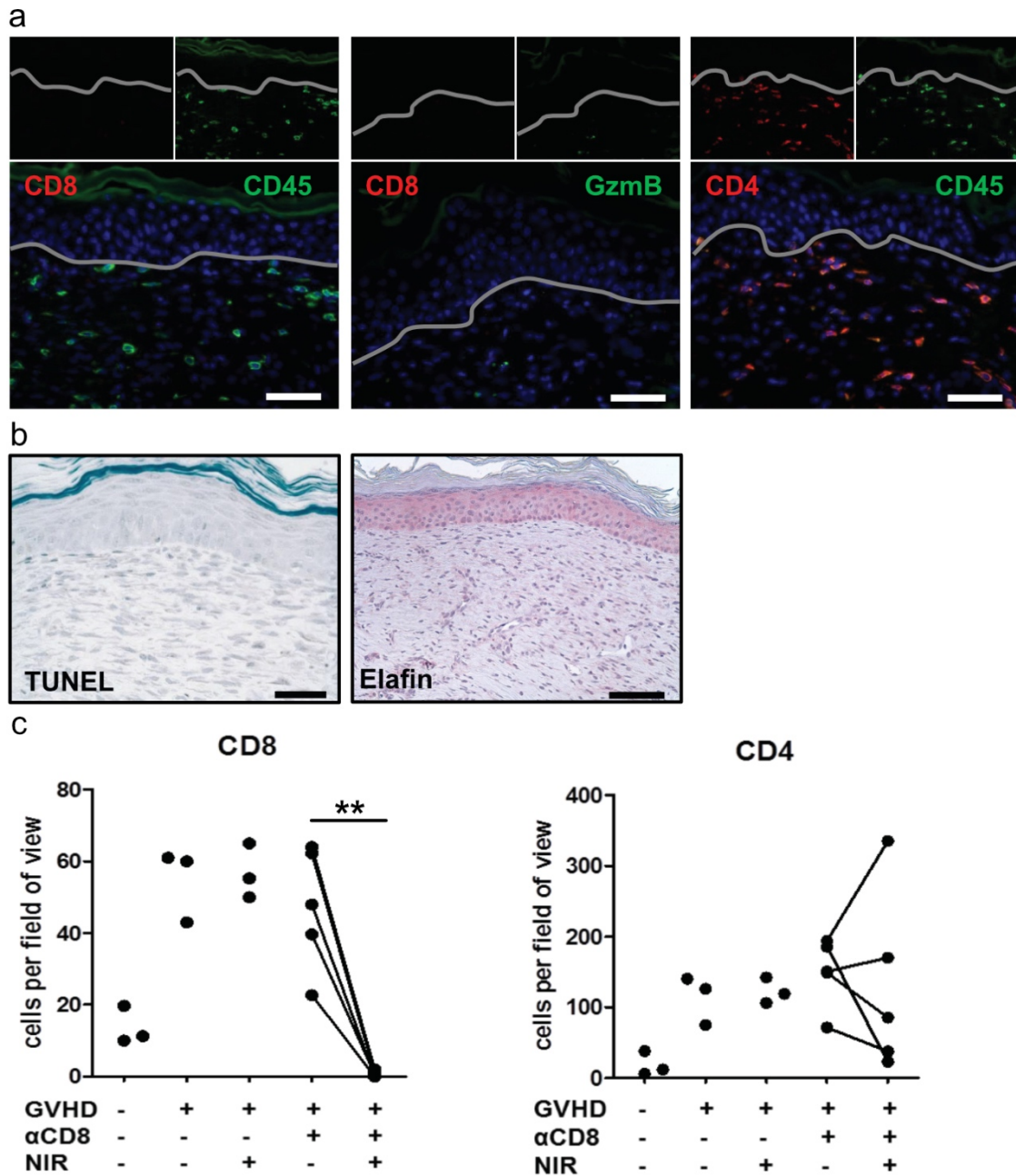


Fig. 11: Combination of CD8-IR700 and NIR light prevents cutaneous aGVHD. **a-b)** Shown are representative skin images from cutaneous aGVHD skin xenograft mice treated with CD8 NIR-PIT (n=5). **a)** Skin sections were stained by IF double staining targeting CD8 or CD4 in combination with CD45 or granzyme B. **b)** Skin sections were processed by TUNEL-assay and stained by IHC using anti-elafin. **c)** CD8 CD45 and CD4 CD45 T cells were counted from three visual fields (200x) per condition of at least three independent experiments. (Published and modified from Freund et al. 2019¹⁰⁰)

3.2.5 NIR-PIT targeting CD8 antigen selectively depletes skin localized CD8 T cells

Because of the former results that showed efficient CD8-IR700-targeted CD8 T cells depletion from NIR light exposed skin grafts, it was questioned if this ablation occurs systemically or is restricted to the NIR light-treated skin. Therefore, splenic tissues were

analyzed for the presence of human lymphoid structures and existence of CD8 T cells. As expected, spleens of control skin xenograft mice without PBMCs injection did not develop human lymphoid structures. In comparison, cutaneous aGVHD mice injected with CD8-IR700 alone or treated with CD8 NIR-PIT displayed humanized lymphoid structures with scattered CD8 T cells, thus reflecting follicle-like structures. Differences in CD8 T cell quantity comparing CD8-IR700 control and CD8 NIR-PIT treated mice could not be detected (Fig. 12).

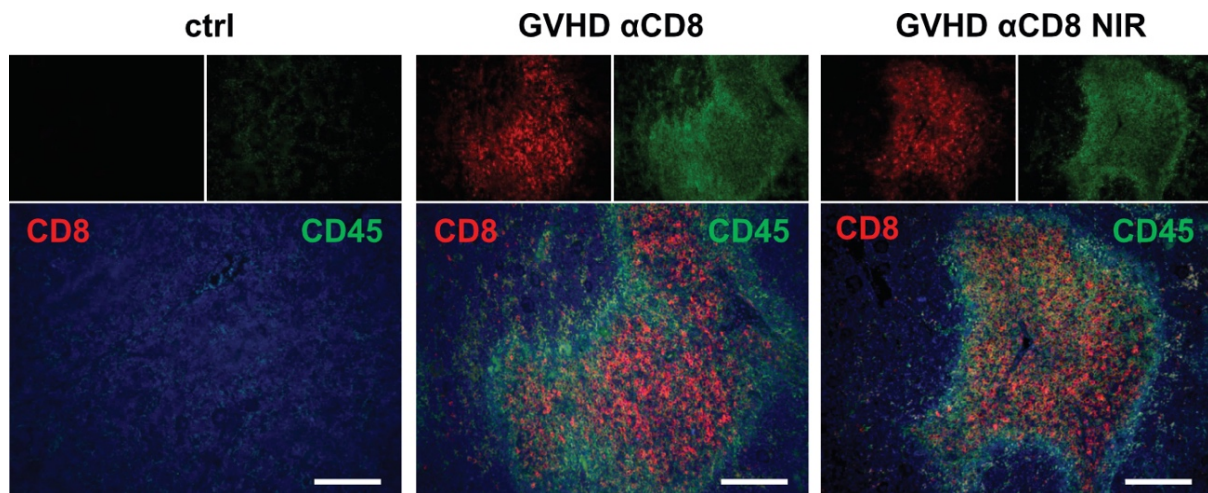


Fig. 12: Skin-selective CD8 depletion by NIR-PIT. Shown are representative spleen sections from skin xenograft mice alone (ctrl), mice with cutaneous GVHD that received CD8-IR700 (GVHD α CD8) as a control and of cutaneous GVHD mice that were treated with CD8 NIR-PIT (GVHD α CD8 NIR). Slides were processed with IF double staining targeting CD8 in combination with CD45 (n=5). (Published in Freund et al. 2019 ¹⁰⁰)

3.2.6 CD8 NIR-PIT inhibits delayed aGVHD

To demonstrate that the initially shown outcomes (Fig. 11) are independent from the selected timepoints, the induction of CD8 NIR-PIT was shifted by one week (Fig. 13a). In comparison to the former model, here, cutaneous aGVHD was manifested for two weeks before modulation with CD8 NIR-PIT was started. Similar to the previous results, CD8 T cell depletion by NIR-PIT inhibited histopathological features of aGVHD, epithelial cell death and reduced elafin production by affected lesional keratinocytes in comparison to CD8-IR700 antibody treated control mice (Fig 13b). Interestingly, in the delayed aGVHD model of antibody treated control mice, elafin was highly detectable in the epidermal as well as dermal tissue. This observation indicates secretion of elafin protein by affected keratinocytes. Pathologically, eosinophilic and DNA-fragmented dead keratinocytes in the basal and suprabasal layers colocalized with cytotoxic CD8 T cells (Fig 13b and c). Similar as in the earlier shown results, CD8 T cells were highly reactive, indicative by the polarized, granzyme

B-rich lytic granule staining. Confirming the previous results, upon treatment with CD8 NIR-PIT, CD8 T cells were completely ablated from the skin graft. Downstream to this depletion, histopathological signs as described before including epithelial cell death were completely reversed. In addition, elafin expression was highly reduced in epithelial keratinocyte layers and moreover abolished from the dermal part. Taken together with the results obtained from the two humanized aGVHD mouse models, it was shown that NIR-PIT efficiently and selectively depletes CD8 T cells from skin grafts and thereby effectively inhibits cutaneous aGVHD.

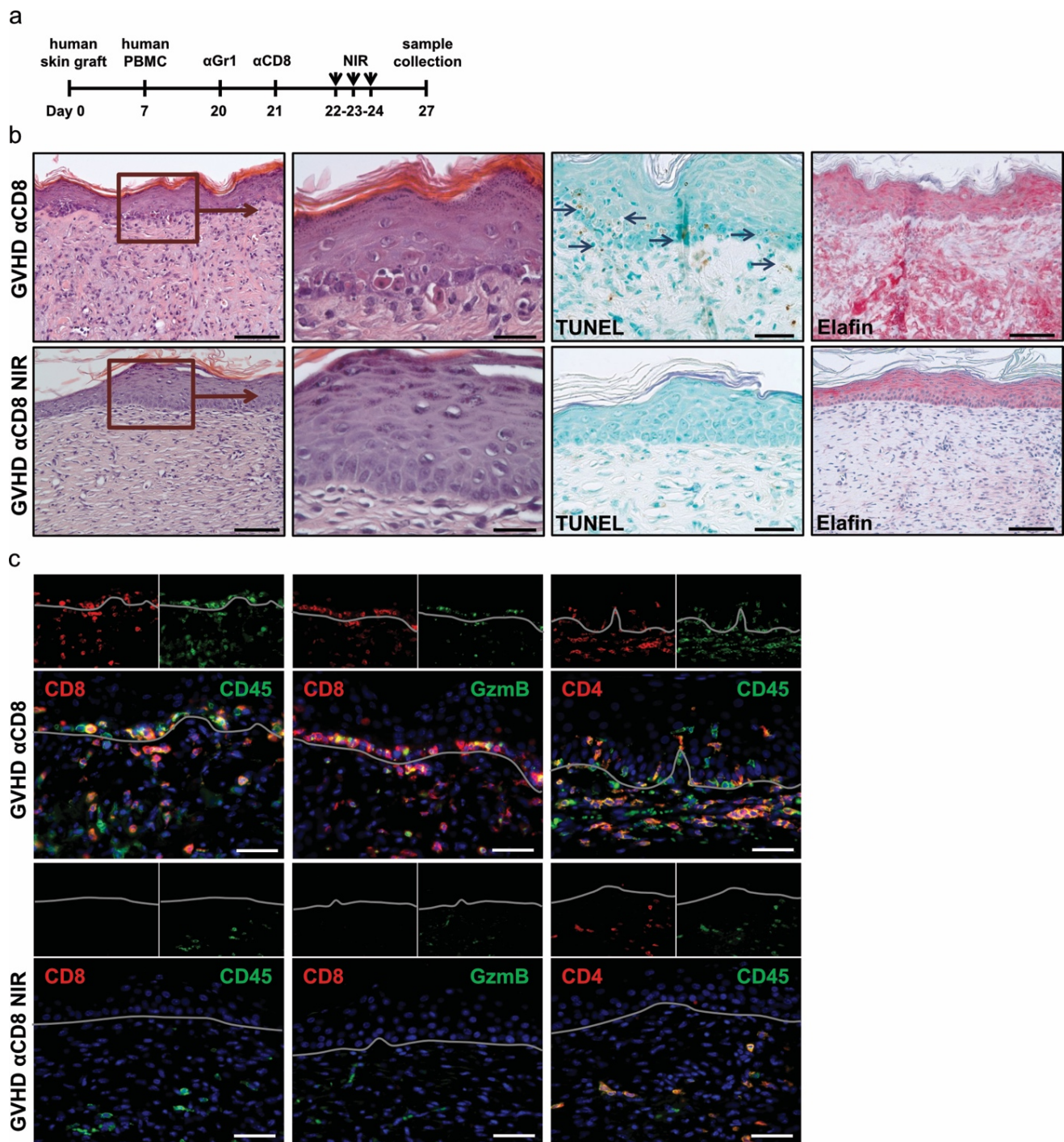


Fig. 13: Delayed cutaneous aGVHD model of CD8 NIR-PIT. **a)** Schematic depiction of the delayed humanized aGVHD mouse model treated with anti-CD8 NIR-PIT. **b-c)** Shown are representative skin images from cutaneous GVHD skin xenograft mice treated with CD8-IR700 alone (GVHD α CD8) or in combination with NIR light (GVHD α CD8 NIR) (n=3). **b)** Displays sections which were stained by H&E, IHC using anti-elafin and processed by TUNEL-assay. **c)** Skin sections were stained by IF double staining targeting CD8 or CD4 in combination with CD45 or granzyme B. (Published in Freund et al. 2019¹⁰⁰)

3.2.7 Purified CD8 T cells alone are incapable of inducing cutaneous aGVHD

Due to the importance of CD8 T cells in the pathogenesis of cutaneous aGVHD, it was questioned if these cells are able to induce and mediate characteristic skin manifestations. Therefore, 7×10^6 isolated CD8 T cells, instead of 30×10^6 bulk PBMCs, were adoptively transferred into skin-transplanted mice (Fig. 14a). However, purified CD8 T cells failed not only to populate splenic lymphoid structures but also to infiltrate mismatched skin grafts in comparison to the results obtained with bulk PBMCs. Merely, few scattered CD8 and CD4 T cells could be detected in the respected skin graft, probably originating from the skin donor (Fig. 14b and c). Therefore, epithelial cell death and elafin expression could not be detected, similar to the control skin grafts without leukocytes transfer (Fig. 14d).

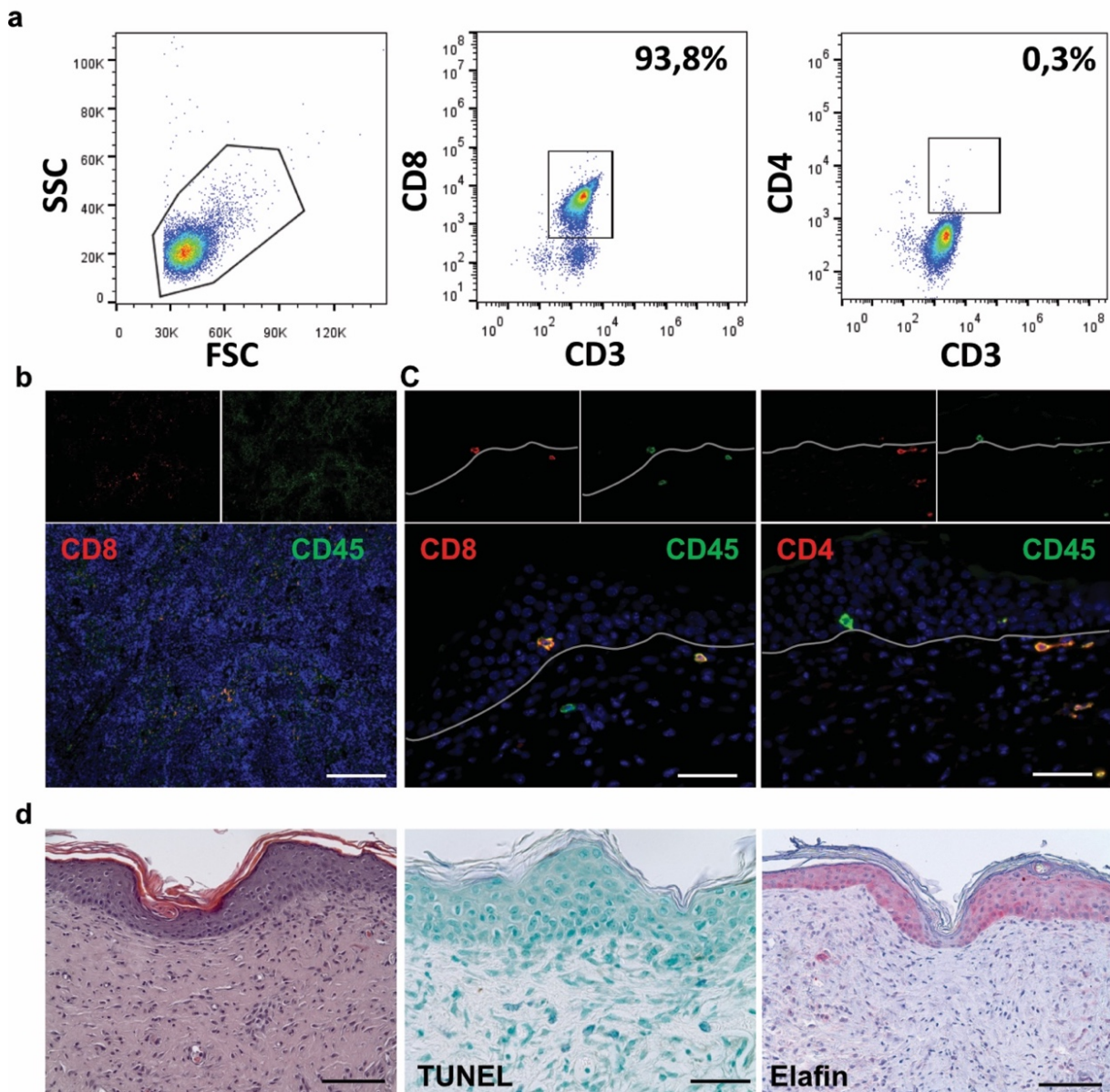


Fig. 14: Purified CD8 T cells do not induce cutaneous aGVHD. **a)** Flow cytometry purity control of MACS isolated CD8 T cells. **b-c)** Displays representative skin and spleen images from skin xenograft mice alone or injected with isolated CD8 T cells on day 20 post skin transplantation (n=3). Spleen (**b**) and skin (**c**) sections were marked by IF double staining targeting CD8 or CD4 in combination with CD45. **d)** Skin sections were stained by H&E, IHC using anti-elafin and processed by TUNEL-assay. (Published in Freund et al. 2019¹⁰⁰)

3.3 Necroptosis in cutaneous aGVHD

3.3.1 Necroptotic signaling is activated in the epidermis of cutaneous aGVHD

Having demonstrated the central role of T cells in mediating skin inflammation in aGVHD, next, keratinocyte cell death was studied in the context of cutaneous aGVHD. Initially, healthy control and lesional skin of aGVHD patients were studied for T-bet expression, a transcription factor of Th1 cells (Fig. 15a). In comparison to healthy controls, biopsies from aGVHD patients showed strong positive staining of infiltrating T-bet positive dermal and intraepithelial leukocytes.

Since epithelial damage, such as keratinocyte cell death, represents a pathological hallmark of aGVHD, it was questioned whether recently described programmed necrosis known as necroptosis is activated in those highly inflamed skin sections. First, to address this question, the expression of terminal-lytic pseudokinase MLKL was assessed by IHC (Fig. 15b). While protein levels of MLKL were highly upregulated in aGVHD, this observation was not to be seen in healthy controls. Of note, protein expression was not restricted to epidermal keratinocytes. However, when studying activation of MLKL by Ser358 phosphorylation, which indicates a shift from monomeric to active oligomeric MLKL, signaling was only detectable in epidermal keratinocytes (Fig. 15c). Phosphorylation staining varied from diminished cytoplasmic to strong polarized plasma membrane associated patterns, indicating a different status in the cascade of necroptotic signaling.

Next, expression analysis of skin biopsies taken from cutaneous aGVHD patients with maculopapular rashes were performed and compared to non-lesional skin of the same patient. In line with the histological staining results (Fig. 15 a-c), qPCR analysis revealed that transcripts of *ZBP1* and *MLKL* were upregulated in aGVHD skin lesions (Fig. 15d). To demonstrate that $\text{IFN}\gamma$ contributes to the inflammatory microenvironment, ISG expression was additionally analyzed. Here, the GVHD-related chemokines *CXCL9* and *CXCL10* as well as transcription factor *STAT1* were formally upregulated (Fig. 15d).

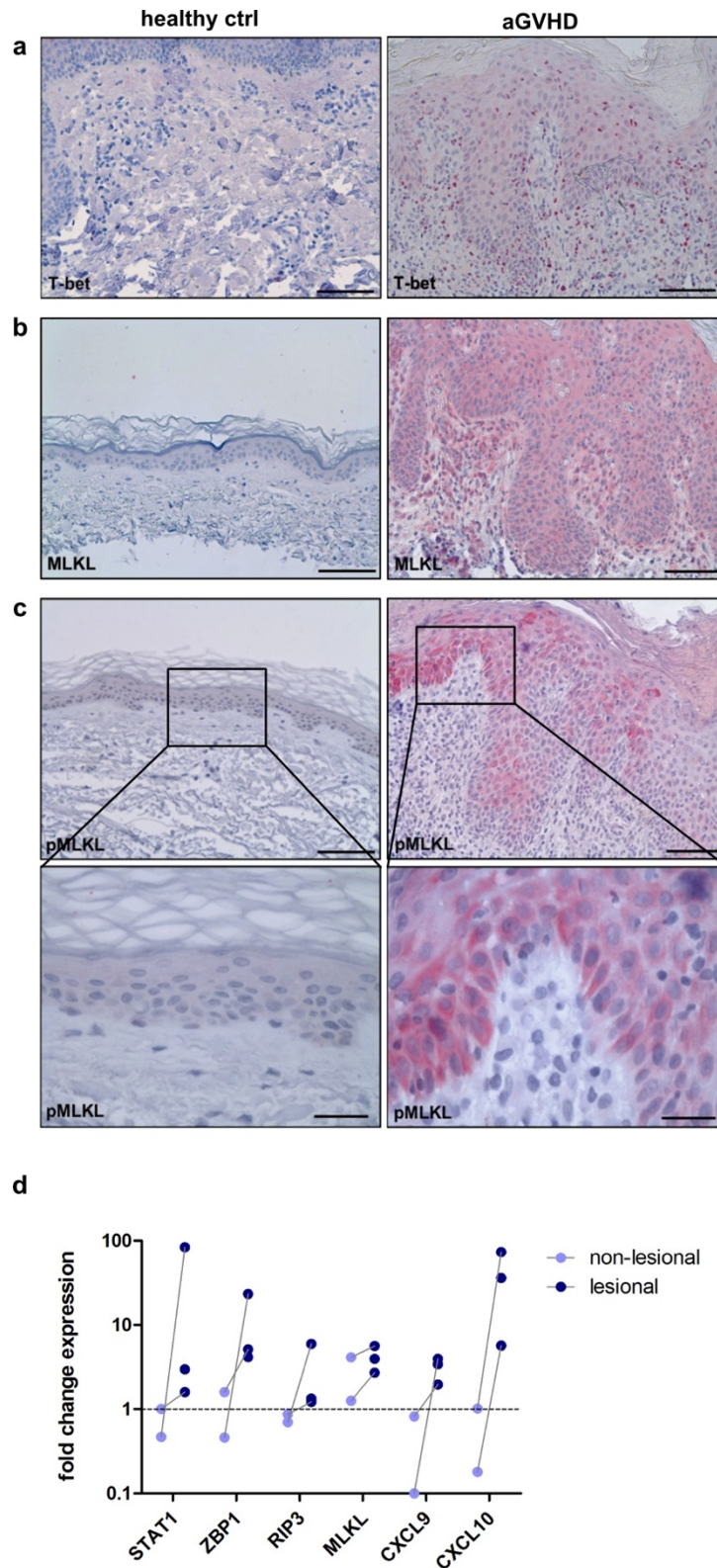


Fig. 15: Necroptotic signaling is activated in cutaneous aGVHD. Skin sections were stained by immunohistochemistry to detect **(a)** T-bet, **(b)** MLKL and **(c)** pMLKL (S358) expression (n=3). Representative images of a healthy controls and a patient with grade II-III aGVHD patient are shown. **d)** Expression of necroptotic markers in paired lesional and non-lesional skin biopsies from the same aGVHD patients (grade I) were analyzed by quantitative real-time PCR and compared to healthy skin (dotted line) (n=3).

3.3.2 Allogeneic leukocyte activation induces necroptotic keratinocyte cell death

Expression analysis of pre-stimulated keratinocytes indicated a priming towards a necroptotic pathway signature by IFN γ , as shown by the upregulation of the proteins *ZBP1*, *RIP3* and *MLKL* but not *RIP1* (Fig. 16a). Interestingly, IFN γ R signaling, which is mediated by JAK kinases-dependent transcription factor STAT1 activation, led itself to a feed forwards signaling loop demonstrated by the increased expression of *STAT1*. In addition, IFN γ induced the expression of the ISGs *CXCL9* and *CXCL10* which are important for the attraction and downstream allogeneic interaction of CXCR3 expressing type I immune cells with keratinocytes. Previous investigations have shown that keratinocyte pre-stimulation with IFN γ is required for their non-professional APC behavior^{18, 58}. In line with this, IFN γ stimulation induced an upregulation of HLA class I and II molecules on the surface of keratinocytes that is necessary for the interaction with allogeneic leukocytes (Fig 16b).

To investigate the possible role of necroptotic keratinocyte cell death in aGVHD, an *in vitro* model was established (Fig. 16c). Therefore, primary IFN γ pre-stimulated (24h) keratinocytes were co-cultured with PBMCs from mismatched healthy donors for 72h. Respective protein lysates of co-cultured keratinocytes were tested for necroptotic signaling. Pre-stimulation of keratinocytes with IFN γ followed by co-culture with allogeneic PBMCs induced a strong phosphorylation of RIP3 at Ser227 and MLKL at Ser358 in comparison to un- or pre-stimulated keratinocytes (Fig. 16d). Of note, western blot analysis using anti-pMLKL displayed a protein band below 55kD in unstimulated keratinocytes (asterisk), slightly smaller than that seen in keratinocytes co-cultured with allogeneic PBMCs. As previously published by Sun et al. who developed pMLKL antibody (clone EPR9514) staining, an upward shift of MLKL upon necroptosis induction by RIP3 was observed. In line with this, RIP3 phosphorylation was absent in unstimulated keratinocytes, which explains a unshifted MLKL version compared to co-culture stimulated keratinocytes. This issue is further addressed by subcellular fractionization in Fig 17b.

Having shown that IFN γ induces necroptotic signaling, it was questioned if this activation correlated with keratinocyte viability. Indeed, flow cytometry analysis of pre-stimulated keratinocytes co-cultured with allogeneic PBMCs demonstrated keratinocyte-directed cellular cytotoxicity detectable by propidium iodide (PI) and annexin V-like, Ca²⁺ independent apotracker staining (Fig. 16e-f). Supernatant analysis of co-cultured keratinocytes with PBMCs demonstrated high level of IFN γ production when keratinocytes were preactivated with IFN γ (Fig. 16g). These findings demonstrate that IFN γ pre-conditions keratinocytes for the induction of necroptotic cell death executed by allogenic PBMCs.

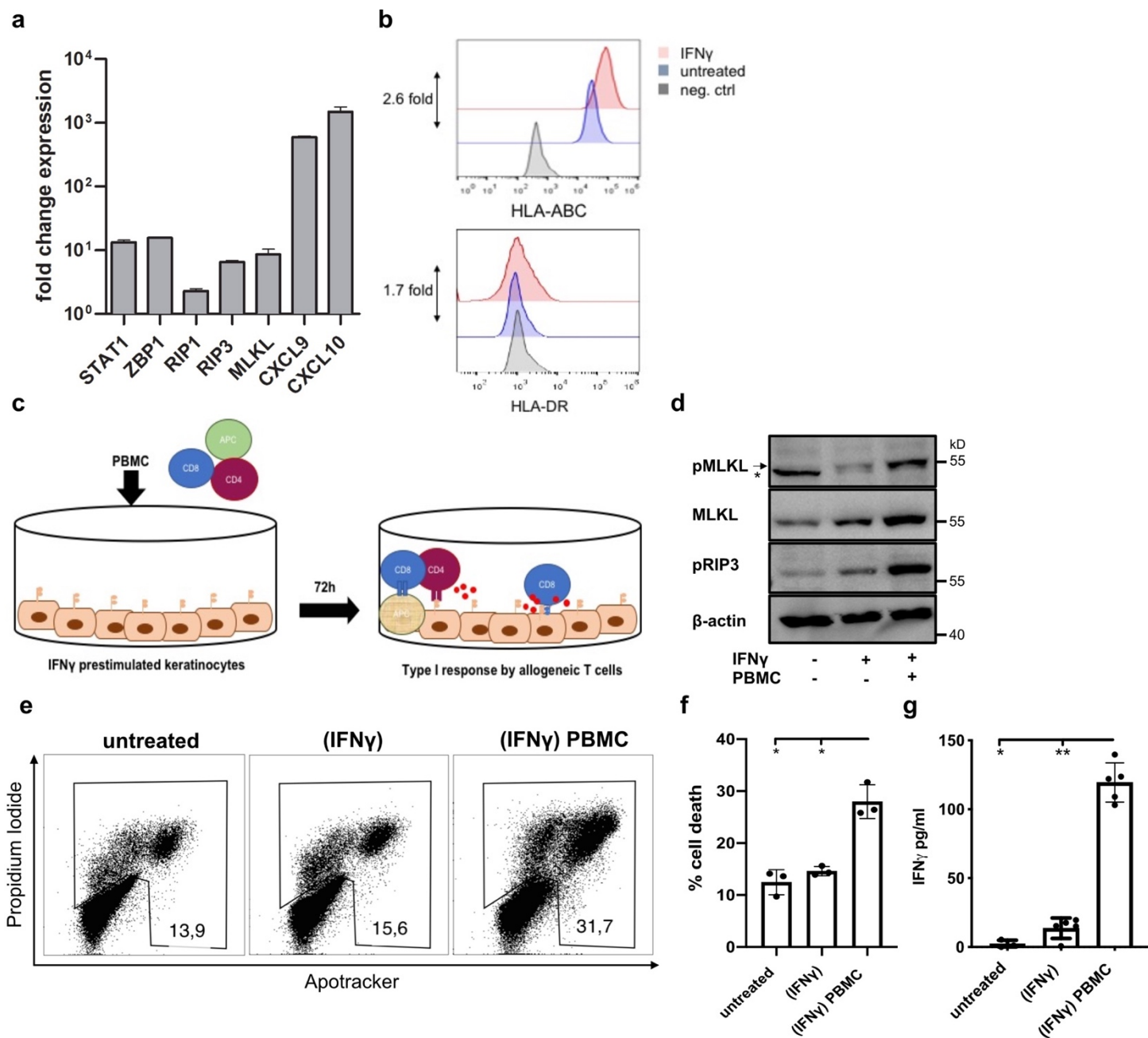


Fig. 16: Alloreactive leukocytes trigger necroptotic cell death of keratinocytes. **a-b)** Culture plate seeded keratinocytes (NHEK) were stimulated with IFN γ for 24h or left untreated. **a)** Following RNA isolation, RNA expression was analyzed using quantitative real-time PCR. Data was normalized to *TBP* and presented as fold change expression relative to untreated keratinocytes. **b)** Trypsinized keratinocytes were surface stained with anti-HLA-ABC and anti-HLA-DR and analyzed by flow cytometry. **c)** Schematic depiction of alloreactive co-culture experiment. Culture plate seeded NHEKs were stimulated with IFN γ for 24h. Following medium renewal, mismatched PBMCs purified from buffy coats were added to the pre-stimulated keratinocytes (ratio 10:1) and let them respond for 72h (d-g). **d)** Keratinocyte lysates from co-culture experiments were analyzed by western blot using antibodies as indicated and compared to untreated or IFN γ pre-treated keratinocytes alone. Arrow indicates an

upward shift from asterisk (*) protein band after necroptosis induction. **e)** Keratinocytes viability (apotracker and propidium iodide positive) after co-culture in comparison to indicated controls are shown from a representative experiment and are displayed grouped in **f)**. **g)** Supernatants from co-culture experiments were analyzed by ELISA for IFN γ production by allogeneic PBMCs and compared to untreated or IFN γ pre-treated keratinocyte supernatants. (* $P < 0.05$, ** $P < 0.01$). Experiments were repeated at least three times.

3.3.3 IFN γ induces RIP3 dependent necroptotic keratinocyte cell death

Necroptosis of keratinocytes was observed under conditions with high levels of IFN γ production in co-cultures of pre-stimulated keratinocytes and allogeneic T cells. Next, it was tested whether prolonged IFN γ was responsible for the necroptotic cell death of keratinocytes. Lysates of IFN γ treated keratinocytes showed a strong phosphorylation of RIP3 and MLKL (Fig 17a). This signaling could not be diminished or increased by pan-caspase inhibitor zVAD demonstrating a caspase independent signaling process (Fig. 17a). To proof that the observed activation of pMLKL, seen in whole cell lysates of IFN γ treated keratinocytes, indicates a final step of the necroptotic signaling cascade and lytic cell death, subcellular fractionation of IFN γ treated and untreated control keratinocytes was performed. Therefore, membrane bound proteins (membrane fraction) were isolated and separated from cytoplasmic and nuclear fractions. As demonstrated, IFN γ stimulation induced translocation of phosphorylated MLKL to the plasma membrane, indicating lytic pore formation and necroptotic cell death in comparison to the membrane fractions of control keratinocytes (Fig. 17b). To delimit IFN γ stimulated necroptotic from apoptotic cell death, cellular viability and proteins of keratinocytes treated with IFN γ (72h) were compared to staurosporine (STS) treated keratinocytes, a selective inducer of caspase dependent apoptosis¹⁰¹. Protein analysis of STS treated but not IFN γ treated keratinocytes showed activation of the apoptotic signaling pathway, detectable by cleaved caspase 3 (CC3) (Fig. 17c). Similarly, flow cytometry analysis showed apotracker (Annexin V) single positive cells by STS treatment (right panel) as known from early apoptotic cells. These apotracker single positive cells were spared in IFN γ treated (middle panel) and untreated (left panel) keratinocytes. Instead, IFN γ treated necroptotic keratinocytes and not staurosporine-induced apoptotic keratinocytes showed a strong single positivity for PI with transition to PI/apotracker double positivity, highlighting its distinct phenotypical cell death (Fig. 17d).

To further demonstrate that keratinocytes undergo necroptotic cell death upon IFN γ stimulation, these cells were treated with increasing concentrations of RIP3 kinase-specific inhibitor GSK'872. Accordingly, IFN γ -induced necroptotic cell death was inhibited by increasing concentrations of GSK'872, as shown by flow cytometry (Fig. 18a-b). Western blot

analysis of the former cell lysates of IFN γ -stimulated keratinocytes showed a complete inhibition of MLKL phosphorylation starting from 3 μ M GSK'872 (Fig. 18c).

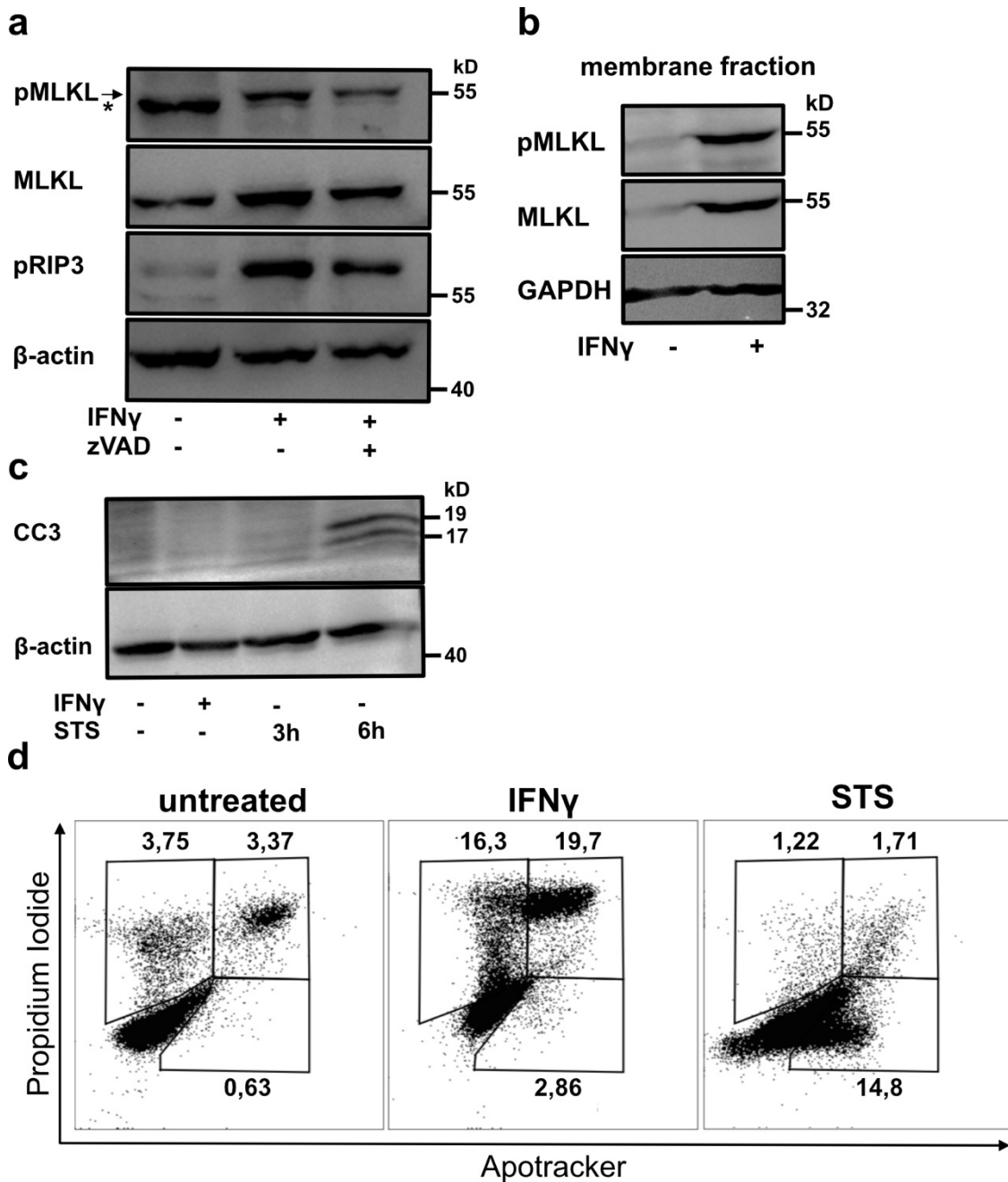


Fig. 17: IFN γ induces keratinocyte necroptotic cell death. a-d) Keratinocytes were stimulated with IFN γ alone or in comparison with **a)** zVAD for 72h or **c)** with staurosporine (STS) for 3h and 6h and were analyzed by western blot with indicated antibodies. Arrow indicates an upward shift from asterisk (*) protein band after necroptosis induction. **b)** Keratinocytes were fractionized into subcellular compartments. Membrane-bound proteins were blotted and analyzed as indicated. **d)** Viability of keratinocytes treated with IFN γ (72h) or staurosporine (6h) were analyzed by flow cytometry. Experiments were repeated three times.

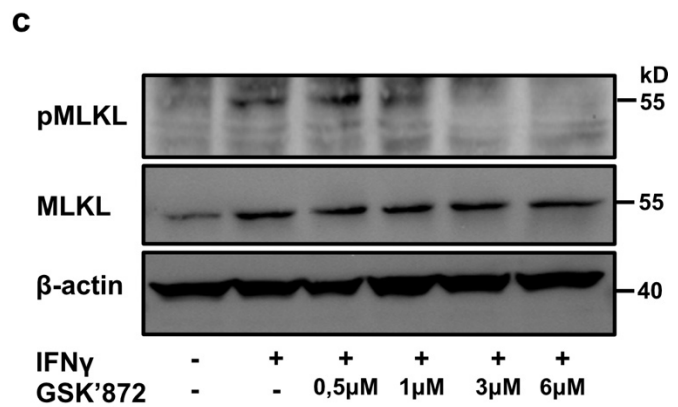
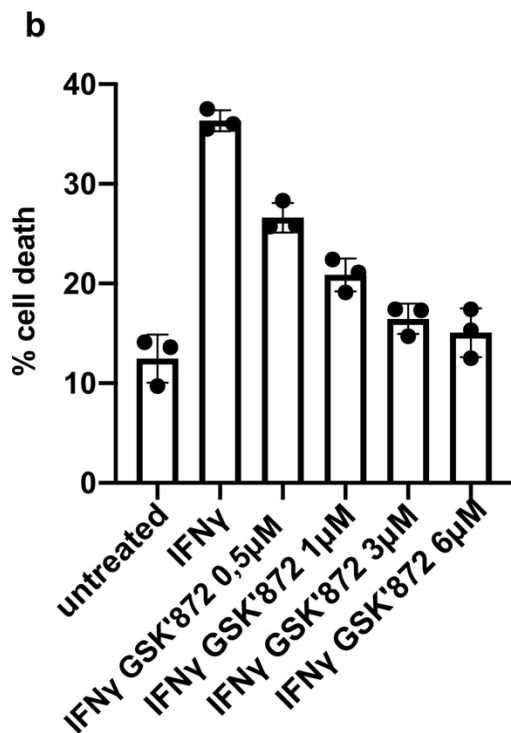
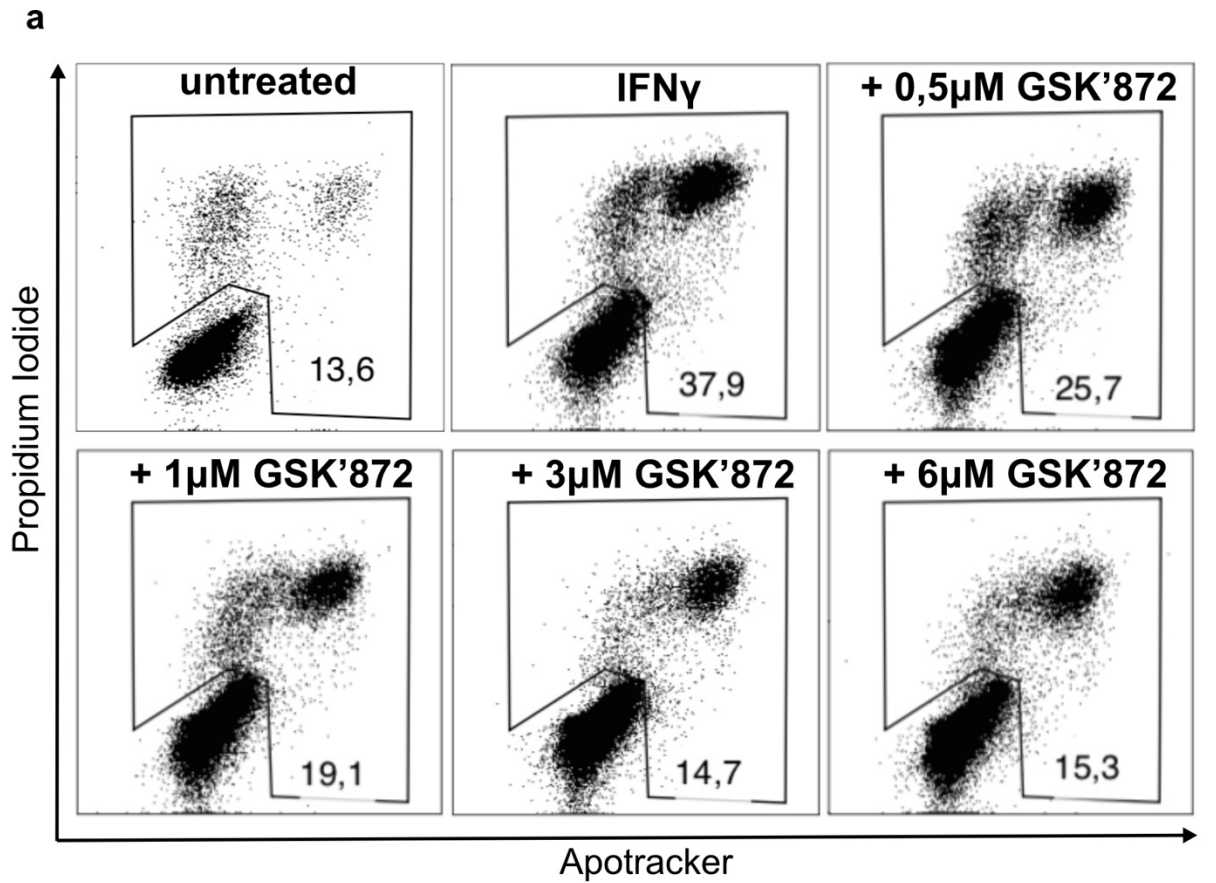


Fig. 18: IFN γ -induced keratinocyte cell death is RIP3 dependent. **a)** Viability of keratinocytes treated with IFN γ (72h) alone or in addition with increasing concentrations of RIP3 inhibitor GSK'872 were analyzed by flow cytometry. **b)** Viability results of three independent experiments were grouped. **c)** Displays corresponding western blot analysis of **a)** using indicated antibodies.

3.3.4 IFN γ -driven keratinocyte cytotoxicity is regulated by STAT1 signaling

To provide further support of an IFN γ dominated immune response in aGVHD, STAT1 phosphorylation (Tyr701) was studied in the epidermis of aGVHD patients. Lesional skin of patients with aGVHD in comparison to healthy control skin showed a strong pSTAT1 activation in the cytoplasm and nucleus of keratinocytes as revealed by immunohistochemistry (Fig. 19a). Inhibition of the JAK/STAT signaling pathway is known to attenuate the alloreactive immune responses and to be of therapeutic value in this disease.^{102, 103}. Next, it was addressed whether inhibition of IFN γ signaling may attenuate necroptotic signaling in the described experimental models. Therefore, cultured keratinocytes were treated for 24h with IFN γ in the presence of increasing concentrations with the JAK1/3 inhibitor tofacitinib (Fig 19b). Complete prevention of STAT1 phosphorylation was reached with tofacitinib concentrations of 5 μ M or higher. Activation of MLKL and RIP3 indicated by phosphorylation was already inhibited with lower tofacitinib concentrations. This may be explained by the finding (see also Fig 16 c) that IFN γ induces the transcription of STAT1, and also of MLKL and RIP3. Consequently, tofacitinib inhibited the IFN γ induced upregulation of MLKL protein expression (Fig. 19b). Ultimately, we can demonstrate that necroptotic cell death induced by IFN γ was efficiently inhibited with tofacitinib (1 μ M) (Fig. 19c-d).

As a final experiment in this series, a side-by-side comparison of different approaches to interfere with IFN γ -induced necroptosis was performed. Tofacitinib, GSK'872 as well as an IFN γ -blocking antibody was studied in the earlier described co-culture system of keratinocytes and allogeneic PBMCs. These studies clearly revealed that the inhibition of necroptosis by GSK'872 or tofacitinib was as efficient as for example an IFN γ -neutralizing mAb in preventing necroptosis to the level of control cells (Fig. 19e-f).

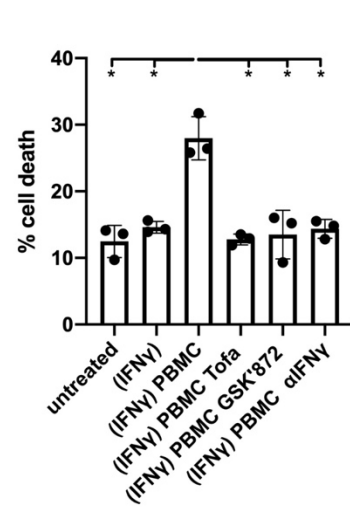
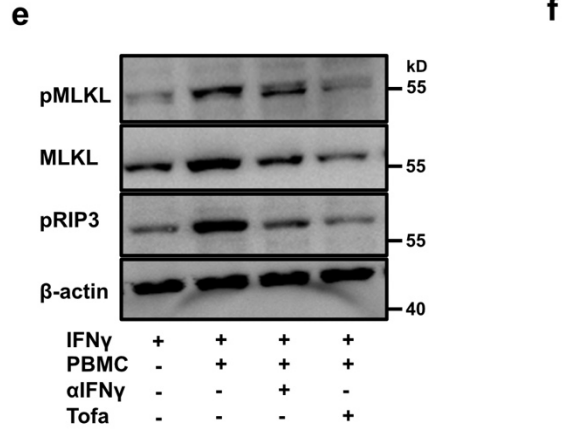
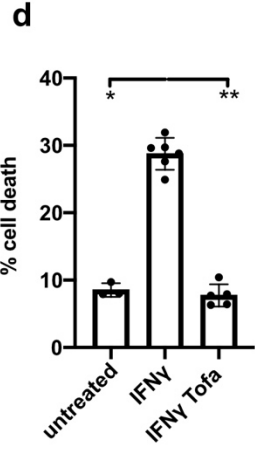
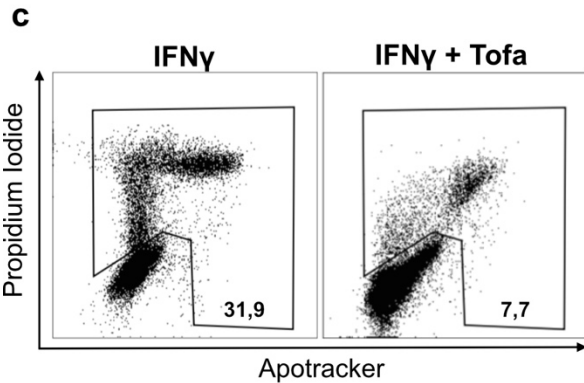
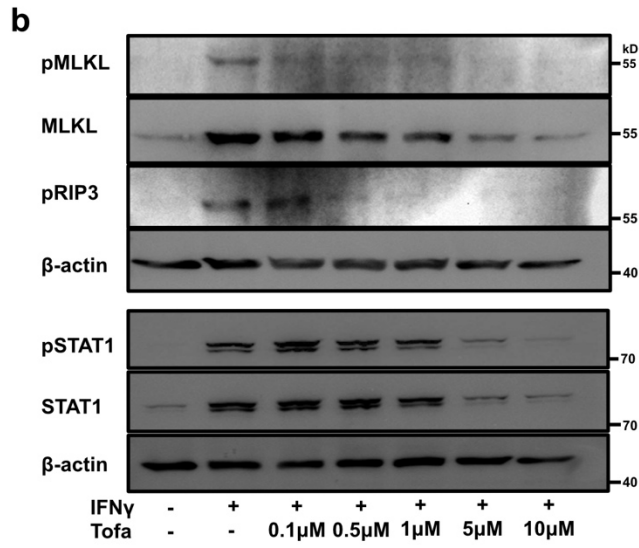
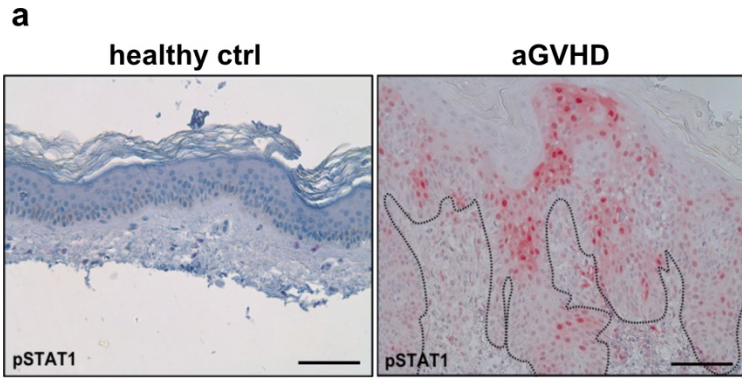


Fig. 19: IFN γ mediates keratinocyte cytotoxicity via STAT1 signaling. **a)** A representative healthy control and acute GVHD patient were stained with anti-pSTAT1 using IHC. **b)** Keratinocytes were stimulated with IFN γ alone or together with increasing concentrations of JAK/STAT inhibitor tofacitinib for 24h and analyzed by western blot. **c-d)** Keratinocytes treated with IFN γ for 72h alone or together with 1 μ M tofacitinib were analyzed for viability using flow cytometry. **e-f)** Keratinocyte lysates of trypsinized cells from co-culture experiments were studied for viability using flow cytometry or western blot using antibodies as indicated and compared to control groups and modifying agents (IFN γ neutralizing antibody 25 μ g/ml, 1 μ M tofacitinib, 3 μ M GSK'872). (* P < 0.05, ** P < 0.01).

3.3.5 *De novo* expressed ZBP1 facilitates keratinocyte necroptosis

It was recently described that the intracellular sensor of nucleic acids ZBP1 is mediating interferon-induced necroptosis⁹². In mice, ZBP1 integrated RHIM motif was shown to recruit and activate RIP3 upon homodimerization leading to necroptotic cell death and inflammation, independent of RIP1⁹². To study the expression of ZBP1 in our aGVHD samples respectively, mAb directed stainings were performed. Indeed, ZBP1 expression was identified in sections of cutaneous aGVHD patients. Here, keratinocytes in active lesions with dense infiltrations of leukocytes showed a strong positivity for ZBP1 (Fig. 20a). Similarly, *in vitro* IFN γ -treated keratinocytes expressed *de novo* ZBP1 on a protein level (Fig. 20b). These results correlate with the data obtained from the previous expression analysis and in relation was completely blocked by the addition of 1 μ M tofacitinib (Fig. 20b), possibly explaining the phenomenon seen in Fig. 19b-d. Furthermore, neither keratinocytes stimulated with IFN γ nor TNF α or the combination induced activation of RIP1. Only caspase inhibition by zVAD in combination with IFN γ and TNF α could induce RIP1 phosphorylation at Ser166 (Fig. 20c).

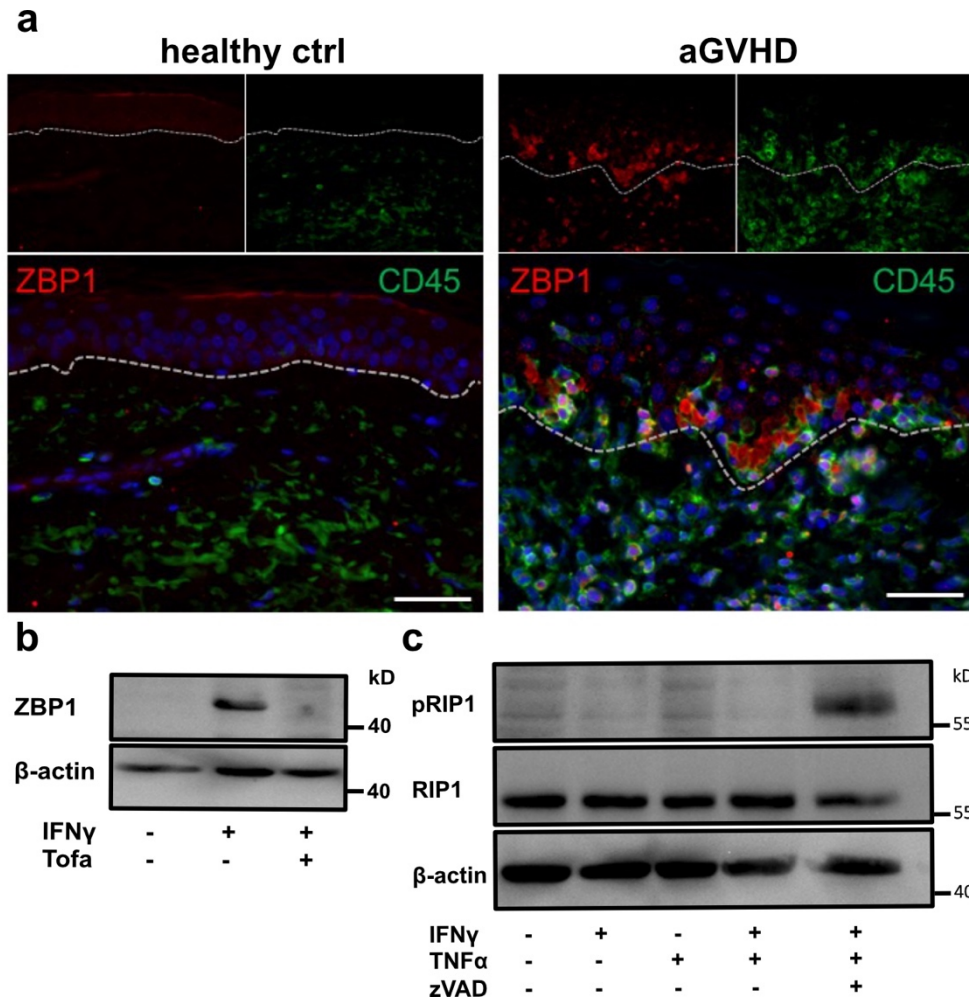


Fig. 20: ZBP1 is de novo expressed in IFN γ stimulated keratinocytes. a) A representative healthy control and acute GVHD patient were stained with anti-ZBP1 and anti-CD45 Abs using IF. **b and c)** Keratinocytes treated with IFN γ and/or TNF α for 72h alone or together with 1 μ M tofacitinib or zVAD were analyzed by western blot as indicated.

3.3.6 IFN γ induces epidermal necroptosis in an *ex vivo* organ culture model

Type I immune responses can provoke different skin diseases in which IFN γ is thought to serve as an orchestrator of the inflammatory responses¹⁰⁴. However, the role of IFN γ in the context of cell death and necroptosis in the skin is barely described. To study this in detail, an *ex vivo* human skin culture system was established. Split skins from healthy donors were cultured with an air-medium interface on a permeable raft for 72h. To induce necroptotic signaling, IFN γ was added to the system alone or in combination with tofacitinib to possibly interfere with signaling and necroptosis induction. During the course of the experiment, unmanipulated *ex vivo* cultured human control split skin appeared completely vital (Fig 21a). IFN γ treatment induced morphological changes in the epidermal basal and suprabasal keratinocyte layers. In particular, vacuolized, pyknotic and eosinophilic keratinocytes that are

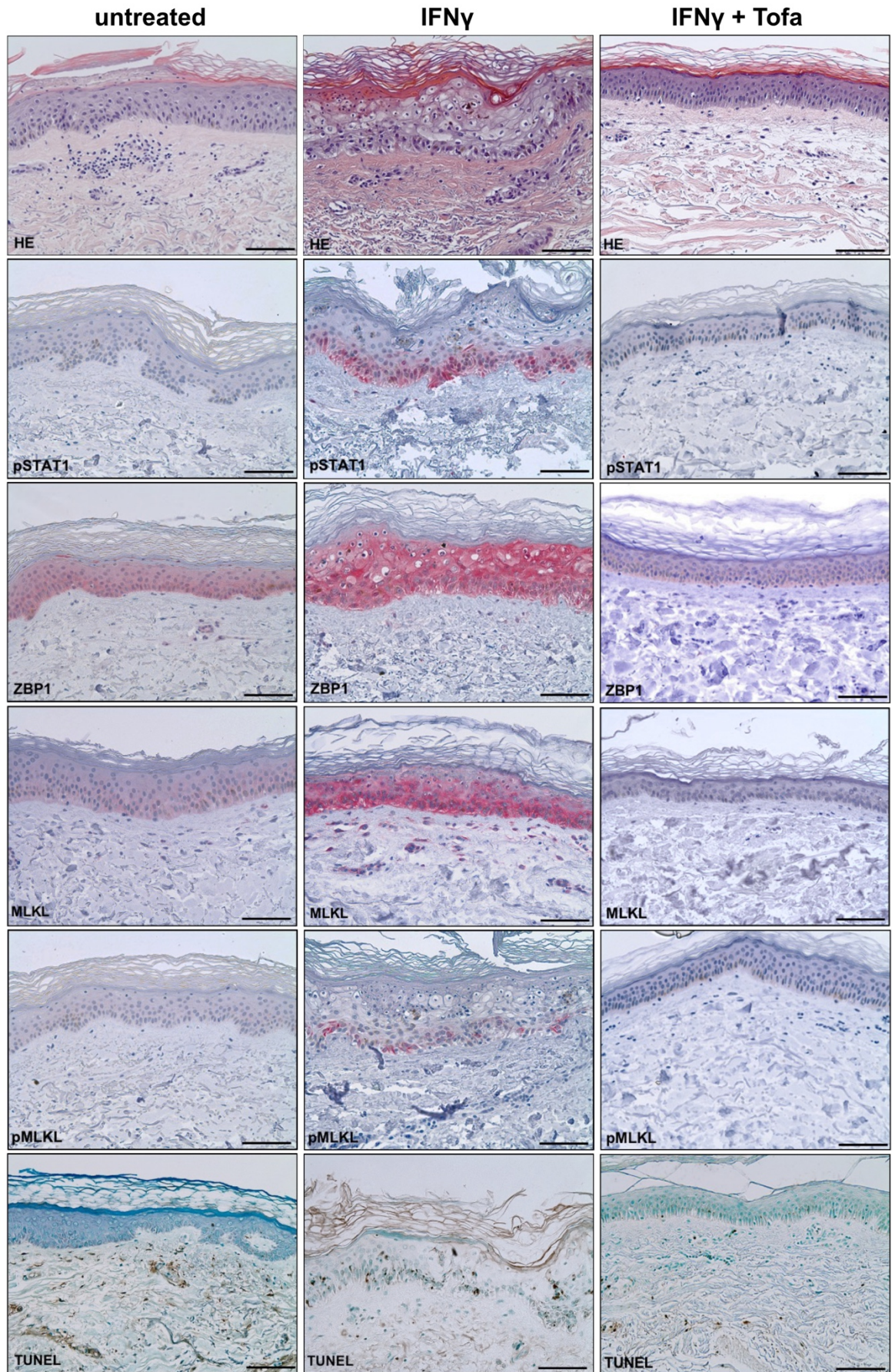
characteristically described for cutaneous aGVHD were seen in settings with IFN γ stimulation (Fig. 21a). Moreover, a strong IFN γ induced phosphorylation of STAT1 could be detected mainly in the basal and suprabasal layers. Expression levels of ZBP1 and MLKL were largely increased. In correlation and downstream to the former described signaling cascade, phosphorylation of MLKL was clearly observed in those affected keratinocytes, but not cleavage of apoptotic caspase 3 (Fig. 21a and 21b). Likely, as a consequence of sufficient MLKL activation, increased keratinocyte cell death as indicated by TUNEL staining could be detected (Fig. 20a). With the addition of tofacitinib as a convenient therapeutically intervention strategy for this pathological manifestation, morphological changes and cell death induced by IFN γ could be reversed. This appeared to be a consequence of silenced STAT1 phosphorylation, protein expression and activation of ZBP1 and MLKL comparable to the untreated control (Fig. 21a). In line with the histological data and earlier shown expression data from cutaneous GVHD patients, transcriptome analyses revealed that *STAT1*, *ZBP1*, *RIP3* and *MLKL* were upregulated in response to IFN γ and again normalized by the addition of tofacitinib (Fig. 21c).

3.3.7 Necroptosis is activated in a mouse model of human aGVHD.

As a valuable extension of the previous observations on necroptosis, the stated hypothesis was studied in a well-defined, T cell dependent model of aGVHD as presented in the figures 1-14¹⁰⁰. In these experiments, human skin grafts with or without cutaneous aGVHD were analyzed and compared for protein expressions of necroptosis-related proteins.

As reported from the skin pathology found in aGVHD patients, human skin grafts of immunodeficient NSG mice showed a clear type I immune response that was illustrated by a strong infiltration of T-bet expressing leukocytes. Moreover, STAT1 signaling was highly activated in lesional keratinocytes, indicating together with T-bet expression a T cell- and IFN γ -dependent inflammation. Downstream to STAT1 signaling, we found increased expression of the inducer of necroptosis ZBP1 and lytic MLKL in comparison to unaffected control skin grafts. This signaling cascade led to a detectable activation and phosphorylation of MLKL (Fig. 22) which correlated with the epithelial cell death shown in figure 8. These results obtained in a T cell dependent model of aGVHD clearly confirm the previous findings obtained by studying patient material, *in vitro* and *ex vivo* experiments.

a



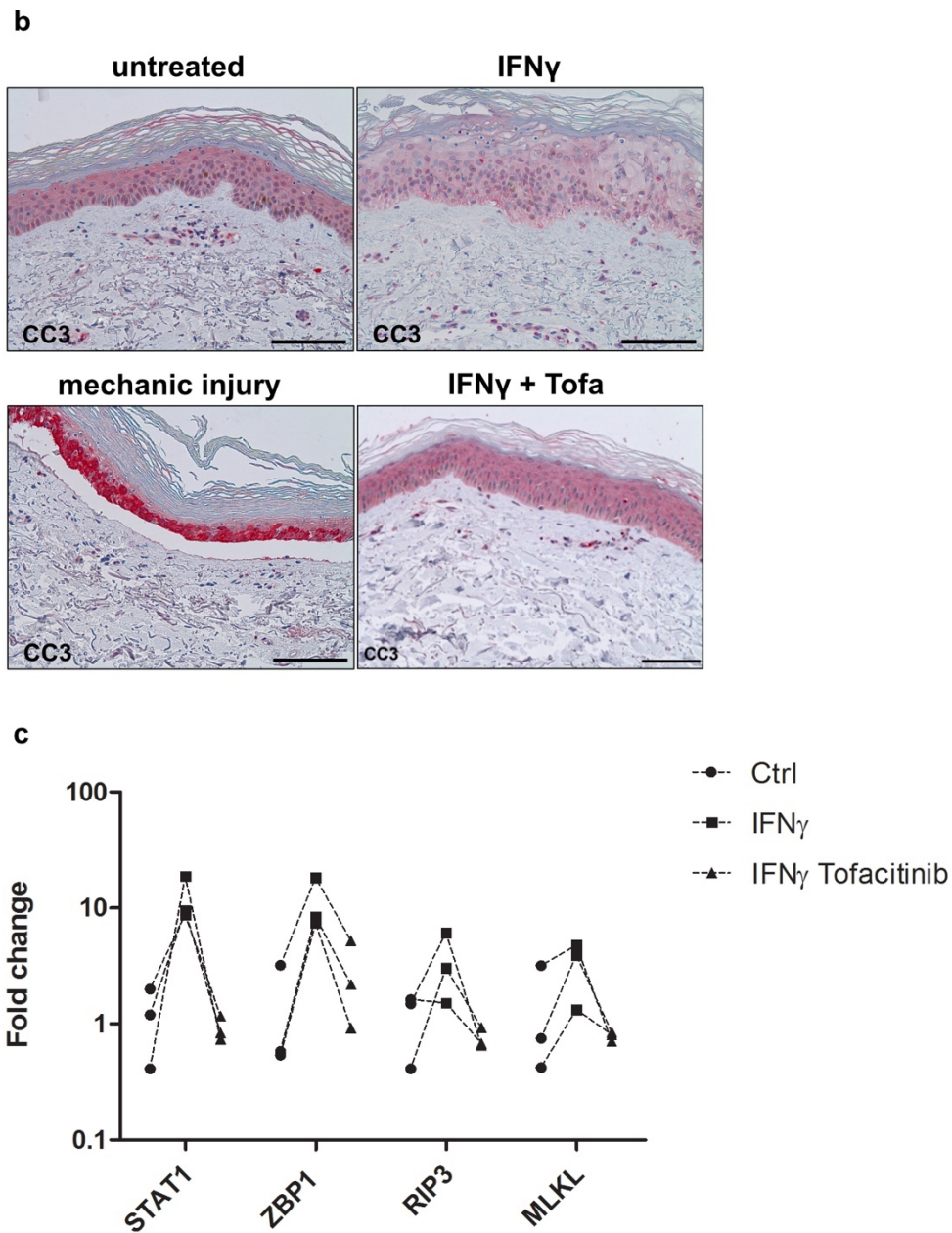


Fig. 21: IFN γ induces necroptosis in *ex vivo* skin organ cultures. Split skins from healthy donors were sewed on cell strainers and cultured *ex vivo* for 72h. Untreated control and IFN γ (500 ng/ml) treated tissues samples alone or in the presents of 10 μ M tofacitinib were analyzed and compared by **(a and b)** H&E and IHC staining as indicated as well as TUNEL assay to detect cell death (n=3). **(b)** For apoptotic CC3 activation, mechanistic injured skin generated by surgical procedure was used as positive control. **(c)** Shows qPCR analysis as biological replicates of skin donors treated with IFN γ (500 ng/ml) alone or in the presents of 10 μ M tofacitinib and normalized to control skin (n=3).

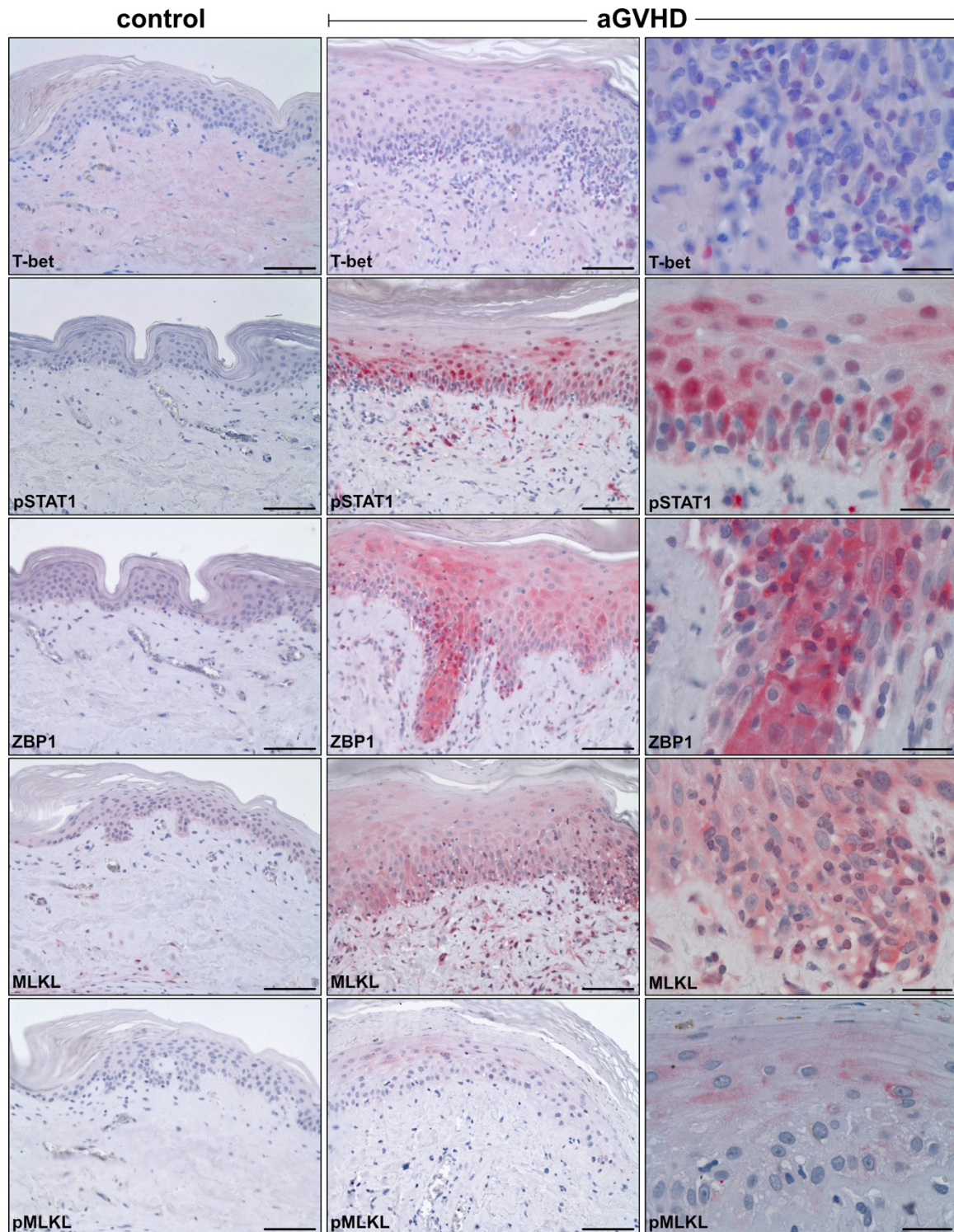


Fig. 22: Necroptotic signaling is activated in humanized aGVHD skin xenografts. Split skins from healthy donors were sewed on immunodeficient NSG mice and subsequently transfused with human mismatched PBMCs to induce cutaneous aGVHD. 20d post skin transplantation and 14d post PBMCs transfusion skin grafts were dissected and analyzed IHC as indicated (n=3).

3.3.8 Serum levels of RIP3 are associated with clinical aGVHD

Excessive induction of necroptosis was reported to cause increased systemic RIP3 levels¹⁰⁵. Regarding to that, increased RIP3 levels may be detectable in serum samples of patients with GVHD. Therefore initially, RIP3 upregulation was tested on protein level in response to IFN γ . Here, IFN γ stimulated keratinocyte cell lysates were immunoblotted for RIP3 detection. Indeed, keratinocytes showed a clear upregulation of RIP3 on protein level *in vitro* (Fig. 23a). Next, serum samples of steroid-refractory intestinal aGVHD patients undergoing extracorporeal photopheresis (ECP), an effective therapeutic manipulation for alloreactive T cell responses, were analyzed. Before the first ECP cycle, refractory patients showed highly elevated levels of RIP3. These levels were found to be significantly decreased in patients clinically responding to ECP therapy, and in accord with the sustained clinical response, serum RIP3 levels remained low (Fig. 23b). These results should foster future studies whether RIP3 protein detection in serum of GVHD patients may serve as a possible diagnostic and treatment response marker.

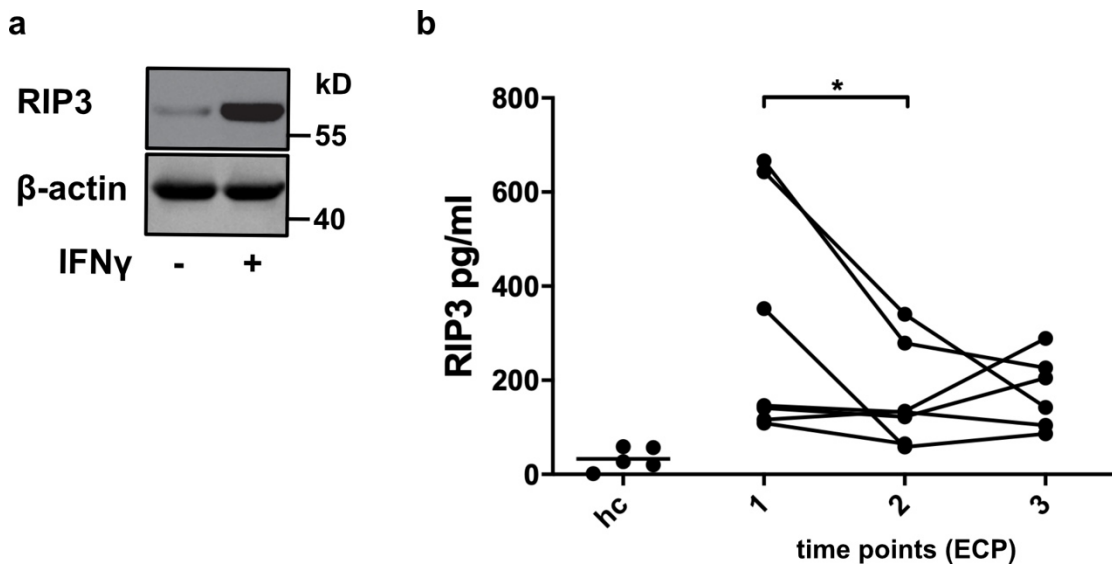


Fig. 23: Association between RIP3 levels and clinical GVHD. (A) Keratinocyte lysates stimulated with IFN γ (50 ng/ml) were analyzed by western blot and stained for RIP3. **(B)** Shows serum levels of RIP3 from steroid-refractory intestinal aGVHD patients (time point 1) in comparison to healthy controls (hc). Consecutive serum levels of RIP3 are shown for patients with clinical response to ECP (time point 2 and 3) (n=7) (* $P < 0.05$).

4 Discussion

Two distinct but closely related topics were the main focus of this presented work on cutaneous aGVHD. First, NIR-PIT was successfully established as a therapeutic approach for inflammatory skin diseases in a humanized mouse model of cutaneous aGVHD. Skin-restricted total depletion of alloreactive CD8 T cells was achieved by applying NIR-PIT. Consequently, this approach completely inhibited target organ manifestations. These findings highlight the role of CD8 T cells in the context of skin aGVHD. In follow up studies focusing on cell death executed by T cells in aGVHD, necroptosis was identified as a novel and dominant inflammatory cell death mechanism occurring in lesional keratinocytes of aGVHD. In different experimental setups, IFN γ was identified as the prime inducer of necroptosis. Finally, therapeutic interference with necroptotic signaling was shown to block keratinocyte cell death. The collected data are discussed in the following sections based on the current literature.

4.1 NIR-PIT for dermatological use

NIR-PIT was initially described for the depletion of EGFR-expressing tumor cells⁷⁷. Based on this first description of efficient tumor therapy, different strategies followed in the context of tumor modulation. However, reports on NIR-PIT-based immune cell modulation are limited. One major report from Sato et al. demonstrated CD4 CD25 regulatory T cell depletion from tumor microenvironment by NIR-PIT. Based on this depletion, the authors could increase tumor reactivity by cytotoxic CD8 T cells as well as NK cells⁹⁷. Here, complete depletion of regulatory T cells could be achieved with 64 J/cm² *in vitro*. Interestingly, in comparison to that, CD8-targeted NIR-PIT already efficiently depleted CD8 T cells with 22 J/cm², indicating CD8 as a promising target. Of note, different light sources were reported to achieve different results. For example, laser-based NIR-PIT is generally considered to be more efficient than light-emitting-diode (LED)-based NIR-PIT, especially when comparing the required total energy (J/cm²). This problem can be overcome by prolonged exposures with LED-based NIR light. In comparison, a disadvantage of laser-based light exposure is the off-target toxicity caused by the strong fluence rate¹⁰⁶. As mentioned before, being developed for the depletion of cancer or cancer-associated cells, sufficient exposure to NIR light is one major difficulty. Therefore, in most *in vivo* models, a high fluence rate is preferred to reach internal tumor tissues with sufficient energy to deplete targeted cells. Although NIR light is reported to penetrate several centimeters deep, methodical improvements by using light collimators or fiber optic diffusers are used to intensify the required light delivery into targeted tumor tissues¹⁰⁷. Therefore, cell depletion in the skin as a terminal tissue, which is easy to access by NIR light, appears promising. Moreover, due to the strong epidermal tropism of CD8 T cells, those alloreactive cells are only few micrometers away from the exterior, therefore optimal to be reached by NIR light.

An important factor that needs to be considered when using antibody-based therapy is penetration efficacy. By using an inflammation model of cutaneous aGVHD, a physiologically increased vascular permeabilization can be assumed. The results presented here have demonstrated that skin exposure to NIR light does not induce histological damage to the epidermal and dermal tissue. Changes in the integrity of cellular composition, increased cell death or changes in the expression of the inflammation marker elafin could not be detected upon treatment with NIR light. Consequently, these results, together with several *in vivo* reports and successful completion of a skin exposed NIR-PIT phase I clinical trial (NCT02422979), emphasize the safety of NIR light for the treatment of skin tissues.

In principle, the published protocol by Sato et al. for NIR-PIT-based regulatory T cell depletion including a single treatment with 100 J/cm² one day after mAb administration, is transferable to perform skin localized CD8 T cell depletion⁹⁷. However, repeated NIR light treatments over three days ensured that subsequently infiltrating CD8 T cells are specifically targeted and depleted from the respective skin graft. This aspect might have contributed to the improved outcome in our studies by returning the skin graft into relatively homeostatic conditions, as discussed later. Although kinetic studies have not been performed *in vivo*, the efficient and permanent effects achieved by repeated NIR-PIT treatment are self-designating. The results presented here are in line with another recent report on NIR-PIT based depletion of cutaneous mast cells, where targeted cells were efficiently depleted from *ex vivo* cultured skin biopsies¹⁰⁸. Therefore, the recently published work created from the here presented CD8-targeted NIR-PIT supports the application of NIR-PIT for dermatological use¹⁰⁰.

4.1.1 NIR-PIT for local therapy of skin diseases

Systemic or topical immunomodulators such as corticosteroids, calcineurin inhibitors or anti-metabolites are the first choice for controlling immune-mediated skin diseases. When given systemically, these drugs have strong immunosuppressive functions causing various severe side effects. Biologicals are widely used to treat several skin and other diseases with great success¹⁰⁹. However, those immunotherapeutic agents function systemically and, in some instances, also cause systemic depletion of immune cells. It is therefore plausible that this immune modulation can lead to systemic and severe side effects. Given the possibility of localized immune cell depletion by NIR-PIT, undesirable systemic effects could be overcome by selectively targeting the central cellular mediator of skin pathology.

In the context of aGVHD, it was demonstrated that CD8 T cells are required for the initiation and progression of skin inflammation. The NIR-PIT mediated local depletion of CD8 T cells from skin grafts completely reversed aGVHD pathology in the applied model. Based on the localized ablative properties of NIR-PIT, CD8 T cell populations were still detectable in splenic tissue demonstrating the possibility to mount a CD8 T cell-mediated immune

response at non-treated sides. In respect of HCT, unwanted pathological processes such as cutaneous aGVHD can be targeted by NIR-PIT while sparing systemic favorable immunological responses such as anti-tumor reactions or protection from opportunistic infections. As indicated, in contrast to their negative impact on the formation of cutaneous aGVHD, CD8 T cells are crucial for the execution of the anti-tumor response upon HCT. Based on the donor-recipient loci miss-match, leukemia-associated minor alloantigens are required for immunosurveillance and protection of recurrent tumors. Therefore, cognate interaction of cytotoxic CD8 T cells and tumor cells is required ^{110, 111}. Moreover, it was shown that infusion of *ex vivo* peptide-primed cytotoxic CD8 T cells or memory CD8 T cells are able to induce a strong anti-tumor response ^{112, 113}. Another important property that was overserved in patients transfused with CD8 T cell-depleted marrow graft was that CD8 T cells are required to prevent graft failure upon transplantation ¹¹⁴. Therefore, especially in patients with cutaneous aGVHD, skin localized depletion of CD8 T cells by using NIR-PIT could overall show beneficial outcomes.

Beyond that, localized depletion of CD8 T cells could be valuable for other dermatological diseases. For instance, it was demonstrated that depletion of CD8 T cells from psoriatic human skin grafts reverses clinical manifestations ¹¹⁵ and depletion of melanocyte-directed cytotoxicity induced by intraepithelial CD8 T cells could protect from progressing vitiligo ¹¹⁶. Nonetheless, NIR-PIT is clearly not limited to CD8 T cells, in theory, any cell can be targeted by the conjugation of a mAb to the photosensitizer IRDye-700DX. For instance, CD4 T cell targeted NIR-PIT depletion could be beneficial in various T_H1/2/17 driven inflammatory skin diseases or could resolve tumor progression of mycosis fungoides. In general, any approach with the aim of exclusively skin immune modulation by circumventing systemic effects is plausible.

4.1.2 Role of CD8 T cells in cutaneous aGVHD

It is well accepted that infiltrating CD8 T cells play a major role in the initiation and progression of interface dermatitis. In aGVHD, a keratinocyte-directed immune response is the driving factor of cutaneous manifestations. Epithelial cells strongly upregulate MHC-I and low MHC-II molecules as well as chemoattractant molecules CXCL9-11 in response to inflammatory stimuli such as IFN γ . The combination of these two incidences might explain the strong epidermal CD8 T cell tropism and thereby make keratinocytes an attractive target for allogeneic recognition in aGVHD by these cells. Still, it was surprising to see that ablation of infiltrating alloreactive CD8 T cells by NIR-PIT inhibited cutaneous manifestations in humanized aGVHD mice. As demonstrated, the reversed pathology was not limited to keratinocyte cell death. Skin localized CD8 T cell depletion led to a reduction of the inflammatory cutaneous aGVHD biomarker elafin and altered recruitment of alloreactive CD4 T cells. One explanation might be that transplanted human split skin is rarely populated with

human leukocytes at the time of aGVHD induction. It is likely that most of the resident APCs, such as LC egress the skin immediately after transplantation to prime the adaptive immune response^{117, 118}. However, this probably occurs before transfusion of allogeneic PBMCs. Therefore, priming and activation of allogeneic CD4 T cells might be a secondary effect due to the absence of human MHC-II molecules. This would support the hypothesis that primed skin infiltrating CD8 T cells produce IFN γ which in turn induces the production of CXCL9-11 chemokines by targeted keratinocytes, finally promoting the recruitment of additional CD8 and CD4 T cells^{119, 40}. Although IFN γ production by infiltrating CD8 T cells could not be detected in the respective histological slides due to methodical difficulties, the reactivity of these cells was demonstrated by granzyme B staining. It is well reported that most of the cytotoxic CD8 T cell co-expresses granzyme B and IFN γ ¹²⁰.

As a consequence of missing intraepidermal and dermal CD8 T cells as well as altered numbers of CD4 T cells, inflammatory markers such as elafin are consequently downregulated. Skin-derived elafin, the best described biomarker for cutaneous GVHD, is generally expressed by keratinocytes upon TNF α stimulation⁵⁰. Therefore, modulated numbers and reactivity of infiltrating T cells could explain the reduced expression, as seen upon CD8-directed NIR-PIT. Both reactive CD4 and CD8 T cells are capable of producing high amounts of TNF α upon allogeneic activation¹²¹. One study could show that skin biopsies with high and low expression levels of elafin correlated with high and low numbers of T cells, respectively, including enriched CD8 T cells populations⁵⁰. The final observation that CD8 T cell depletion by NIR-PIT inhibited keratinocytes' cell death seems very plausible. Collectively, in these studies, all skin grafts of humanized cutaneous aGVHD mice showed highly reactive cytotoxic CD8 T cells. Therefore, it is very likely that depletion or inhibition of these cells influenced this pathologic phenomenon. However, as discussed later, it is questionable whether this cytotoxic activity leads to enhanced apoptotic cell death. Data from GVHD-like mouse models of ovalbumin-expressing basal keratinocytes revealed that OT-I-derived CD8 T cells clearly induce histopathology of cutaneous aGVHD. Moreover, the authors have demonstrated that the cytotoxic function of reactive CD8 T cells derives from secreted IFN γ ^{122, 123}. In line with that, a similar study using the same mouse model demonstrated that PD-1 deficient OT-I CD8 T cells caused severe skin manifestations due to their unregulated activity¹²⁴. Studies using human skin explants demonstrated that CD8 T cells clearly induce phenotypic cutaneous aGVHD upon pulsing with allogeneic dendritic cells. Here, the authors have shown that the infiltration into *ex vivo* cultured skin biopsies depends on the recruitment of CXCR3 expressing CD8 T cells by IFN γ -regulated CXCL10/11. Additionally, the keratinocyte-directed damage was prevented by the addition of regulatory T cells¹²⁵.

Similar to the present work, published characterization of the cellular skin infiltrate in aGVHD and lichenoid cGVHD samples revealed high numbers of CD8 and CD4 T cells detectable in the dermis and epidermis. Here, an outstanding observation was the high frequency of IFN γ producing T cells, while overall CD8 T cells outnumbered CD4 T cells. Consistent with this, the authors could detect a clear immunological type I response in both aGVHD and lichenoid cGVHD as indicated by an increased expression of CXCL9, CXCL10 and CCL5⁵⁰.

4.2 Epidermal homeostasis

Tissue homeostasis is generally regulated by immunologic silent programmed cell death mediated by apoptosis or autophagy. Apart from that, evolution developed alternative pathways such as the cornification of epidermal keratinocytes. This differentiation enables an epithelial barrier function by generating a lipid rich final layer of the skin which is largely impermeable to water. These corneocytes are not only constantly lost through mechanistic influence, but are also renewed by stable proliferation of basal keratinocytes and their subsequent differentiation. Therefore, caspase-dependent apoptosis is not part of skin homeostasis compared to other terminal differentiated cell types. Caspase-14 is the only known active caspase in normal skin involved in keratinocyte differentiation by filaggrin remodeling independent of apoptosis¹²⁶.

Apoptotic cell death of keratinocytes occurs for example in the basal layer following irradiation with UVB light and subsequent DNA damage, known as sunburn, representing the most intensively studied pathomechanisms in this context. In this context, it was shown that cell death of keratinocytes can be blocked by caspase inhibition or transfection with anti-apoptotic protein BCL-2 downstream to intrinsic activation, mediated by mitochondrial depolarization, cytochrome c release and p53 activation¹²⁷. Similar to intrinsic cell death activation, extrinsic initiation by TNF α -dependent DR-ligation is thought to result in the activation of the apoptotic machinery in epidermal cell death-related diseases such as GVHD and adverse drug reactions^{128, 127}. However, in psoriasis, known as a TNF α dominated skin disease, aberrant keratinocyte cell death is not described. It is generally postulated, that NF κ B signaling in response to TNF α suppresses premature keratinocyte cell death by causing hyperproliferation and acanthosis due to the expression of apoptotic regulators¹²⁹. In this regard, NF κ B-dependent inhibitor of apoptosis (IAP) expression such as XIAP, c-IAP1 and c-IAP2 blocks the activity of caspase 3, 7 and 9 leading to pro-survival signaling and apoptosis resistance of primary keratinocytes^{130, 131}. In line with that, mitochondrial regulatory entity, second mitochondria-derived activator of caspase (Smac/DIABLO), in turn blocks IAPs leading to pro-apoptotic signaling. Another important regulator in the skin represents cFLIP, which is highly expressed in basal keratinocytes¹³². The different isoforms interact with caspase 8 upon recruitment to FADD after death-receptor-ligation, thereby

inhibiting its activity and protecting keratinocytes from TNF α -dependent apoptosis¹³³. To confirm this statement, the presence of cFLIP was observed in primary keratinocytes upon different stimuli. After TNF α or IFN γ stimulation, cFLIP remained unchanged; however, upon STS stimulation, protein levels were completely lost, correlating with caspase 3 activation and apoptotic cell death (data not shown). Similar to that, regulatory authorities of necroptotic cell death and inflammation were additionally described. Probably the most studied enzyme represents A20 (TNF inducible protein 3). This enzyme regulates NF κ B activation and RIP3-dependent necroptosis through its deubiquitinating properties upon TNF α signaling. It was shown that deficiency of A20 results in strong inflammation and MLKL dependent cell death^{134, 135, 136}. Based on these characteristics, several units developed to protect the skin from pre-mature cell death. Studies focusing on DR-dependent apoptotic signaling often combine TNF α with Smac/DIABLO to investigate downstream signaling. Finally, the combination of caspase inhibitor zVAD with TNF α and Smac/DIABLO, or A20 deficiency leads to necroptotic signaling and inflammatory cell death enabling specific investigations.

4.3 Pathology of type I driven interface dermatitis

Interface dermatitis is characterized by band-like, suprabasal epidermal cell injury that is traditionally described to be mediated by the adaptive immune system and here specifically by T cells. Lichen planus is well known for its histologic changes encompassing interface dermatitis. In addition to being part of a systemic disorder, interface dermatitis is a hallmark of histologic changes found in lupus erythematosus, stevens-johnson syndrome (SJS), toxic epidermal necrolysis (TEN), and GVHD¹³⁷. Pathogens and drugs are described to cause cross-reactivity between self- and foreign-antigens driving keratinocyte-directed cytotoxicity. In contrast to other interface dermatitis manifestations, GHVD results from MHC-recognition on the background of allogenicity. An overarching commonality is the orchestration of pathology by different members of the IFN family (I-III). Histopathological liquefaction or vacuolization of the basal keratinocytes appearing as “cloudi swelling”, also termed as oncosis, is a characteristic feature of interface dermatitis¹³⁸. The phenomenon results from rapid cytoplasmic swelling, membrane rupture, and organelle breakdown as known from necrotic cell death and independent of caspase activity. However, in contrast to apoptosis, markers indicating vacuolization and subsequent cell death are missing¹³⁹. Mechanistically, it is believed that the damage of basal keratinocytes results from exocytosis of cytotoxic granular and the exposure to FAS or TNF α , released or presented by reactive infiltrating cytotoxic CD8 T cells. These cells are primarily recruited into epidermal sides by keratinocyte-secreted chemokines CXCL9-11 and the respective receptor CXCR3 expressed on reactive T cells¹⁴⁰. Here, CD8 T cells exhibit a leading role, based on the interaction between TCR-CD8 complex and MHC-I molecules, which are highly expressed on epithelial cells causing subsequent CD8 T cell activation^{140, 141}.

4.4 Necroptosis in interface dermatitis

Several recent investigations demonstrated that necroptosis occurs as an alternative regulated cell death pathway in lesional keratinocytes of lichenoid tissue reactions/interface dermatitis. Firstly, this was reported in the context of adverse drug reactions by the observation that keratinocytes rather undergo phenotypic necrotic cell death instead of the well known apoptotic cell death ¹⁴². Here, the authors recognized annexin A1, secreted by CD14 monocytes, as a cytotoxic molecule that induces keratinocyte RIP3-dependent necroptosis. Interestingly, the cytotoxic response depended on drug-primed, IFN γ producing CD8 T cells and could be prevented by MHC-I blocking ¹⁴³. A follow up study revealed that extracellular serum levels of RIP3 correlated with pathological signs such as skin detachment, keratinocytes cell death and clinical parameters in patients with SJS/TEN. Moreover, supernatant analysis of necroptotic keratinocytes revealed the presence of extracellular RIP3 ¹⁴⁴. Similarly, transcriptomic analysis of patients with lichen planus or cutaneous lupus erythematosus termed as lichenoid tissue reactions/interface dermatitis, showed a clear pathway association with IFN (type I and II) signaling. Furthermore, flow cytometry analysis of isolated infiltrating T cells demonstrated strong production of IFN γ and TNF α and in relation to that, histological data revealed strong expression of RIP3 in affected keratinocytes. Additionally, the authors could show that keratinocyte cell death induced by TNF α /IFN γ could be reduced by silenced expression of RIP3 and MLKL phosphorylation ¹⁰⁴. In line with that, recently published transcriptomic analysis of lichen planus and hypertrophic lichen planus skin biopsies demonstrated strongest association of IFN γ and upregulated gene expression based on gene ontology. The same study could show that the keratinocyte-directed cytotoxic response induced by activated PBMCs is enhanced by IFN γ pre-stimulation of the same keratinocytes. Although the authors described apoptosis as a primary cause of keratinocyte cell death, they could additionally detect activation of the necroptotic pathway. Moreover, the authors could prevent keratinocyte cell death by inhibiting JAK/STAT pathway using baricitinib (JAK1/2 inhibitor) or by MHC-I blocking ⁵⁸.

4.5 Concept of IFN γ in the context GVHD

The role of IFN γ following HCT is extremely versatile and cannot be simplified for a single pathway. However, depending on the responding cell, favorable or adverse outcomes influence the condition of the allogeneic recipient. First of all, by amplifying the reactivity of allogeneic T cells in line with increased MHC expression, engrafted T cells patrol the recipient organism to detect and fight recurrent tumors or are recruited to the neoplastic side. Moreover, it was demonstrated that IFN γ itself has direct anti-proliferative, anti-angiogenic, and pro-apoptotic effects on tumor cells. As the major cause of post-HCT mortality,

neutralization or deficiency might have an unfavorable outcome ²². Second, this immunogenicity might have protective effects against opportunistic infections, a major cause of non-relapse mortality.

For GVHD, IFN γ was demonstrated to have a dual role in the pathogenesis and progression of the disease depending on the target cell and tissue. Here, much of our knowledge about the pathomechanisms in GVHD comes from *in vivo* studies. Importantly, mice that received allogeneic IFN γ R KO splenocytes experienced reduced GVHD manifestations with prolonged survival. This effect was shown to depend on impaired recruitment of CXCR3-expressing donor T cells into target organs ¹⁴⁵. Early studies of experimental aGVHD demonstrated that exogenous IL-12 injections worsen target organ pathology in aGVHD; however, they protect from cGVHD by polarizing the immune response from a T_H2 to a T_H1 driven reaction ¹⁴⁶. On the other side, mice receiving allogeneic grafts experienced less GVHD when they received single injections with exogenous IL-12 on the day of HCT. The curative effects of IL-12 were attributed to secondary produced IFN γ and the upregulation of checkpoint inhibitors FASL, PD-L1, and indolamine 2,3-dioxygenase (IDO). These molecules dampen the adaptive immune response by the induction of T cell apoptosis and anergy ^{147, 148}. Another study demonstrated that mice, which received allogeneic IFN γ KO CD4 T cells, had reduced liver and intestinal GVHD score but ameliorated lung and skin pathology. The authors hypothesized that this phenomenon is driven by a polarized T_H17 immune response ¹⁴⁹. Profiling of murine cutaneous aGVHD revealed a strong T_C1 and to a lesser extent T_C17 polarization of reactive CD8 T cells. Here, transcriptional analysis revealed high expression of IFN γ , especially by intraepithelial donor CD8 T cells. When these mice were depleted for LC, skin pathology was reversed, probably due to the reduced reactivity of skin resident CD8 T cells ¹².

However, pre-clinical mouse models have their limitations which make an imperfect translation into the human system. Therefore, researchers have to consider microbiota and housing conditions, genetic disparity, and therefore reactivity of the immune system when interpreting murine data ⁶⁴. Moreover, the discussed observations are generally comprehensive for the organism or respective organ, and investigations on the cellular level might differ from those observations.

4.6 Necroptosis in cutaneous aGVHD

Generally, epithelial damage that occurs during aGVHD is thought to result from regulated caspase-dependent apoptotic or unregulated necrotic cell death. However, the present data demonstrate for the first time that regulated necrosis - called necroptosis – is highly activated in cutaneous lesions of aGVHD patients and might resemble a major pathological pathway.

In the context of aGVHD and cGVHD, despite the controversy about the type of immune response, it was reported that overall IFN γ in comparison to IL-4, IL-17 or IL-22 was the most abundant produced inflammatory cytokine detected in respective skin biopsies. TNF α and Fas expressions for instance, as established apoptosis and necroptosis inducers, were not affected or even downregulated in aGVHD⁴². In line with that, sections studied in the present work from aGVHD patients showed a strong infiltration of T-bet positive cells indicating IFN γ production and signaling. However, profiling of T-bet negative lymphocytes was not addressed in this work; therefore, a statement about the infiltration of GATA3 expressing T_{H/C}2 or ROR γ T expressing T_{H/C}17 cells cannot be made.

4.6.1 Pro-necroptotic properties of IFN γ on epidermal keratinocytes

Several studies demonstrated that IFN γ has a strong cytotoxic property on human keratinocytes which is thought to be a consequence of immunological silent apoptosis^{150, 151, 58}. However, here it could be demonstrated that keratinocytes rather undergo necroptotic cell death due to a polarized expression profile. Especially *de novo* expression and upregulation of ZBP1 and MLKL respectively, licensed keratinocytes for this novel cell death pathway. Moreover, due to upregulated expression of STAT1, constitutive signaling of IFN γ led to an autoregulated amplification of this cytotoxic pathway. Much of our knowledge of necroptosis and its signaling pathway comes from DR-signaling in combination with caspase inhibition or genetic modification, leading to RIP1 activation¹⁵². However, physiological activation in regard to inflammation remains a riddle. In respect to that, a surprising novel initiator of necroptosis function was recently described for ZBP1. Here, the authors demonstrate that keratinocytes and gut stem cells undergo necroptotic cell death upon RNA binding of endogenous retro-elements by ZBP1 when RIP1 is mutated. Since this was holding true even under sterile conditions, it remains to be determined which elements are finally leading to ZBP1 homodimerization. In respect of the present data, it could be shown that IFN γ -mediated cell death depends on the presence of ZBP1, RIP3 and MLKL, independent of caspase activation. Surprisingly, both human and murine keratinocytes and fibroblasts react differently to stimulation with IFN γ , as murine keratinocytes show phosphorylation of RIP3 and MLKL only when RIP1 is genetically mutated^{153, 154, 155, 156}. In contrast to that, stimulation with IFN γ in human keratinocytes results in RIP1 independent RIP3 and MLKL activation.

Apart from RIP1 activation, necroptotic signaling and downstream cell death can be induced by ZBP1-dimerization and TRL-3/4-dependent TRIF signaling. Only these three molecules are reported to contain a RHIM domain and are therefore licensed to initiate necroptotic signaling via the interaction with RIP3. Since it was shown here that IFN γ stimulation does not induce RIP1 phosphorylation and microbial activation of TLR-3/4 can be excluded by the

experimental setup under sterile conditions, an activation through ZBP1 seems very likely. Therefore, this work can present for the first time, the occurrence of ZBP1-mediated necroptotic cell death in context of inflammatory skin disease and demonstrate its natural signaling behavior in human keratinocytes.

In line with that, viability analysis of IFN γ stimulated primary keratinocytes revealed a clear and distinct pattern that was different from STS stimulated apoptotic keratinocytes. It is well accepted that annexin V (Apotracker) single positive cells mark early apoptotic cells; whereas late apoptotic double positive cells are indistinguishable from necrotic or necroptotic cells. PI single positive cells were described to be early necrotic or necroptotic cells^{157, 158}. Therefore, as demonstrated by flow cytometry analysis, Apotracker single positive cells were not detectable in IFN γ stimulated keratinocytes, excluding the occurrence of apoptotic cell death as seen with STS.

Histopathologically, cutaneous aGVHD is categorized by vacuolization of the basal layer (grade I), satellite cell necrosis (grade II), pyknotic nuclei and eosinophilic cytoplasm, often with subepidermal clefts (grade III), and finally complete loss of the epidermis (grade IV). Translationally, by using IFN γ in our *ex vivo* system, we could partially recapitulate these clinical manifestations, thereby clarifying and elaborating previously reported observations on morphological changes induced by IFN γ /TNF α in three-dimensional skin models¹⁰⁴. This data set demonstrates that keratinocytes in the basal layer showed an active STAT1 signaling transduction with highly positive signals for phosphorylated MLKL, colocalized with vacuolized and dead keratinocytes. The morphological changes in the suprabasal layers with increased numbers of pyknotic keratinocytes were clearly induced by the treatment with IFN γ , although STAT1 signaling was not detectable but reversible by tofacitinib. Probably, a kinetic investigation would open further insights. Moreover, the hypothesized pathway of ZBP1 induced, RIP3 mediated and MLKL executed necroptotic cell death was overall upregulated in these skin sections, indicating the consistency of this novel IFN γ regulated pathological pathway. Generally, the observed pathological changes match the reported results seen in mice with an epidermal deficiency for Fas-associated death receptor domain (FADD) or RIP1. These mice developed inflammatory skin lesions with necrotic and pyknotic keratinocytes depending on necroptotic signaling, which was reversible by RIP3 mutation. In addition and parallel to our observations, the authors showed how epidermal cell death was independent from apoptotic CC3 signaling¹⁵⁹.

Allogeneic interactions of primary keratinocytes with mismatched leukocytes used to result in unresponsiveness. Recently described co-culture models with prior stimulation by using IFN γ , however, resulted in activation of the adaptive immune response. This was based on increased MHC-TCR interaction capability and costimulation by the primary keratinocytes⁵⁸.

⁵⁹. Consistent with this, the results presented here show that in turn production of IFN γ after allogeneic activation displays the central cytokine in keratinocyte-directed cytotoxicity resulting in necroptotic cell death.

4.6.2 Clinical implication of necroptosis during acute GVHD

In the context of inflammation, DAMPs ejected from dying cells are thought to function as a fire-accelerator in aGVHD. Therefore, it is considerable that necroptosis contributes to the inflammatory environment, as it has been shown that, for instance HMGB1, ATP, DNA, IL-33 (ST2-ligand) IL-6, TNF α , and IL-1 α/β are released from these dying cells. Moreover, different studies showed that a RIP3-dependent NF κ B activation leads to the expression of such inflammatory mediators or the expression of chemoattractant molecules. Therefore, it can be hypothesized that specific inhibition of the necroptotic signaling cascade in aGVHD might reduce inflammation on the one hand and epithelial cell death with improved barrier function on the other hand. Regarding necroptosis inhibition, a potential target displays RIP3 as an activator of cell death and inflammation. By using well-described GSK'872, necroptotic cell death could effectively be blocked *in vitro*. However, its usability and efficiency *in vivo* remains to be proven, since higher concentrations were reported to result in apoptotic cell death activation ¹⁶⁰. Also, a very recent publication demonstrated prevention of intestinal epithelial necroptotic cell death by GSK'872 treatment in mice, genetically suffering from inflammatory bowel disease. Similar to RIP3 KO mice, here GSK'872-treated mice showed an improved overall survival, proposing GSK'872 as a potential therapeutic agent ¹⁶¹. Another potential target for the specific inhibition of necroptotic cell death is MLKL. Treatment with necrosulfonamid, a specific MLKL inhibitor, prevented epidermal cell death in xenogeneic mice induced by adverse drug reactions ¹⁴³. However, additional positive reports on specific MLKL inhibition or the usage of necrosulfonamide are currently lacking. With RIP1 as the first necroptosis associated molecule, specific kinase inhibition has been intensively studied. In this regard, several investigations described necrostatin-1 as a potential molecule to inhibit necroptotic cell death ^{86, 162}. However, compared with the exclusive pro-necroptotic function of RIP3 and MLKL, RIP1 was shown to activate both the necroptotic and apoptotic signaling pathway downstream to DR-signaling ¹⁶³. Moreover, RIP1 was reported to prevent spontaneous formations of necroptotic lesions at epithelial sides, mediated by ZBP1 ^{155, 164}. These data challenge its suitability as a therapeutical target to prevent necroptosis.

Because HCT is usually performed on the background of hematologic malignancies, recurrence of the malignant cells remains the primary cause of post-HCT mortality. Here, tumor cells developed mechanisms to escape from chemotherapy-induced apoptosis ¹⁶⁵. Therefore, it is indispensable to persist an immunoreactive state in post-HCT patients in

order to perform a GVL effect mediated by the engrafted donor leukocytes. This protective state is often lost in patients treated with potent immunosuppressive agents such as calcineurin-inhibitors or anti-metabolites. A mechanistic separation of GVHD-driven damage to healthy non-hematopoietic tissue from GVL-driven tumor-directed cytotoxicity remains a major goal ¹⁶⁶. One idea is to induce necroptosis pharmacologically in tumor cells. Here, a combined treatment with chemotherapy and Smac/DIABOLO, a specific IAP inhibitor leading to the deubiquitylation and downstream activation of RIP1, can induce apoptosis and necroptosis of chemotherapy resistant tumor cells ^{167, 168}. In contrast, with the data presented here, it can be hypothesized that low dose immunosuppressive treatment in combination with necroptotic cell death inhibition at affected GVHD target organs could reduce its selective severity. Moreover, by the circumstance of reduced epithelial damage in the skin or intestine, barrier function would be retained, thereby protecting patients from microbial infections. Finally, by the fact that necroptotic inhibition acts downstream to donor immune cell activity, reactive T cells remain potent to induce apoptosis-dependent tumor-directed cytotoxicity.

4.6.3 Keratinocyte cell death in aGVHD

Based on the strong infiltration of granzyme B-expressing cytotoxic CD8 T cells, it was somehow surprising that caspase activation, indicated by cleaved caspase 3, was rather low in keratinocytes of active lesions (data not shown). Granzyme B is a member of the serine proteases family that is enriched in granules of activated cytotoxic T cells and NK cells. Upon degranulation in the immunological synapse, pore-forming perforin enables granzyme B to enter targeted cells. Here, for instance granzyme B cleaves BID (BH3-interacting domain agonist), which in turn demolishes mitochondrial membrane integrity and leads to cytochrome c-dependent apoptotic cell death ¹⁶⁹. Possibly, the weak activity of caspase 3 in cutaneous aGVHD results from the previously discussed apoptotic-resistance of primary keratinocytes. Literature focusing on degranulation and keratinocyte cytotoxicity in response to allogeneic interaction is limited and was not further addressed in this work. However, due to the ratio of severe histopathology and weak caspase 3 activation, alternative pathological pathways such as necroptosis were addressed to elucidate pathomechanisms of cutaneous aGVHD.

Accordingly, early reports of apoptotic keratinocytes in cutaneous GVHD can be challenged by novel insights and the use of more accurate methods. Thus, epithelial apoptosis was generally detected by TUNEL-assay performance of respective skin sections. Here DNA-fragmented keratinocytes correlated with ascending aGVHD grading ^{170, 171, 172}. However, recent investigations demonstrated that TUNEL-positive staining does not exclusively indicate apoptotic cell death but rather any regulated cell death that induces DNA damage, also including necroptosis ⁸³. In respect to that, PARP-1 (Poly(ADP-ribose)-polymerase-1), a

DNA-repair machinery, was shown to be activated in response to necroptotic stimuli and necrosome activation. These observations demonstrated DNA-damage during necroptosis processes ¹⁷³. In line with that, an early study described that the voluminous, large TUNEL-positive cells outnumber the small condensed TUNEL-positive cells in the epidermis of murine cutaneous aGVHD ¹⁷⁴. Finally, the literature search revealed rather limited or no information about caspase dependent apoptotic cell death during cutaneous aGVHD. One report demonstrated caspase 3-activation in skin biopsies of severe aGVHD patients with Fanconi anemia. Here, patients with this rare disease are hypersensitive to DNA-crosslinking due to defects in their DNA-repair mechanisms ¹⁷⁵. So far, apart from this report no other publication demonstrated caspase-dependent cell death of epidermal keratinocytes during cutaneous aGVHD. Experimental murine models of aGVHD showed that keratin 15 expressing basal keratinocyte “stem cells” located in the rete ridges of the epidermis are primary targets of allogeneic T cells. It was hypothesized that loss of keratin 15 and occurrence of TUNEL positivity in the murine skin indicate targeted apoptotic cell death ¹⁷⁶. However, later investigation demonstrated how those keratin 15 expressing murine keratinocytes showed a clear anti-apoptotic expression profile and were protected from apoptotic cell death ⁴⁴. As mentioned before, it is noteworthy that these observations were made in murine GVHD models and have not been described for human samples.

4.7 JAK/STAT inhibitors for aGVHD

On the basis of strong STAT1 activation and autoregulation detected in lesional keratinocytes from cutaneous aGVHD patients, the therapeutic use of JAK/STAT inhibitors seems plausible. However, it was surprising to see that complete prevention of cell pathology was observed by the addition of JAK/STAT inhibitor tofacitinib in *in vitro* and *ex vivo* IFN γ stimulated keratinocytes and split skin, respectively. Indeed, as a first generation JAK/STAT inhibitor, tofacitinib was shown to be safe and highly efficient in treating inflammatory diseases. For example, tofacitinib was recently approved by the Food and Drug Administration (USA) for therapeutical use in patients with psoriasis arthritis and is currently being tested in several clinical trials for its usage in atopic dermatitis, psoriasis and sjögrens' syndrome ¹⁷⁷. In line with that, CD8 T cell-mediated mucocutaneous GVHD-like disease proved to be dependent on the cytotoxic properties of IFN γ and could be inhibited by treating with tofacitinib ¹²². Additionally, a group studying experimental humanized aGVHD *in vivo* showed attenuation of cutaneous manifestations due to decreased T_H1 polarization mediated by pacritinib, a JAK2 inhibitor. In addition, the authors observed induction of regulatory CD8 T cells that contribute to the control of aGVHD ⁶⁹. Finally, ruxolitinib, a novel JAK1/2 inhibitor, was recently approved for the treatment of steroid-refractory aGVHD by inducing efficient immunosuppression and reversing pathological manifestations ^{102, 178}. Mechanistically, it has

been shown that these effects result from impaired differentiation of IFN γ and IL-17 producing T_{H/C}1/17 T cells¹⁷⁹. However, beneficial effects for the responding non-hematopoietic cells are underrepresented, although epithelial damage strongly correlates with disease-associated morbidity and mortality. In line with this, promising topical administrations of ruxolitinib are currently being tested in clinical trials for the treatment of cutaneous non-sclerotic (NCT03954236) and sclerotic (NCT03395340) cGVHD. In agreement with the literature, the results demonstrated here highlight the efficacy and support the oral or topical use of JAK/STAT inhibitors in IFN γ -driven cutaneous aGVHD and other lichenoid tissue reactions/interface dermatitis such as adverse drug reactions¹⁸⁰, lichen planus⁵⁸, or cutaneous lupus erythematosus¹⁸¹.

4.8 Conclusion

Improvements in infrastructure and emerging economical changes, in combination with the growing use of unpretentiously accessible peripheral blood stem cells, allowed annual frequencies of curative stem cell transplantations to dramatically increase^{182, 183}. Along with this indispensable medical treatment, incidences of lethal GVHD are rising too²⁷. Therefore, understanding the pathomechanisms of aGVHD remains a major goal for the development of new therapeutic strategies.

Isolated non-advanced (grade I) cutaneous aGVHD is generally treated successfully with topical steroids. However, steroid-refractory or advanced (grade II-IV) cutaneous aGVHD patients are generally treated with systemic immunosuppressive agents or second-line therapy. The here described CD8-directed NIR-PIT represents an effective alternative strategy for the treatment of cutaneous aGVHD, thereby modulating the local immune system at pathological sites to circumvent systemic immune suppression, which is essential for the GVL effect and protection from opportunistic infections. Moreover, as a universal approach by targeting different cell types in the context of different pathological conditions, this makes NIR-PIT a promising tool for scientists and clinicians in dermatology. In addition, the results presented here demonstrate the importance of alloreactive CD8 T cells in the context of cutaneous aGVHD manifestation and progression.

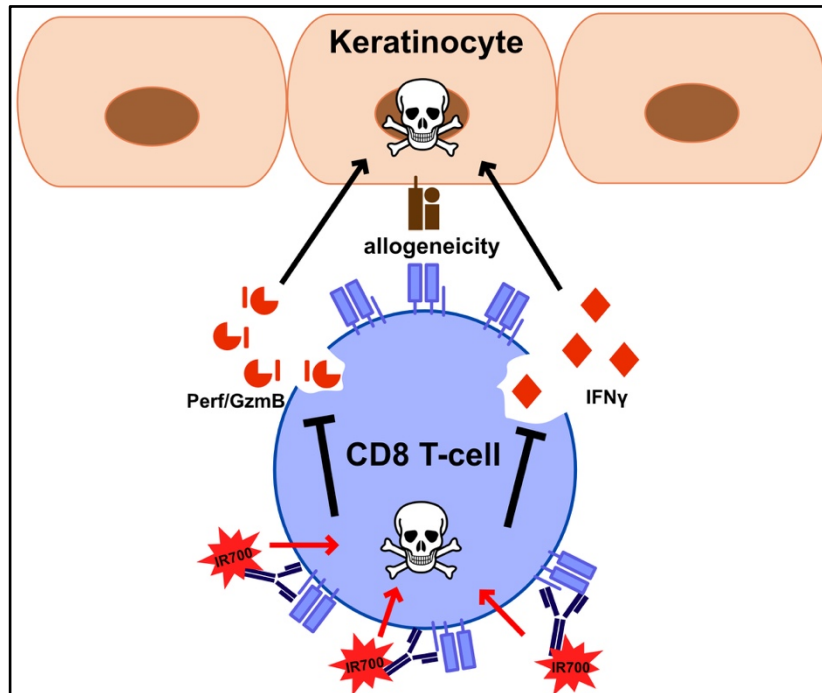


Fig. 24: CD8 NIR-PIT for the treatment of cutaneous aGVHD. During cutaneous aGVHD, alloreactive CD8 T cells infiltrate the skin causing damage to targeted keratinocytes by the release of $\text{IFN}\gamma$ and cytotoxic granzyme B/perforin. Upon binding to CD8 T cells by CD8-IR700 and subsequent exposure to NIR light, targeted cells are depleted from the skin. Therefore, pathological manifestations including downstream reactions are inhibited.

Investigations on pathological processes downstream to allogeneic activation revealed that necroptosis, as an immunogenic form of regulated cell death, is activated in cutaneous lesions of aGVHD. The present work could describe a new pathological role of $\text{IFN}\gamma$ in the context of keratinocyte pathology and alloreactive consequences. It is hypothesized that necroptotic cell death in keratinocytes is induced by an altered expression profile regulated by STAT1 transcription factor mediated through *de novo* expression of ZBP1 and formation of the necrosome complex including activation of RIP3 and MLKL. Investigations unrevealing the initiation phase of necroptosis in respect to ZBP1 ligation and activation are necessary to predict its manifestation in health and disease in order to develop specific therapeutic interventions.

The identification of necroptosis as a highly regulated and relevant form of cell death of human keratinocytes paves the way for well-designed and targeted interventions. JAK/STAT inhibitors, blocking $\text{IFN}\gamma$ production and signaling, are already used as a second line therapy to treat aGVHD, thereby likely inhibiting the induction of necroptosis as an additional

favorable effect, so far not specifically recognized. Specific RIP3 kinase inhibitors such as GSK'872 would allow for a more selective intervention.

Increased extracellular levels of RIP3, measured in the serum of patients with intestinal aGVHD, suggest the occurrence of necroptosis at this organ site in addition to the skin. It clearly needs to be studied in further detail, if other target organs such as the gut in aGVHD also show necroptotic cell death activation. Still, interference of necroptotic signaling could prevent excessive damage to epithelial cells and thereby lower the inflammatory response in target tissues induced by necroptotic cell death. Moreover, a possible strategy of low-dose immunosuppressive agents in combination with necroptotic inhibitors could dampen GVHD while persisting GVL responses.

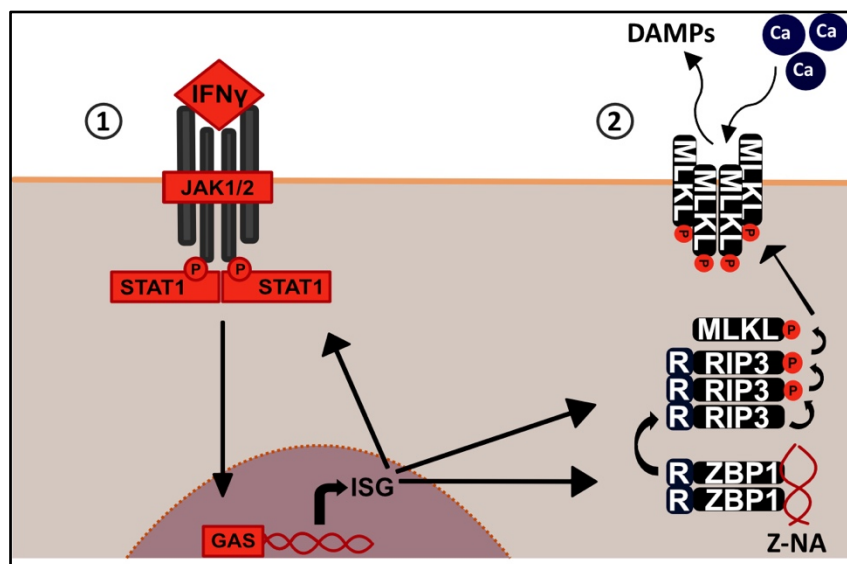


Fig. 25: Hypothesized model of IFN γ -regulated keratinocyte necroptosis. (1) IFN γ R signaling induces the activation and homodimerization of transcription factor STAT1. Upon translocation to the nucleus, ISG expression of *MLKL* and *STAT1* is increased whereas *ZBP1* is *de novo* expressed. (2) Newly synthesized ZBP1 is activated by left-handed Z-NA which leads to the formation of the necrosome complex, comprised of activated RIP3 and MLKL. As a consequence, MLKL-oligomers are transferred to the plasma membrane where they execute the lytic immunogenic cell death.

5 References

1. Litman, G. W. & Cooper, M. D. Why study the evolution of immunity? *Nat. Immunol.* **8**, 547–548 (2007).
2. Gasteiger, G. *et al.* Cellular Innate Immunity: An Old Game with New Players. *J. Innate Immun.* **9**, 111–125 (2017).
3. Bonilla, F. A. & Oettgen, H. C. Adaptive immunity. *J. Allergy Clin. Immunol.* **125**, S33–S40 (2010).
4. Pasparakis, M., Haase, I. & Nestle, F. O. Mechanisms regulating skin immunity and inflammation. *Nat. Rev. Immunol.* **14**, 289–301 (2014).
5. Nestle, F. O., Di Meglio, P., Qin, J. Z. & Nickoloff, B. J. Skin immune sentinels in health and disease. *Nat. Rev. Immunol.* **9**, 679–691 (2009).
6. Belkaid, Y. & Segre, J. A. Dialogue between skin microbiota and immunity. *Science (80-.)*. **346**, 954–959 (2014).
7. Iwasaki, A. & Medzhitov, R. Control of adaptive immunity by the innate immune system. *Nat. Immunol.* **16**, 343–353 (2015).
8. Laidlaw, B. J., Craft, J. E. & Kaech, S. M. The multifaceted role of CD4+ T cells in CD8+ T cell memory. *Nat. Rev. Immunol.* **16**, 102–111 (2016).
9. Annunziato, F., Romagnani, C. & Romagnani, S. The 3 major types of innate and adaptive cell-mediated effector immunity. *J. Allergy Clin. Immunol.* **135**, 626–635 (2015).
10. Chaplin, D. D. Overview of the immune response. *J. Allergy Clin. Immunol.* **125**, S3–S23 (2010).
11. Abbas, A. K., Murphy, K. M. & Sher, A. L2 (not recommended) Functional diversity of helper T lymphocytes. 787–793.
12. Santos E Sousa, P. *et al.* Peripheral tissues reprogram CD8+ T cells for pathogenicity during graft-versus-host disease. *JCI insight* **3**, (2018).
13. Kabashima, K., Honda, T., Ginhoux, F. & Egawa, G. The immunological anatomy of the skin. *Nat. Rev. Immunol.* **19**, 19–30 (2019).
14. Watt, F. M. & Green, H. Stratification and terminal differentiation of cultured epidermal cells. *Nature* **295**, 434–436 (1982).
15. Simpson, C. L., Patel, D. M. & Green, K. J. Deconstructing the skin: Cytoarchitectural determinants of epidermal morphogenesis. *Nat. Rev. Mol. Cell Biol.* **12**, 565–580 (2011).
16. Freedberg, I. M., Tomic-Canic, M., Komine, M. & Blumenberg, M. Keratins and the keratinocyte activation cycle. *J. Invest. Dermatol.* **116**, 633–640 (2001).
17. Guttman-Yassky, E., Zhou, L. & Krueger, J. G. The skin as an immune organ:

- Tolerance versus effector responses and applications to food allergy and hypersensitivity reactions. *J. Allergy Clin. Immunol.* **144**, 362–374 (2019).
18. Orlik, C. *et al.* Keratinocytes costimulate naive human T cells via CD2: a potential target to prevent the development of proinflammatory Th1 cells in the skin. *Cell. Mol. Immunol.* **17**, 380–394 (2020).
 19. Ho, A. W. & Kupper, T. S. T cells and the skin: from protective immunity to inflammatory skin disorders. *Nat. Rev. Immunol.* **19**, 490–502 (2019).
 20. Afkarian, M. *et al.* T-bet is a STAT1-induced regulator for IL-12R expression in naïve CD4⁺ T cells. *Nat. Immunol.* **3**, 549–557 (2002).
 21. Hu, X. & Ivashkiv, L. B. Cross-regulation of Signaling Pathways by Interferon- γ : Implications for Immune Responses and Autoimmune Diseases. *Immunity* **31**, 539–550 (2009).
 22. Falk, C. S. & Oliveira, M. J. Interferon-Gamma at the Crossroads of Tumor Immune Surveillance or Evasion. **9**, 1–19 (2018).
 23. Corporation, U. C. & Setlow, J. K. Interferon-Like Virus-Inhibitor. **149**, 0–2 (1965).
 24. Zaidi, M. R. & Merlino, G. The two faces of interferon- γ in cancer. *Clin. Cancer Res.* **17**, 6118–6124 (2011).
 25. Johnson-Huang, L. M. *et al.* A single intradermal injection of IFN- γ induces an inflammatory state in both non-lesional psoriatic and healthy skin. *J. Invest. Dermatol.* **132**, 1177–1187 (2012).
 26. Faragallah, W. H. Historical review. 330–339 (1988) doi:10.1007/0-306-48100-6_1.
 27. Styczynski, J. *et al.* Death after hematopoietic stem cell transplantation: changes over calendar year time, infections and associated factors. *Bone Marrow Transpl.* **55**, 126–136 (2020).
 28. Manuscript, A. Gyurkocza B, Rezvani A, Storb RF. Allogeneic hematopoietic cell transplantation: the state of the art. *Expert Rev Hematol.* 2010;3(3):285–299. **3**, 285–299 (2011).
 29. Lee, S. J. *et al.* High-resolution donor-recipient HLA matching contributes to the success of unrelated donor marrow transplantation. *Blood* **110**, 4576–4583 (2007).
 30. Koyama, M. & Hill, G. R. Alloantigen presentation and graft-versus-host disease: Fuel for the fire. *Blood* **127**, 2963–2970 (2016).
 31. Marino, J., Paster, J. & Benichou, G. Alloreognition by T lymphocytes and allograft rejection. *Front. Immunol.* **7**, 1–9 (2016).
 32. Blander, J. M. Regulation of the Cell Biology of Antigen Cross-Presentation. *Annu. Rev. Immunol.* **36**, 717–753 (2018).
 33. Fürst, D., Neuchel, C., Tsamadou, C., Schrezenmeier, H. & Mytilineos, J. HLA Matching in Unrelated Stem Cell Transplantation up to Date. *Transfus. Med.*

- Hemotherapy* **46**, 326–336 (2019).
34. Siu, J. H. Y., Surendrakumar, V., Richards, J. A. & Pettigrew, G. J. T cell allorecognition pathways in solid organ transplantation. *Front. Immunol.* **9**, 1–14 (2018).
 35. Zeiser, R. & Blazar, B. R. Acute graft-versus-host disease - Biologic process, prevention, and therapy. *N. Engl. J. Med.* **377**, 2167–2179 (2017).
 36. Arai, S. *et al.* Increasing Incidence of Chronic Graft-versus-Host Disease in Allogeneic Transplantation: A Report from the Center for International Blood and Marrow Transplant Research. *Biol. Blood Marrow Transplant.* **21**, 266–274 (2015).
 37. Ferrara, J. L., Levine, J. E., Reddy, P. & Holler, E. Graft-versus-host disease. *Lancet* **373**, 1550–1561 (2009).
 38. Schoemans, H. M. *et al.* EBMT–NIH–CIBMTR Task Force position statement on standardized terminology & guidance for graft-versus-host disease assessment. *Bone Marrow Transplant.* **53**, 1401–1415 (2018).
 39. Reddy, P. & Ferrara, J. L. M. Immunobiology of acute graft-versus-host disease. *Blood Rev.* **17**, 187–194 (2003).
 40. Santos e Sousa, P., Bennett, C. L. & Chakraverty, R. Unraveling the mechanisms of cutaneous graft-versus-host disease. *Front. Immunol.* **9**, (2018).
 41. Hofmeister, C. C. *et al.* Graft-versus-host disease of the skin: life and death on the epidermal edge. *Biol Blood Marrow Transpl.* **10**, 366–372 (2004).
 42. Brügggen, M. C. *et al.* Diverse T-cell responses characterize the different manifestations of cutaneous graft-versus-host disease. *Blood* **123**, 290–299 (2014).
 43. Du, W. & Cao, X. Cytotoxic Pathways in Allogeneic Hematopoietic Cell Transplantation. *Front Immunol* **9**, 2979 (2018).
 44. Zhan, Q. *et al.* Cytokeratin15-positive basal epithelial cells targeted in graft-versus-host disease express a constitutive antiapoptotic phenotype. *J. Invest. Dermatol.* **127**, 106–115 (2007).
 45. Murphy, G. F. Target cells in graft-versus-host disease: Implications for cancer therapy. *Clin. Rev. Allergy Immunol.* **33**, 113–123 (2007).
 46. Piper, K. P. *et al.* CXCL10-CXCR3 interactions play an important role in the pathogenesis of acute graft-versus-host disease in the skin following allogeneic stem-cell transplantation. *Blood* **110**, 3827–3832 (2007).
 47. Kitko, C. L. *et al.* Plasma CXCL9 elevations correlate with chronic GVHD diagnosis. *Blood* **123**, 786–793 (2014).
 48. Choi, J. *et al.* IFN γ R signaling mediates alloreactive T-cell trafficking and GVHD. *Blood* **120**, 4093–4103 (2012).
 49. Reichenbach, D. K. *et al.* The IL-33/ST2 axis augments effector T-cell responses

- during acute GVHD. *Blood* **125**, 3183–3192 (2015).
50. Brügger, M. C. *et al.* Epidermal Elafin Expression Is an Indicator of Poor Prognosis in Cutaneous Graft-versus-Host Disease. *J. Invest. Dermatol.* **135**, 999–1006 (2015).
 51. Paczesny, S. *et al.* Elafin is a biomarker of graft-versus-host disease of the skin. *Sci. Transl. Med.* **2**, (2010).
 52. Collin, M. P. *et al.* The fate of human Langerhans cells in hematopoietic stem cell transplantation. *J. Exp. Med.* **203**, 27–33 (2006).
 53. Penack, O. *et al.* Prophylaxis and management of graft versus host disease after stem-cell transplantation for haematological malignancies: updated consensus recommendations of the European Society for Blood and Marrow Transplantation. *Lancet Haematol.* **7**, e157–e167 (2020).
 54. Törlén, J. *et al.* A prospective randomized trial comparing cyclosporine/methotrexate and tacrolimus/sirolimus as graft-versus-host disease prophylaxis after allogeneic hematopoietic stem cell transplantation. *Haematologica* **101**, 1417–1425 (2016).
 55. Finke, J. *et al.* Standard graft-versus-host disease prophylaxis with or without anti-T-cell globulin in haematopoietic cell transplantation from matched unrelated donors: a randomised, open-label, multicentre phase 3 trial. *Lancet Oncol.* **10**, 855–864 (2009).
 56. Ruutu, T. *et al.* Prophylaxis and treatment of GVHD: EBMT-ELN working group recommendations for a standardized practice. *Bone Marrow Transplant.* **49**, 168–173 (2014).
 57. Nickoloff, B. J., Basham, T. Y., Merigan, T. C., Torseth, J. W. & Morhenn, V. B. Human keratinocyte-lymphocyte reactions in vitro. *J. Invest. Dermatol.* **87**, 11–18 (1986).
 58. Shao, S. *et al.* IFN-gamma enhances cell-mediated cytotoxicity against keratinocytes via JAK2/STAT1 in lichen planus. *Sci Transl Med* **11**, (2019).
 59. Orlik, C. *et al.* Keratinocytes costimulate naive human T cells via CD2: a potential target to prevent the development of proinflammatory Th1 cells in the skin. *Cell Mol Immunol* **17**, 380–394 (2020).
 60. Wang, X. N. *et al.* Skin explant model of human graft-versus-host disease: Prediction of clinical outcome and correlation with biological risk factors. *Biol. Blood Marrow Transplant.* **12**, 152–159 (2006).
 61. Dickinson, A. M. *et al.* Use of a skin explant model for predicting GVHD in HLA-matched bone marrow transplants: Effect of GVHD prophylaxis. *Bone Marrow Transplant.* **24**, 857–863 (1999).
 62. Wallstabe, J. *et al.* Inflammation-induced tissue damage mimicking GvHD in human skin models as test-platform for immunotherapeutics. *ALTEX* **37**, (2020).
 63. Lange, J. *et al.* Interactions of donor sources and media influence the histo-

- morphological quality of full-thickness skin models. *Biotechnol. J.* **11**, 1352–1361 (2016).
64. Zeiser, R. & Blazar, B. R. Preclinical models of acute and chronic graft-versus-host disease: How predictive are they for a successful clinical translation? *Blood* **127**, 3117–3126 (2016).
 65. Salgado, G., Ng, Y. Z., Koh, L. F., Goh, C. S. M. & Common, J. E. Human reconstructed skin xenografts on mice to model skin physiology. *Differentiation* **98**, 14–24 (2017).
 66. Shultz, L. D. *et al.* Human Lymphoid and Myeloid Cell Development in NOD/LtSz-scid IL2R γ null Mice Engrafted with Mobilized Human Hemopoietic Stem Cells . *J. Immunol.* **174**, 6477–6489 (2005).
 67. Racki, W. J. *et al.* NOD-scid IL2rnull mouse model of human skin transplantation and allograft rejection. *Transplantation* **89**, 527–536 (2010).
 68. Yamauchi, T. *et al.* Polymorphic Sirpa is the genetic determinant for NOD-based mouse lines to achieve efficient human cell engraftment. *Blood* **121**, 1316–1325 (2013).
 69. Betts, B. C. *et al.* Targeting JAK2 reduces GVHD and xenograft rejection through regulation of T cell differentiation. *Proc. Natl. Acad. Sci. U. S. A.* **115**, 1582–1587 (2018).
 70. Sagoo, P. *et al.* Human regulatory T cells with alloantigen specificity are more potent inhibitors of alloimmune skin graft damage than polyclonal regulatory T cells. *Sci. Transl. Med.* **3**, (2011).
 71. Ehrlich, P. Über Antigene und Antikörper. *Handbuch der Technik und Methodik der Immunitätsforschung* 1–10 (1908).
 72. Weiner, L. M., Surana, R. & Wang, S. Monoclonal antibodies: Versatile platforms for cancer immunotherapy. *Nat. Rev. Immunol.* **10**, 317–327 (2010).
 73. Dobosz, P. & Dzieciatkowski, T. The Intriguing History of Cancer Immunotherapy. *Front. Immunol.* **10**, (2019).
 74. Liu, J. K. H. The history of monoclonal antibody development - Progress, remaining challenges and future innovations. *Ann. Med. Surg.* **3**, 113–116 (2014).
 75. Deligne, C., Milcent, B., Josseaume, N., Teillaud, J. L. & Sibénil, S. Impact of depleting therapeutic monoclonal antibodies on the host adaptive immunity: A bonus or a malus? *Front. Immunol.* **8**, 1–11 (2017).
 76. Inamoto, Y. *et al.* Influence of immunosuppressive treatment on risk of recurrent malignancy after allogeneic hematopoietic cell transplantation. *Blood* **118**, 456–463 (2011).
 77. Mitsunaga, M. *et al.* Cancer cell-selective in vivo near infrared photoimmunotherapy

- targeting specific membrane molecules. *Nat. Med.* **17**, 1685–1691 (2011).
78. Sato, K. *et al.* Photoinduced Ligand Release from a Silicon Phthalocyanine Dye Conjugated with Monoclonal Antibodies: A Mechanism of Cancer Cell Cytotoxicity after Near-Infrared Photoimmunotherapy. *ACS Cent. Sci.* **4**, 1559–1569 (2018).
 79. Queirós, C., Garrido, P. M., Maia Silva, J. & Filipe, P. Photodynamic therapy in dermatology: Beyond current indications. *Dermatol. Ther.* 1–7 (2020)
doi:10.1111/dth.13997.
 80. Grandi, V. *et al.* Standardization of regimens in Narrowband UVB and PUVA in early stage mycosis fungoides: position paper from the Italian Task Force for Cutaneous Lymphomas. *J. Eur. Acad. Dermatology Venereol.* **32**, 683–691 (2018).
 81. Kobayashi, H. & Choyke, P. L. Near-Infrared Photoimmunotherapy of Cancer. *Acc. Chem. Res.* **52**, 2332–2339 (2019).
 82. Green, D. R. The Coming Decade of Cell Death Research: Five Riddles. *Cell* **177**, 1094–1107 (2019).
 83. Weinlich, R., Oberst, A., Beere, H. M. & Green, D. R. Necroptosis in development, inflammation and disease. *Nat Rev Mol Cell Biol* **18**, 127–136 (2017).
 84. Wajant, H. & Siegmund, D. TNFR1 and TNFR2 in the control of the life and death balance of macrophages. *Front. Cell Dev. Biol.* **7**, 1–14 (2019).
 85. Johnstone, R. W., Ruefli, A. A. & Lowe, S. W. Apoptosis: A link between cancer genetics and chemotherapy. *Cell* **108**, 153–164 (2002).
 86. Degtarev, A. *et al.* Chemical inhibitor of nonapoptotic cell death with therapeutic potential for ischemic brain injury. *Nat. Chem. Biol.* **1**, 112–119 (2005).
 87. He, S. *et al.* Receptor Interacting Protein Kinase-3 Determines Cellular Necrotic Response to TNF- α . *Cell* **137**, 1100–1111 (2009).
 88. Sun, L. *et al.* Mixed lineage kinase domain-like protein mediates necrosis signaling downstream of RIP3 kinase. *Cell* **148**, 213–227 (2012).
 89. Gong, Y. N., Guy, C., Crawford, J. C. & Green, D. R. Biological events and molecular signaling following MLKL activation during necroptosis. *Cell Cycle* **16**, 1748–1760 (2017).
 90. Wallach, D., Kang, T. B., Dillon, C. P. & Green, D. R. Programmed necrosis in inflammation: Toward identification of the effector molecules. *Science (80-.)*. **352**, (2016).
 91. Kaiser, W. J., Upton, J. W. & Mocarski, E. S. Receptor-Interacting Protein Homotypic Interaction Motif-Dependent Control of NF- κ B Activation via the DNA-Dependent Activator of IFN Regulatory Factors. *J. Immunol.* **181**, 6427–6434 (2008).
 92. Kesavardhana, S. & Kanneganti, T. D. ZBP1: A STARGATE to decode the biology of Z-nucleic acids in disease. *J. Exp. Med.* **217**, 1–4 (2020).

93. Rickard, J. A. *et al.* RIPK1 regulates RIPK3-MLKL-driven systemic inflammation and emergency hematopoiesis. *Cell* **157**, 1175–1188 (2014).
94. Gong, Y. N. *et al.* ESCRT-III Acts Downstream of MLKL to Regulate Necroptotic Cell Death and Its Consequences. *Cell* **169**, 286-300.e16 (2017).
95. Kaczmarek, A., Vandenabeele, P. & Krysko, D. V. Necroptosis: the release of damage-associated molecular patterns and its physiological relevance. *Immunity* **38**, 209–223 (2013).
96. Berthold, F. Isolation of human monocytes by ficoll density gradient centrifugation. *Blut* **43**, 367–371 (1981).
97. Sato, K. *et al.* Spatially selective depletion of tumor-associated regulatory T cells with near-infrared photoimmunotherapy. *Sci. Transl. Med.* **8**, (2016).
98. Venema, K. *The TNO in vitro model of the colon (TIM-2). The Impact of Food Bioactives on Health: In Vitro and Ex Vivo Models* (2015). doi:10.1007/978-3-319-16104-4_26.
99. van Dijk, A. M. C. *et al.* Primary human keratinocytes as targets in predicting acute graft-versus-host disease following HLA-identical bone marrow transplantation. *Br. J. Haematol.* **111**, 791–796 (2000).
100. Freund, L. *et al.* Skin-Selective CD8 T-Cell Depletion by Photoimmunotherapy Inhibits Human Cutaneous Acute Graft-Versus-Host Disease. *J. Invest. Dermatol.* **140**, 1455-1459.e6 (2020).
101. Belmokhtar, C. A., Hillion, J. & Ségal-Bendirdjian, E. Staurosporine induces apoptosis through both caspase-dependent and caspase-independent mechanisms. *Oncogene* **20**, 3354–3362 (2001).
102. Zeiser, R. *et al.* Ruxolitinib for Glucocorticoid-Refractory Acute Graft-versus-Host Disease. *N Engl J Med* **382**, 1800–1810 (2020).
103. Schroeder, M. A. *et al.* A phase 1 trial of itacitinib, a selective JAK1 inhibitor, in patients with acute graft-versus-host disease. *Blood Adv.* **4**, 1657–1669 (2020).
104. Lauffer, F. *et al.* Type I Immune Response Induces Keratinocyte Necroptosis and Is Associated with Interface Dermatitis. *J Invest Dermatol* **138**, 1785–1794 (2018).
105. Choi, M. E. *et al.* Necroptosis : a crucial pathogenic mediator of human disease Find the latest version : Necroptosis : a crucial pathogenic mediator of human disease. **4**, (2019).
106. Sato, K. *et al.* Comparative effectiveness of light emitting diodes (LEDs) and lasers in near infrared photoimmunotherapy. *Oncotarget* **7**, 14324–14335 (2016).
107. Okuyama, S. *et al.* Interstitial near-infrared photoimmunotherapy: Effective treatment areas and light doses needed for use with fiber optic diffusers. *Oncotarget* **9**, 11159–11169 (2018).

108. Plum, T. *et al.* Human Mast Cell Proteome Reveals Unique Lineage, Putative Functions, and Structural Basis for Cell Ablation. *Immunity* **52**, 404-416.e5 (2020).
109. Nast, A. *et al.* S3 - Leitlinie zur Therapie der Psoriasis vulgaris. Update 2017, AWMF-Register-Nr. 013/001. 1–156 (2017).
110. Biernacki, M. A. *et al.* T cell optimization for graft-versus-leukemia responses. **5**, (2020).
111. Bleakley, M. *et al.* Leukemia-associated minor histocompatibility antigen discovery using T-cell clones isolated by in vitro stimulation of naive CD8² T cells. **115**, 4923–4933 (2010).
112. Zhang, Y. *et al.* Dendritic cell – activated CD44^{hi} CD8² T cells are defective in mediating acute graft-versus-host disease but retain graft-versus-leukemia activity. **103**, 3970–3978 (2004).
113. Muffly, L. *et al.* Infusion of donor-derived CD8⁺ memory T cells for relapse following allogeneic hematopoietic cell transplantation. *Blood Adv.* **2**, 681–690 (2018).
114. Martin, P. J. *et al.* A phase I-II clinical trial to evaluate removal of CD4 cells and partial depletion of CD8 cells from donor marrow for HLA-mismatched unrelated recipients. *Blood* **94**, 2192–2199 (1999).
115. Di Meglio, P. *et al.* Targeting CD8⁺ T cells prevents psoriasis development. *J. Allergy Clin. Immunol.* **138**, 274-276.e6 (2016).
116. Cheuk, S. *et al.* CD49a Expression Defines Tissue-Resident CD8⁺ T Cells Poised for Cytotoxic Function in Human Skin. *Immunity* **46**, 287–300 (2017).
117. Hemmerling, J. *et al.* Human Epidermal Langerhans Cells Replenish Skin Xenografts and Are Depleted by Alloreactive T Cells In Vivo. *J. Immunol.* **187**, 1142–1149 (2011).
118. Merad, M. *et al.* Depletion of host Langerhans cells before transplantation of donor alloreactive T cells prevents skin graft-versus-host disease. *Nat. Med.* **10**, 510–517 (2004).
119. Wenzel, J. *et al.* CXCR3 <-> ligand-mediated skin inflammation in cutaneous lichenoid graft-versus-host disease. *J. Am. Acad. Dermatol.* **58**, 437–442 (2008).
120. Bratke, K., Kuepper, M., Bade, B., Virchow, J. C. & Luttmann, W. Differential expression of human granzymes A, B, and K in natural killer cells and during CD8⁺ T cell differentiation in peripheral blood. *European Journal of Immunology* vol. 35 2608–2616 (2005).
121. Ewing, P. *et al.* Donor CD4⁺ T-cell production of tumor necrosis factor alpha significantly contributes to the early proinflammatory events of graft-versus-host disease. *Exp. Hematol.* **35**, 155–163 (2007).
122. Okiyama, N. *et al.* Reversal of CD8 T-cell-mediated mucocutaneous graft-versus-host-like disease by the JAK inhibitor tofacitinib. *J Invest Dermatol* **134**, 992–1000 (2014).

123. Shibaki, A., Sato, A., Vogel, J. C., Miyagawa, F. & Katz, S. I. Induction of GVHD-like skin disease by passively transferred CD8 + T-cell receptor transgenic T cells into keratin 14-ovalbumin transgenic mice. *J. Invest. Dermatol.* **123**, 109–115 (2004).
124. Okiyama, N. & Katz, S. I. Programmed cell death 1 (PD-1) regulates the effector function of CD8 T cells via PD-L1 expressed on target keratinocytes. *J. Autoimmun.* **53**, 1–9 (2014).
125. Mavin, E. *et al.* Regulatory T cells inhibit CD8+ T-cell tissue invasion in human skin graft-versus-host reactions. *Transplantation* **94**, 456–464 (2012).
126. Eckhart, L. *et al.* Terminal differentiation of human keratinocytes and stratum corneum formation is associated with caspase-14 activation. *J. Invest. Dermatol.* **115**, 1148–1151 (2000).
127. Raj, D., Brash, D. E. & Grossman, D. Keratinocyte apoptosis in epidermal development and disease. *J. Invest. Dermatol.* **126**, 243–257 (2006).
128. Eckhart, L., Lippens, S., Tschachler, E. & Declercq, W. Cell death by cornification. *Biochim. Biophys. Acta - Mol. Cell Res.* **1833**, 3471–3480 (2013).
129. Zhang, Q., Lenardo, M. J. & Baltimore, D. 30 Years of NF- κ B: A Blossoming of Relevance to Human Pathobiology. *Cell* **168**, 37–57 (2017).
130. Leverkus, M. *et al.* Proteasome Inhibition Results in TRAIL Sensitization of Primary Keratinocytes by Removing the Resistance-Mediating Block of Effector Caspase Maturation. *Mol. Cell. Biol.* **23**, 777–790 (2003).
131. Salvesen, G. S. & Duckett, C. S. IAP proteins: Blocking the road to death's door. *Nat. Rev. Mol. Cell Biol.* **3**, 401–410 (2002).
132. Panayotova-Dimitrova, D. *et al.* CFLIP Regulates Skin Homeostasis and Protects against TNF-Induced Keratinocyte Apoptosis. *Cell Rep.* **5**, 397–408 (2013).
133. Hughes, M. A. *et al.* Co-operative and Hierarchical Binding of c-FLIP and Caspase-8: A Unified Model Defines How c-FLIP Isoforms Differentially Control Cell Fate. *Mol. Cell* **61**, 834–849 (2016).
134. Polykratis, A. *et al.* A20 prevents inflammasome-dependent arthritis by inhibiting macrophage necroptosis through its ZnF7 ubiquitin-binding domain. *Nat. Cell Biol.* **21**, 731–742 (2019).
135. Feoktistova, M. *et al.* A20 Promotes Ripoptosome Formation and TNF-Induced Apoptosis via cIAPs Regulation and NIK Stabilization in Keratinocytes. *Cells* **9**, 351 (2020).
136. Devos, M. *et al.* Keratinocyte Expression of A20/TNFAIP3 Controls Skin Inflammation Associated with Atopic Dermatitis and Psoriasis. *J. Invest. Dermatol.* **139**, 135–145 (2019).
137. Wenzel, J. & Tüting, T. An IFN-associated cytotoxic cellular immune response against

- viral, self-, or tumor antigens is a common pathogenetic feature in 'interface dermatitis'. *J. Invest. Dermatol.* **128**, 2392–2402 (2008).
138. Sontheimer, R. D. Lichenoid tissue reaction/interface dermatitis: clinical and histological perspectives. *J Invest Dermatol* **129**, 1088–1099 (2009).
 139. Galluzzi, L. & Kroemer, G. Necroptosis: A Specialized Pathway of Programmed Necrosis. *Cell* **135**, 1161–1163 (2008).
 140. Meller, S., Gilliet, M. & Homey, B. Chemokines in the pathogenesis of lichenoid tissue reactions. *J. Invest. Dermatol.* **129**, 315–319 (2009).
 141. Iijima, W. *et al.* Infiltrating CD8⁺ T cells in oral lichen planus predominantly express CCR5 and CXCR3 and carry respective chemokine ligands RANTES/CCL5 and IP-10/CXCL10 in their cytolytic granules: A potential self-recruiting mechanism. *Am. J. Pathol.* **163**, 261–268 (2003).
 142. Hasegawa, A. & Abe, R. Recent advances in managing and understanding Stevens-Johnson syndrome and toxic epidermal necrolysis. *F1000Research* **9**, (2020).
 143. Saito, N. *et al.* An annexin A1-FPR1 interaction contributes to necroptosis of keratinocytes in severe cutaneous adverse drug reactions. *Sci Transl Med* **6**, 245ra95 (2014).
 144. Hasegawa, A. *et al.* RIP3 as a diagnostic and severity marker for Stevens-Johnson syndrome and toxic epidermal necrolysis. *J Allergy Clin Immunol Pr.* **8**, 1768-1771 e7 (2020).
 145. Choi, J. *et al.* IFN γ R signaling mediates alloreactive T-cell trafficking and GVHD. *Blood* **120**, 4093–4103 (2012).
 146. Via, C. S., Rus, V., Gately, M. K. & Finkelman, F. D. IL-12 stimulates the development of acute graft-versus-host disease in mice that normally would develop chronic, autoimmune graft-versus-host disease. *J. Immunol.* **153**, 4040–7 (1994).
 147. Yang, Y., Wang, H., Asavaroengchai, W. & Dey, B. R. Role of Interferon- γ in GVHD and GVL. **2**, (2005).
 148. Wang, H. & Yang, Y. G. The complex and central role of interferon-gamma in graft-versus-host disease and graft-versus-tumor activity. *Immunol Rev* **258**, 30–44 (2014).
 149. Yi, T. *et al.* Reciprocal differentiation and tissue-specific pathogenesis of Th1, Th2, and Th17 cells in graft-versus-host disease. *Blood* **114**, 3101–3112 (2009).
 150. Rebane, A. *et al.* Mechanisms of IFN- γ -induced apoptosis of human skin keratinocytes in patients with atopic dermatitis. *J. Allergy Clin. Immunol.* **129**, 1297–1306 (2012).
 151. Konur, A., Schulz, U., Eissner, G., Andreesen, R. & Holler, E. Interferon (IFN)- γ is a main mediator of keratinocyte (HaCaT) apoptosis and contributes to autocrine IFN- γ and tumour necrosis factor- α production. *Br. J. Dermatol.* **152**, 1134–1142 (2005).
 152. Molnar, T. *et al.* Current translational potential and underlying molecular mechanisms

- of necroptosis. *Cell Death Dis* **10**, 860 (2019).
153. Devos, M. *et al.* Sensing of endogenous nucleic acids by ZBP1 induces keratinocyte necroptosis and skin inflammation. *J Exp Med* **217**, (2020).
 154. Yang, D. *et al.* ZBP1 mediates interferon-induced necroptosis. *Cell Mol Immunol* **17**, 356–368 (2020).
 155. Lin, J. *et al.* RIPK1 counteracts ZBP1-mediated necroptosis to inhibit inflammation. *Nature* **540**, 124–128 (2016).
 156. Jiao, H. *et al.* Z-nucleic-acid sensing triggers ZBP1-dependent necroptosis and inflammation. *Nature* **580**, 391–395 (2020).
 157. Tait, S. W. G., Bouchier-hayes, L., Oberst, A., Connell, S. & Green, D. R. Chapter 3 Live to Dead Cell Imaging. *Business* **559**, 33–48 (2013).
 158. Wei, L., Sun, X. J., Wang, Z. & Chen, Q. CD95-induced osteoarthritic chondrocyte apoptosis and necrosis: Dependency on p38 mitogen-activated protein kinase. *Arthritis Res. Ther.* **8**, 1–10 (2006).
 159. Bonnet, M. C. *et al.* The adaptor protein FADD protects epidermal keratinocytes from necroptosis in vivo and prevents skin inflammation. *Immunity* **35**, 572–582 (2011).
 160. Mandal, P. *et al.* RIP3 induces apoptosis independent of pronecrotic kinase activity. *Mol Cell* **56**, 481–495 (2014).
 161. Wang, R. *et al.* Gut stem cell necroptosis by genome instability triggers bowel inflammation. *Nature* **580**, 386–390 (2020).
 162. Degterev, A., Ofengeim, D. & Yuan, J. Targeting RIPK1 for the treatment of human diseases. *Proc. Natl. Acad. Sci. U. S. A.* **116**, 9714–9722 (2019).
 163. Laurien, L. *et al.* Autophosphorylation at serine 166 regulates RIP kinase 1-mediated cell death and inflammation. *Nat. Commun.* **11**, (2020).
 164. Dannappel, M. *et al.* RIPK1 maintains epithelial homeostasis by inhibiting apoptosis and necroptosis. *Nature* **513**, 90–94 (2014).
 165. Letai, A. Cell Death and Cancer Therapy: Don't Forget to Kill the Cancer Cell! *Clin. Cancer Res.* **21**, 5015–5020 (2015).
 166. Chang, Y. J., Zhao, X. Y. & Huang, X. J. Strategies for Enhancing and Preserving Anti-leukemia Effects Without Aggravating Graft-Versus-Host Disease. *Front. Immunol.* **9**, 3041 (2018).
 167. Gong, Y. *et al.* The role of necroptosis in cancer biology and therapy. *Mol. Cancer* **18**, 1–17 (2019).
 168. Mezzatesta, C. & Bornhauser, B. C. Exploiting necroptosis for therapy of acute lymphoblastic leukemia. *Front. Cell Dev. Biol.* **7**, 1–8 (2019).
 169. Lieberman, J. The ABCs of granule-mediated cytotoxicity: New weapons in the arsenal. *Nat. Rev. Immunol.* **3**, 361–370 (2003).

170. Jarvis, M. *et al.* The detection of apoptosis in a human in vitro skin explant assay for graft versus host reactions. *J. Clin. Pathol.* **55**, 127–132 (2002).
171. Langley, R. G. B., Walsh, N., Nevill, T., Thomas, L. & Rowden, G. Apoptosis is the mode of keratinocyte death in cutaneous graft-versus-host disease. *J. Am. Acad. Dermatol.* **35**, 187–190 (1996).
172. Gilliam, A. C., Whitaker-Menezes, D., Korngold, R. & Murphy, G. F. Apoptosis is the predominant form of epithelial target cell injury in acute experimental graft-versus-host disease. *J. Invest. Dermatol.* **107**, 377–383 (1996).
173. Jouan-Lanhouet, S. *et al.* TRAIL induces necroptosis involving RIPK1/RIPK3-dependent PARP-1 activation. *Cell Death Differ.* **19**, 2003–2014 (2012).
174. Yoo, Y. H., Gilliam, A. C., Whitaker-Menezes, D., Korngold, R. & Murphy, G. F. Experimental induction and ultrastructural characterization of apoptosis in murine acute cutaneous graft-versus-host disease. *Arch. Dermatol. Res.* **289**, 389–398 (1997).
175. Wang, L. *et al.* Increased apoptosis is linked to severe acute GVHD in patients with Fanconi anemia. *Bone Marrow Transplant.* **48**, 849–853 (2013).
176. Whitaker-Menezes, D., Jones, S. C., Friedman, T. M., Korngold, R. & Murphy, G. F. An epithelial target site in experimental graft-versus-host disease and cytokine-mediated cytotoxicity is defined by cytokeratin 15 expression. *Biol. Blood Marrow Transplant.* **9**, 559–570 (2003).
177. Solimani, F., Meier, K. & Ghoreschi, K. Emerging Topical and Systemic JAK Inhibitors in Dermatology. *Front. Immunol.* **10**, 1–19 (2019).
178. Zeiser, R. *et al.* Ruxolitinib in corticosteroid-refractory graft-versus-host disease after allogeneic stem cell transplantation: A multicenter survey. *Leukemia* **29**, 2062–2068 (2015).
179. Spoerl, S. *et al.* Activity of therapeutic JAK 1/2 blockade in graft-versus-host disease. *Blood* **123**, 3832–3842 (2014).
180. Stern, R. S. & Divito, S. J. Stevens-Johnson Syndrome and Toxic Epidermal Necrolysis: Associations, Outcomes, and Pathobiology—Thirty Years of Progress but Still Much to Be Done. *J. Invest. Dermatol.* **137**, 1004–1008 (2017).
181. Fetter, T. *et al.* Selective Janus Kinase 1 Inhibition Is a Promising Therapeutic Approach for Lupus Erythematosus Skin Lesions. *Front. Immunol.* **11**, 1–9 (2020).
182. Gratwohl, A. *et al.* Original Articles Changes in the use of hematopoietic stem cell transplantation: a model for diffusion of medical technology. *Ferrata Storti Foundation* 637–643 doi:10.3324/haematol.2009.015586.
183. Baldomero, H. *et al.* Narrowing the gap for hematopoietic stem cell transplantation in the East-Mediterranean / African region: comparison with global HSCT indications

and trends. *Bone Marrow Transplant*. 402–417 (2019) doi:10.1038/s41409-018-0275-5.

Acknowledgements

First of all, I would like to thank my supervisor Prof. Knut Schäkel who gave me the opportunity to perform my dissertation project at the Department of Dermatology in Heidelberg. Throughout the years your support, supervision, feedback and intensive discussions on equal terms shaped my scientific education tremendously. Retrospectively, I am thankful for all the opportunities and challenges you gave to promote our projects such as the internships in Dresden and Zürich as well as all the meetings that I could join and cooperation's I could make. Furthermore, I want to thank Prof. Rodewald, Prof. Dalpke, Prof. Haefeli and Prof. Umansky for attending and supervising my TAC meetings and examining my thesis.

I am extremely grateful for the past years in the Hautklinik lab, for all the people I met, friendships that were formed and moments that remain unforgettable. (Chronological) Therefore, special thanks to Stefanie Häberle being the good sole of the lab and organizer of all the activities. Your laugh is missing. Diego, thanks for all the crazy imaginations, I hope you remain an eternal dreamer. Special thanks to my brother Hao, for all the Hot Pot nights and "bottoms up" that we made. Hope to see you one day again. Thanks to Stephanie Oehrl who was not just a strong support in my every day laboratory work but a companion in spirit. Better times will come. Thank you Cinthia for the intensive discussions covering any topic. I hope you remember me this time. Thanks to Felix, for the common lab time, talks about travelling and funny party moments. Big thanks to Stefan, even if we do not always agree I appreciate you very much. Galina, thanks that you were the order in my daily life, histology times forever connect us. Thanks to Martin and the intensive friendship whether spending our nights in the lab or at Vater Rhein. I wish you all the best. I am especially thankful for Julius, a friend you will not meet a second time. Moreover, I want to thank all the people that have accompanied me on my way: Adriana, Jing, Florian, Lisa, Silvi, Fareed, Sophie, Priscilla, Akira, Yutaka, Karsten, Sabine, Carmen, Halina, Josefina, Frauhammer, Florina, Meihong, Mr. Lee, Mustafa, Sonja, Paul and many more.

Zuletzt möchte meinem privaten Umfeld danken. Meiner Familie und Angehörigen, namentlich meinem Großvater Martin, meiner Mutter Wilma, meinem Vater Harald, meinen Brüdern Josef und Alexander, meinen Schwestern Vera und Franziska sowie meinen Nichten und Neffen die mich in meiner Persönlichkeit und meinem Dasein formen und mir einen Halt geben.

Zum Schluss danke ich meiner Frau Rumina für das Vergangene,
die Gegenwart und die Zukunft.